

INSTITUTE OF BUILDING DESIGN

Report no. **174**

KRISTIAN HERTZ

ANALYSES OF PRESTRESSED CONCRETE STRUCTURES EXPOSED TO FIRE

Den polytekniske Lærestalt, Danmarks tekniske Højskole
Technical University of Denmark. DK-2800 Lyngby 1985

INSTITUTE OF BUILDING DESIGN

Report no. **174**

KRISTIAN HERTZ

ANALYSES OF PRESTRESSED CONCRETE STRUCTURES EXPOSED TO FIRE

Den polytekniske Lærestalt, Danmarks tekniske Højskole
Technical University of Denmark. DK-2800 Lyngby 1985

It is forbidden to sell or rent computer programs based on
the theory of this report without the authors permission.

© Kristian Hertz

CONTENTS

Contents	2
Preface	3
Acknowledgements	4
Summary	5
Symbols	9
Introduction	14
Idealized Mechanical Properties of Reinforcing Steels	15
Idealized Mechanical Properties of Concrete ..	22
Idealized Strain Properties of Concrete	35
Stress Distribution	41
Ultimate Limit State Analysis of Beams in Bending	53
Slabs and T-Sections	63
Shear	67
Analysis of Rectangular Cross-Sections	73
Deflections	81
Columns	89
The Fully Developed Fire Course	101
Literature	105
Appendix A: Derivation of Formulas for the Ana- lysis of Rectangular Cross-sections.	113
Appendix B: Strength and Temperature Distributions	121
Appendix C: Examples	127
References to the Examples	150



Eugène Freyssinet

PREFACE

It was the idea of Eugène Freyssinet that a pre-tensioned reinforcement would provide a concrete construction with a prestress counteracting the formation of tensile cracks.

Doing so, the total cross-section of the concrete contributes to the stiffness, the deflections can be minimized for dead load and service load, and a smaller cross-section is required to obtain deflections within certain limits.

Freyssinet was fully aware that the prestressing steel should have a high strength, and that the concrete should arise a minimum of shrinkage and creep.

However, when a prestressed structure is exposed to fire the smaller cross-section is heated more than the larger slack-reinforced cross-section, causing the high strength of the prestressing steel to be rapidly reduced and the loaded concrete to be compressed.

This means that prestressed concrete structures are especially susceptible to fire exposure, and that an analysis for the load-case "Fire" is of a special importance for these structures.

The analysis is a main topic for the present report.

Lyngby, december 1985

Kristian Hertz

M.Sc. Ph.D. Struct.Eng.

ACKNOWLEDGEMENTS

I wish to express my gratitude to the Danish Technical Research Council for financial support of the project and to the staff of the Institute of Building Design for typing and printing the report.

A special thank should be given to senior lecturer T. Jakobsen for reading the manuscript thoroughly and for many fruitful lingual discussions.

SUMMARY

Based on the data and discussions of the Ph.D. thesis Hertz [14] idealized properties of fire exposed concrete are derived, and especially a relation is found between the reductions of the compressive strength, the reduction of the E-modulus and the increment of the ultimate strain defined as the strain at the ultimate compressive stress.

Introducing the relation proposed by Ritter between the E-modulus and the compressive stress the idealized stress-strain curves are derived for the fire exposed concrete, and these curves ensure a homogeneity in the calculations of deflections of beams and the stability of centrally loaded- and cross-loaded columns.

Idealized properties of reinforcing steels exposed to high temperatures are determined, and a relation between the strength reductions of mild steel and cold worked prestressing steel is formulated.

The distribution of the ultimate stresses through a fire exposed concrete cross-section is described by simple parameters, and the influence of hindered thermal strains is discussed.

The distribution of the E-modulus through a fire exposed cross-section is analysed, and simple methods

are developed for the estimation of the stiffness of the cross-section subjected to compression and to bending.

Methods are established for the analysis in the ultimate limit state of beams and slabs in positive and negative bending, where negative bending is defined by fire exposure at the more compressed edge of the cross-section. Further, a method is developed for estimating the shear capacity of beams and walls.

The methods mentioned can be applied analysing the load-bearing capacity of a structure with or without prestressing at any time of any fire course.

A new procedure is derived for the analysis of a rectangular cross-section subjected to a service load in bending or an eccentrically normal load, which can be an external normal load, a prestressing force or a combination of both.

The procedure operates with cracked or uncracked cross-sections and the idealized curved stress-strain relation of the concrete, and it determines the complete distribution of stresses and strains of the cross-section and the curvature in particular.

The procedure is advantageous for structures without a fire exposure, but in this context it is utilized as a subroutine in a more complex procedure, which

is developed for the estimation of the deflections of fire exposed concrete beams at any time of any fire course.

Based on the above procedure an algorithm is described for the analysis of fire exposed cross-loaded concrete columns comprising an estimation of the deflection and the stability of the columns.

As a marginal case an extended Renkine formula is derived for the calculation of the load bearing capacity of a centrally loaded reinforced concrete column with or without the impact of a fire exposure.

This formula further represents an improvement related to the commonly used design formulas for structures without a fire exposure.

Finally a survey is given of the calculation of the load-bearing capacity through a fully developed fire course.

In Appendix B drawings are shown of the distribution of temperature and strength through cross-sections of various thicknesses and exposed to various fire courses.

In Appendix C examples are shown of the development of the load-bearing capacity and the deflections

of fire exposed concrete columns and beams.

The data are presented in standardised schedules in order to facilitate the comparison, and the structural elements and the main results are illustrated.

The calculated values are compared with test results on the same structural elements as reported in the literature.

In general it appears that the calculational procedures are on the safe side and quite close to the data observed.

σ	stress
σ_o	concrete stress at minimum compressed edge
σ_c	concrete stress at maximum compressed edge
σ_p	prestress of steel
σ_s	stress of steel

Indices:

B	bottom of a slab
c	concrete
cc	concrete compression
cr	critical
ct	concrete tension
cu	concrete ultimate
fict.	fictive
i	index number
M	middle
N	normal force
P	prestressing
s	steel
su	steel ultimate
sy	steel yield
T	top of a slab
th	thermal
tr	transient
u	ultimate
w	web
20	at 20 C
0.2	0.2 pct. proof (stress)

INTRODUCTION

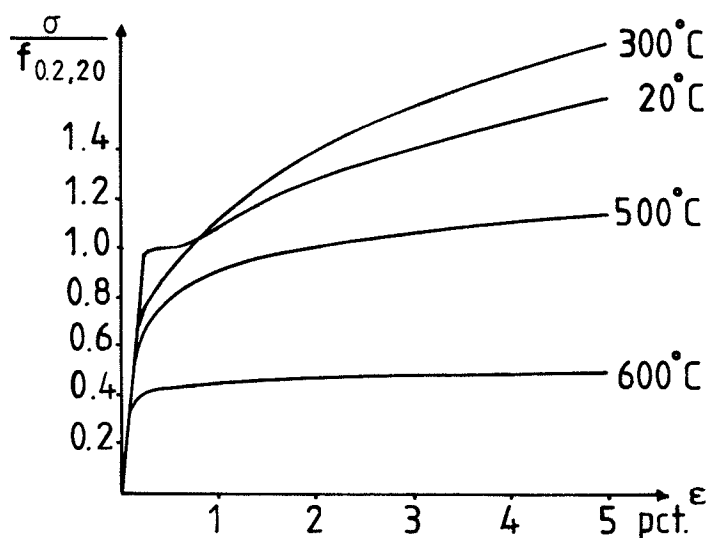
The changes of the material properties of fire exposed concrete are discussed in details in the ph.D. thesis Hertz [14], and in this context only a short description is made of the chemical and physical processes involved.

After the Ph.D. work the behaviour of fire exposed concrete structures were studied, and in the report Hertz [15] a first draft was made of methods for calculating the loadbearing capacities of fire exposed concrete structures by means of a stress distribution factor.

The chapter on this matter for beams in this text is based on the report; but it is extended and totally rewritten.

The remainder of this text is based on completely new research, and thus it substitutes the report [15].

First of all the text presents new methods for the calculation of the load-bearing capacities of fire exposed reinforced concrete columns and of the deflections of fire exposed concrete beams with slack or prestressed reinforcement.



Stress-strain curves for a mild steel (St 37, $f_{0.2,20} = 253$ MPa, $d\epsilon/dt = 0.2$ pct./min.) Skinner [26].

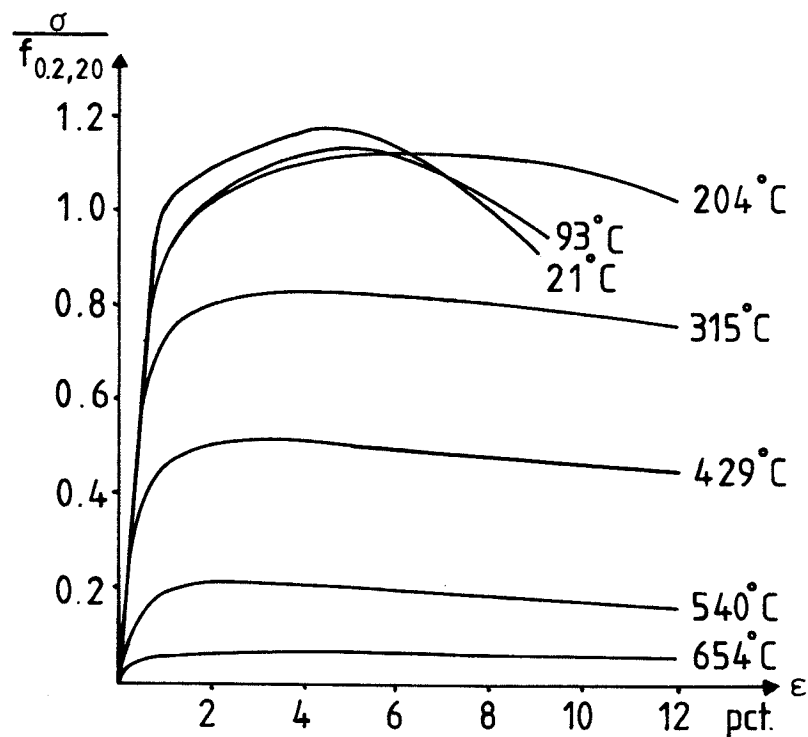
IDEALIZED MECHANICAL PROPERTIES OF REINFORCING STEELS

As regards the stress-strain curves of mild steel and hot rolled bars at normal and elevated temperatures the yield point disappears and the elastic linear part appears to become slightly more curved when the temperature increases.

The value of the strain, at which the steel becomes more plastic, seems to be almost a constant for all temperature levels.

As regards the corresponding stress-strain curves of cold-worked and prestressing steels the same observations can be made, although the yield point does not exist at any temperature.

For mild steel and hot rolled bars the yield stress and the 0.2 pct. proof stress appears to decrease by



Stress-strain curves for a prestressing steel
 (ASTM A 421, $f_{0.2,20} = 1470$ MPa, $d\epsilon/dt = 2$ pct./min.)
 Harmathy and Stanzak [13].

the same percentual reductions for increasing temperature levels, and the original strengths are regained, when the steels are cooled.

For cold-worked prestressing steels the 0.2 pct. proof stresses are percentually reduced much more than for hot rolled bars, and the original strengths are not regained at cooling.

The permanent loss of strength at heating is due to a reduction of the effects of cold-working.

For all three categories of reinforcing steels the idealized elasto-plastic stress-strain curves are almost changed by a linear affinity in the strain axis when heated.

Therefore, in the context of analysing fire exposed reinforced concrete structures it is suggested considering the stress-strain curves of heated reinforcing steels as linear affinities in the strain axis of their stress-strain curves at 20°C.

The coefficient of affinity is the ratio between the yield stress or the 0.2 pct. proof stress of the heated steel and of the steel at 20°C, which ratio is denoted

$$\xi_s = f_{0.2}/f_{0.2,20}$$

This means that stresses due to a certain strain of the steel are reduced by the factor ξ_s , when the steel is heated, and relaxation is not being considered.

The Danish code of practice for steel structures [7] defines the values of ξ_s by the formulas

$$\xi_s = \left(1 + \frac{T}{767 \ln\left(\frac{T}{1750}\right)} \right) \text{ for } 0 < T \leq 600^\circ\text{C}$$

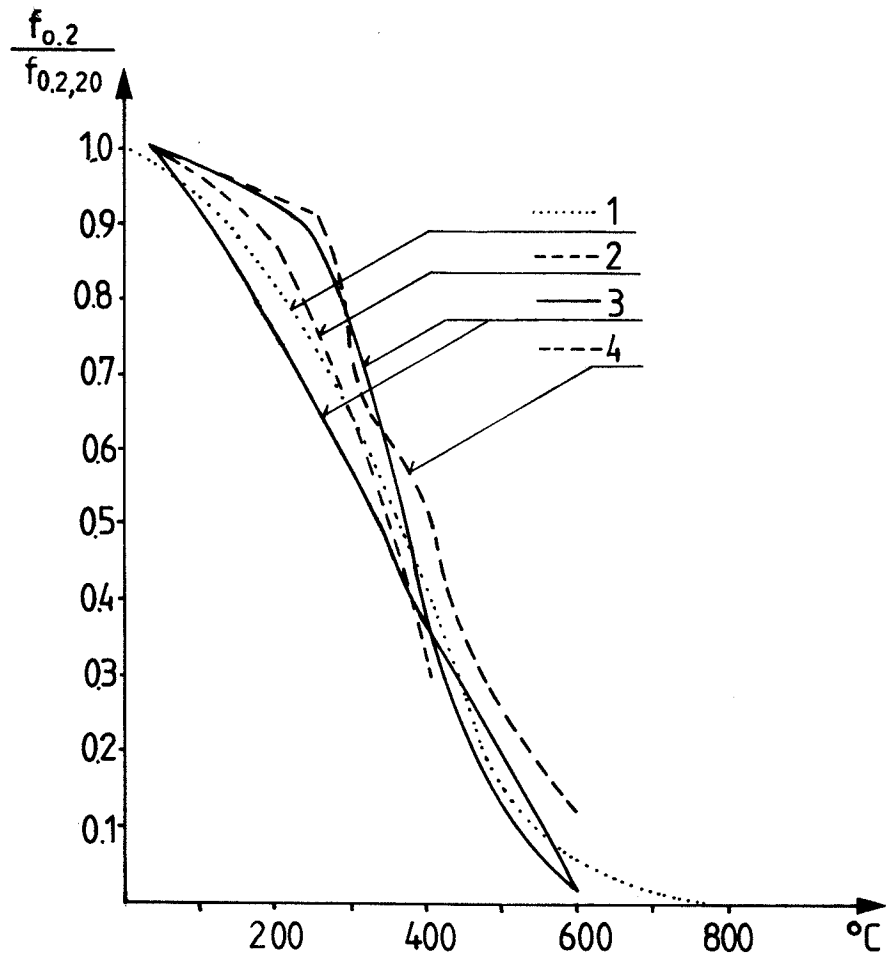
$$\xi_s = \frac{0.108(750 - T)}{T - 440} \quad \text{for } 600 < T \leq 1000^\circ\text{C}$$

This curve is found to fit very precisely to the strength reduction curves of hot rolled bars and reinforcing bars of St.37.

For prestressing steels of cold drawn wire which often have 0.2 pct. proof stresses of more than 1300 MPa, the values of ξ_s are smaller at all temperature levels.

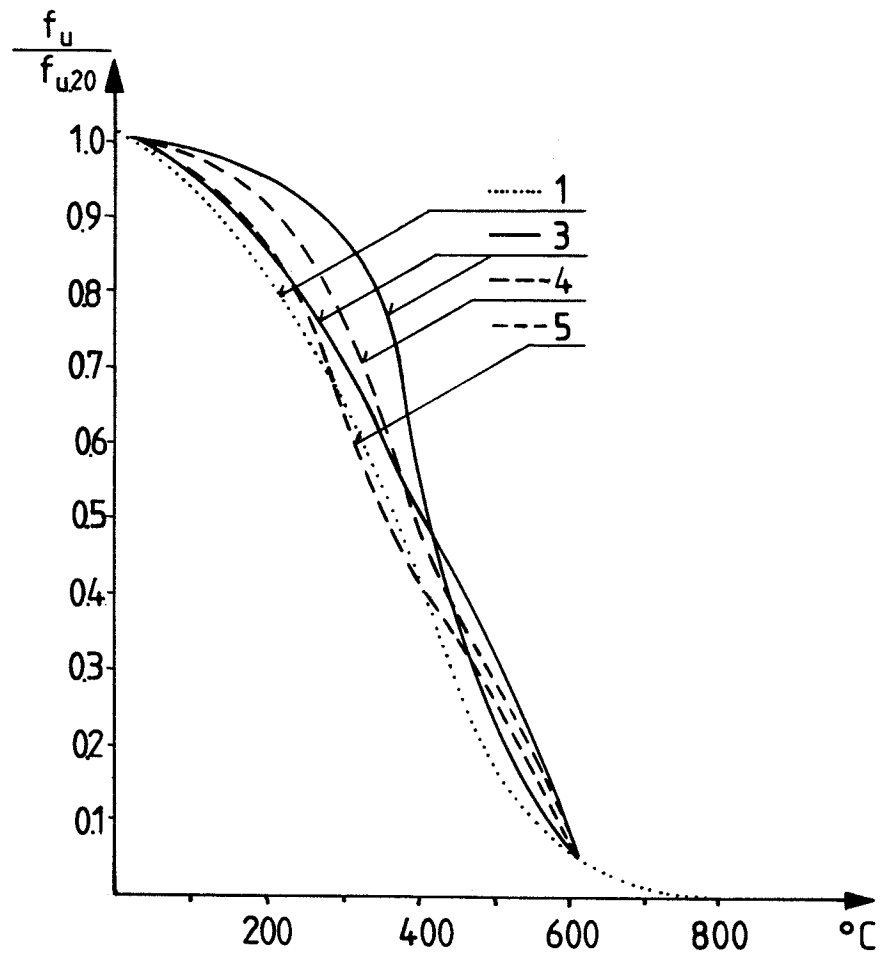
For these steels a good approximation for ξ_s at the temperature T is attained from the above expressions using a fictive temperature of

$$T_{\text{fict.}} = \frac{4}{3}T$$



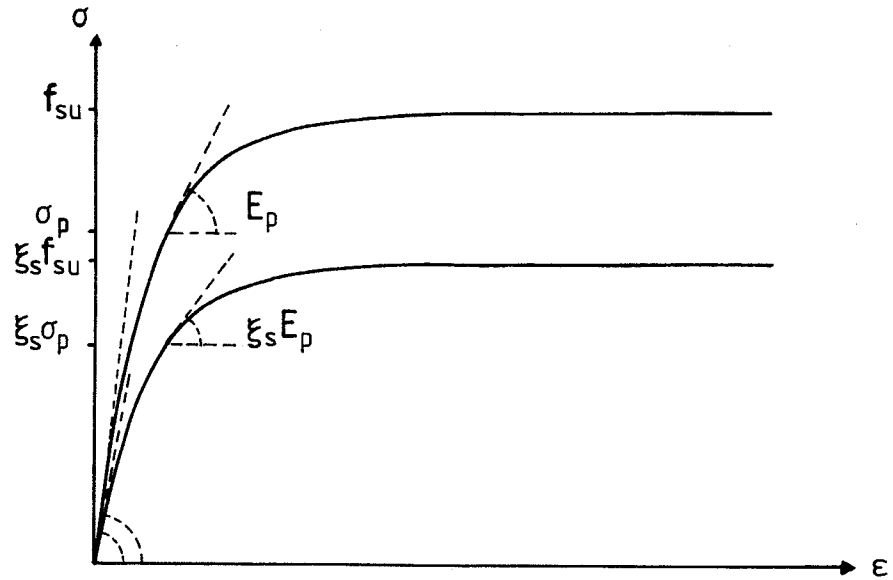
Reduction of 0.2 pct. proof strength
of cold drawn prestressing steels.

- 1) Idealized curve
- 2) Cahill [2]
- 3) Dannenberg [8]
- 4) Voves [28]



Reduction of ultimate stress
of cold drawn prestressing steels.

- 1) Idealized curve
- 3) Dannenberg [8]
- 4) Voves [28]
- 5) Anderberg [1]



Linear affinity of the stress-strain curve of a prestressing steel.

The E-modulus of a prestressing steel to be used for stress-strain calculations of a loaded prestressed cross-section is the tangent modulus E_p at the level of prestress σ_p .

Using the definitions given above, this tangent modulus is reduced by the factor ξ_s .

Likewise, the ultimate stress f_{su} as well as the ultimate stress increment $f_{su} - \sigma_p$ are both reduced by the factor ξ_s .

IDEALIZED MECHANICAL PROPERTIES OF CONCRETE

The physical and chemical processes causing a decrepitation of fire exposed concrete are described in detail in the Ph.D. thesis Hertz [14].

In the thesis more than 160 curves from the literature are redrawn in standardized coordinate systems showing test results concerning the influence of high temperatures on the mechanical properties of concrete in a hot condition as well as the corresponding residual properties after the cooling phase.

These data are utilized in this context deriving conservative idealizations for the mechanical properties as functions of the temperature.

A brief description of the decrepitation of concrete exposed to heating and subsequent cooling can be made as follows:

When the concrete is heated the free water evaporates, and above approximately 150°C the water chemically bound in the hydrated calcium silicates begins releasing.

In some cases the surface layer of a concrete specimen is not able to resist the pressure of the water and steam, and a spalling occurs.

If the concrete is dense, the moisture content is high or the heating rate is fast the spalling can become a steam exploding comprising large parts of the specimen, Hertz [16].

In case the concrete does not spall the release of water causes a shrinkage of the hydrated cement paste, while the aggregate and the reinforcing bars are subjected to a thermal expansion.

Consequently, stresses will develop in the composite material, and from approximately 300°C microcracks will pierce through the matrix.

The microcracks will cause a reduction of the compressive strength, the tensile strength and the modulus of elasticity, and an unloaded specimen will be subject to an irreversible expansion.

Above approximately 400°C the crystals of calcium hydroxide will begin decomposing into calcium oxide and water - a process reaching its highest intensity at about 535°C.

This weakens the concrete, but during the cooling phase and within the first week after the heat exposure, the calcium oxide absorbs water from the ambient air, giving rise to an expansion which opens the cracks already formed.

Thus, the reduction of strength of the heated concrete is dependent on the temperature level, the load, the aggregate used and the amount of calcium hydroxide crystals in the matrix, and the strength parameters are typically reduced by 20 pct. during the cooling phase from a hot condition to the time of minimum of strength, which is mostly about one week after the time of fire exposure.

Pozzolanas are able to react chemically with the calcium hydroxide of the Portland cement, and in case the pozzolana used has a sufficient content of aluminium oxide, the resulting crystals may become heat resistant.

Using proper pozzolanas and aggregates of a modest heat expansion a fire resistant concrete can be made from Portland cement.

The technique has been used for decades in the Soviet Union, where the aggregate used is chamotte and the pozzolana is pulverised chamotte (Nekrassov and Tarasova [29]).

At the authors laboratory a fire resistant concrete has been developed using Danish mo-clay powder as pozzolana and burnt mo-caly as aggregate (Muff [22]).

It was shown that it is possible to improve the heat resistance of concrete based on Portland cement up to at least a temperature level of 1150°C .

At 573°C the quartz crystals change from the twisted structure of "low quartz" to the symmetrical structure of "high quartz" causing a volume expansion of about 1 pct.

Above approximately 650°C carbon dioxide is released from limestone aggregates, and the insulation properties of the concrete may be improved, but during the cooling phase the hydratisation of the remaining calcium oxide will increase the formation of cracks.

At the temperature level about 710°C the rate of decomposition of the remaining calcium silicates becomes a maximum.

Above 900°C the volumes of the quartz aggregates become unstable. Above 1150°C aggregates containing felspar, among which aggregates made of burnt caly, will melt.

The close relationship between the properties of the aggregate and the properties of the concrete show that the natural found composition of the aggregate may very well cause improvements of the mechanical

properties of an ordinary concrete as compared to another based on a less suitable aggregate, when both are heated to the same temperature level.

These facts and the ability of deliberate making a composition of a fire resistant concrete of Portland cement lead to the conclusion that *calculational procedures for analysing fire exposed concrete structures should be able to take into account different relationships of the mechanical properties of the concrete and the temperature.*

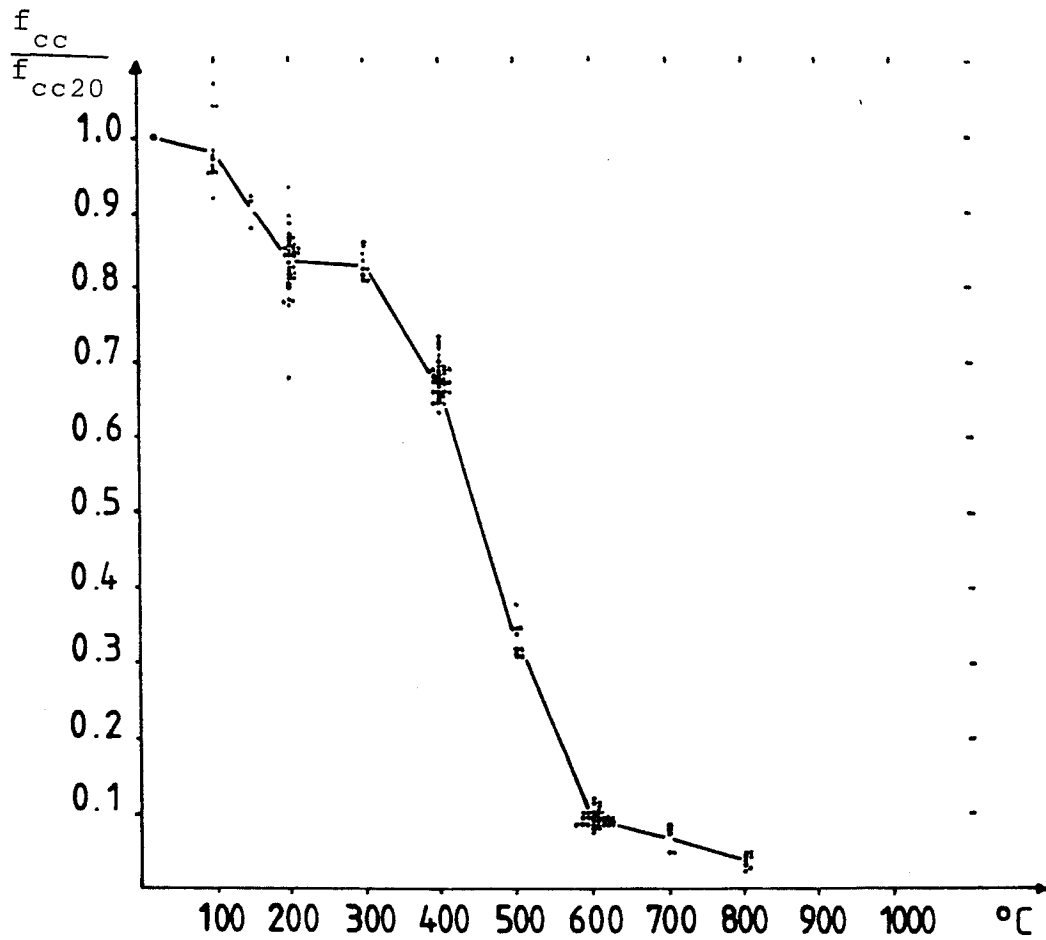
Furthermore, since the percentual reduction of the compressive strength of a heat exposed concrete within a wide range is not dependent on the water-cement ratio and thus is not dependent on the original compressive strength (Hertz [14]), it would be advantageous, if the original compressive strength was an independent parameter in the calculational procedures.

These requirements are fulfilled by the procedures presented in this context.

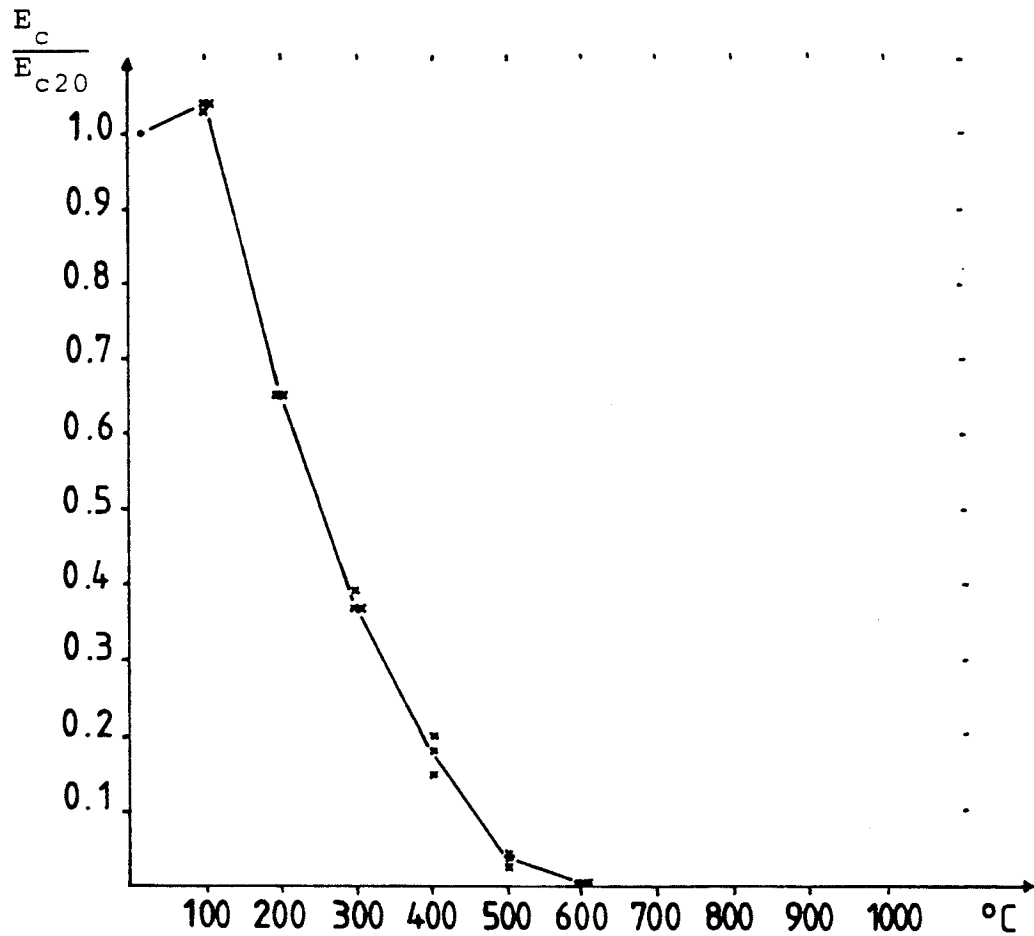
In case the reduction of the compressive strength is not known as a function of the temperature for the actual concrete, it must be estimated by a conservative assessment.

The author has tested a series of 230 cylindrical concrete specimens of diameter 150 mm and height 300 mm with an aggregate of Danish sea gravel.

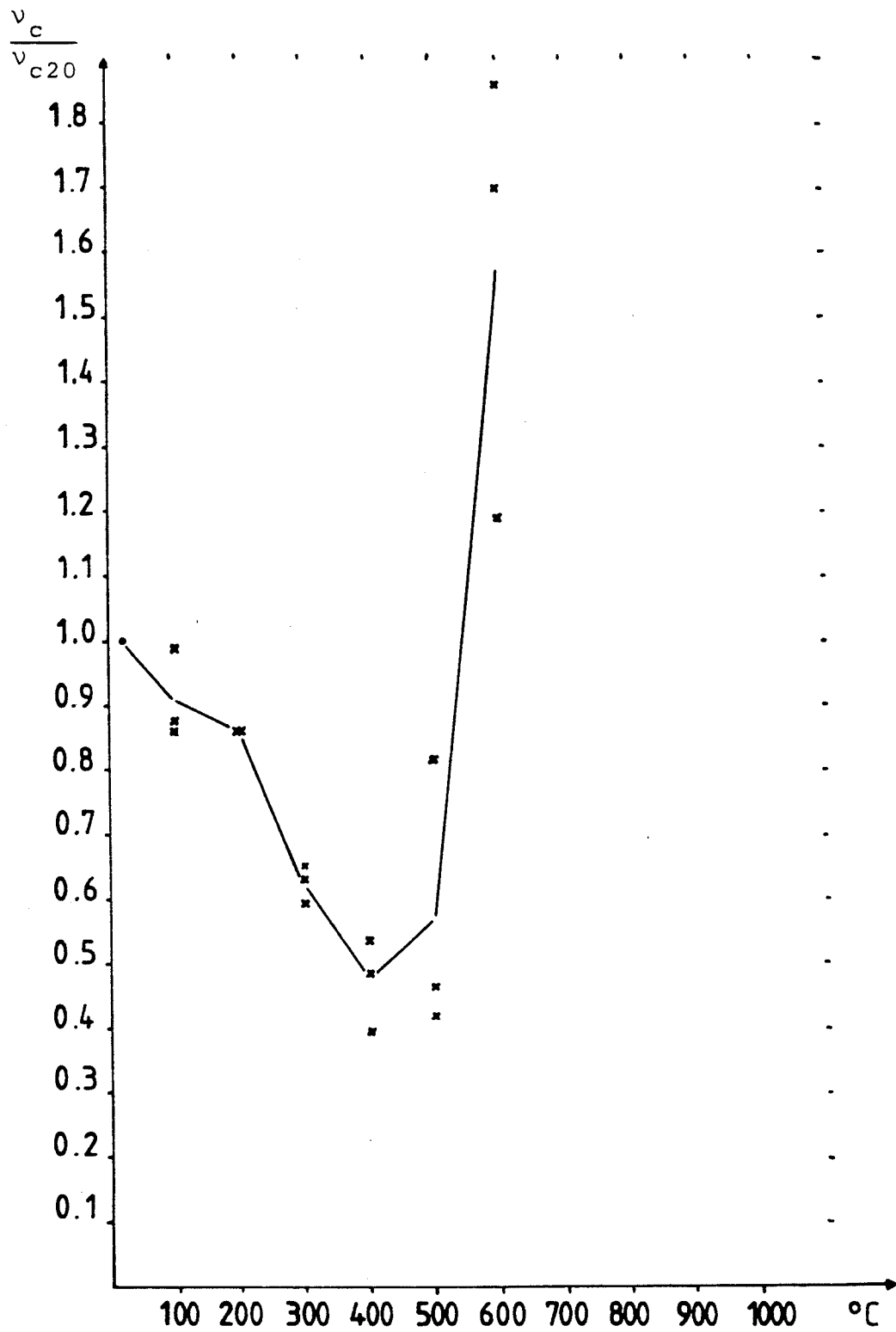
From Hertz [14] it is seen that the percentual residual strengths of such a concrete and of most concretes based on quartz aggregates heated to various maximum temperatures form the lower bounds of the temperature-strength curves of most concretes.



Residual ultimate stress of concrete with Danish sea gravel, $w/c = 0.87$, $f_{cc20} = 19.5$ MPa. Hertz [14].



Residual modulus of elasticity of concrete with Danish sea gravel, $w/c = 0.87$, $E_{c20} = 27.9$ GPa. Hertz [14].



Residual Poisson's ratio of concrete with
 Danish sea gravel, $w/c = 0.87$, $v_{c20} = 0.16$.
 Hertz [14].

An idealization of this curve therefore represents a conservative estimation of the real curve for most structural concretes.

The ratio between the reduced compressive strength of the concrete damaged by heat, f_{cc} , and of the unheated concrete, f_{cc20} , is called ξ_c :

$$\xi_c = f_{cc} / f_{cc20}$$

The idealized curve mentioned above of ξ_c versus the temperature T could be straight lines between the points

$$(T, \xi_c) = (20, 1.0)$$

$$(T, \xi_c) = (300, 0.8)$$

$$(T, \xi_c) = (650, 0.0)$$

for the residual strength after cooling (labelled "COLD") and

$$(T, \xi_c) = (20, 1.0)$$

$$(T, \xi_c) = (200, 1.0)$$

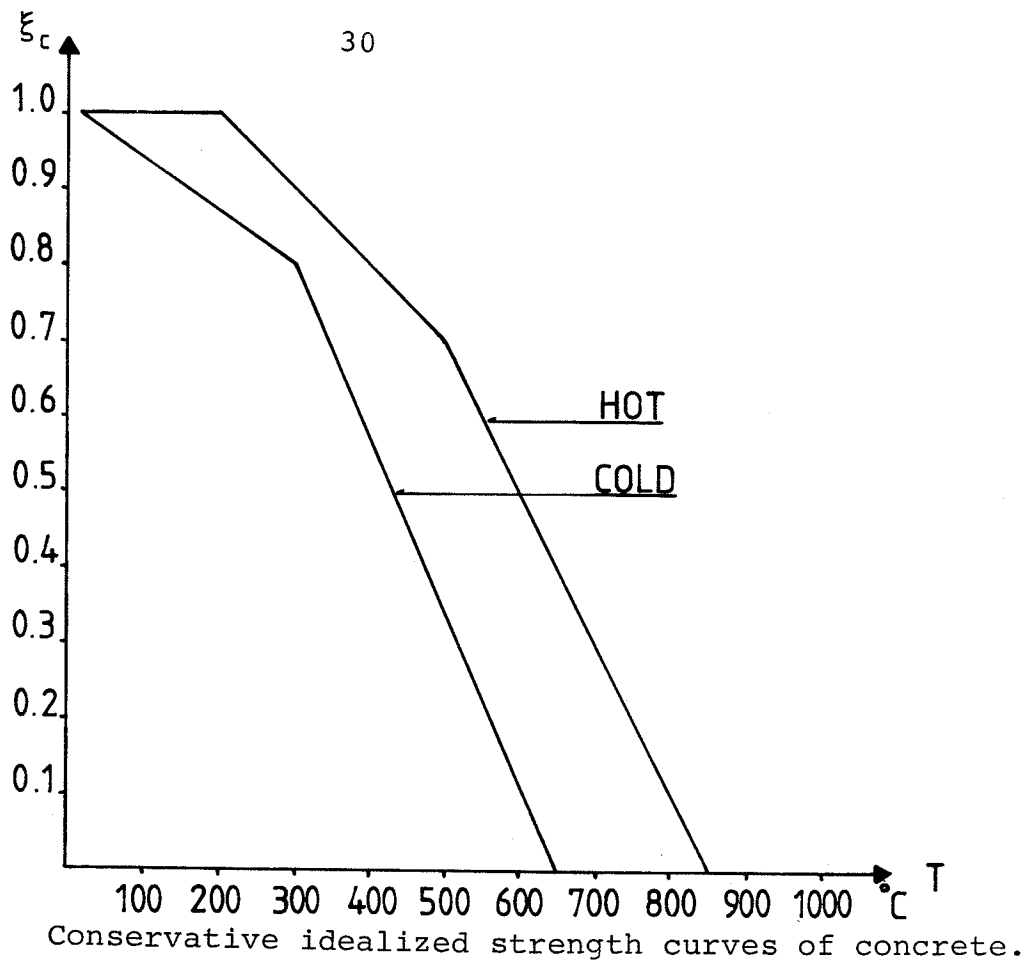
$$(T, \xi_c) = (500, 0.7)$$

$$(T, \xi_c) = (850, 0.0)$$

for the strength at the maximum temperature (labelled "HOT").

These curves are valid for a description of the reduction of strength of slowly heated concrete, which is predominant in large cross-sections exposed to ordinary fire courses.

However, by means of microwave power heating the author has shown that the curve for residual compressive strength becomes much more straight, if the concrete is heated rapidly, i.e. by 10^0C per minute.



Therefore, for cross-sections of thicknesses less than 250 mm exposed to fires with opening factors of the compartment of $0.04 \text{ m}^{\frac{1}{2}}$ or more, the residual strength curve (COLD) could be given by the points

$$(T, \xi_c) = (20, 1.00)$$

$$(T, \xi_c) = (400, 0.55)$$

$$(T, \xi_c) = (650, 0.00)$$

as an idealization of the results in Hertz [18].

Comparing curves on the development of the modulus of elasticity to curves on the development of the compressive strength with temperature for the same concretes exposed to the same temperature-time courses and subjected to the same loading, it appears to be a universal truth, that the reduction of the modulus of elasticity is the square of the reduction of the com-

pressive strength. (See for example the curves in Hertz [14]).

$$E_{co} = \xi_c^2 E_{co20}$$

The relation appears to be valid for a large variety of concretes in a hot condition as well as after the cooling phase, and applicable for maximum temperatures above 200°C, where the effects of the initial moisture condition are negligible.

During the investigation previously mentioned on concrete based on Danish sea gravel, the author has noticed a considerable increase of the ultimate strain ϵ_{cu} with temperature (Hertz [14]).

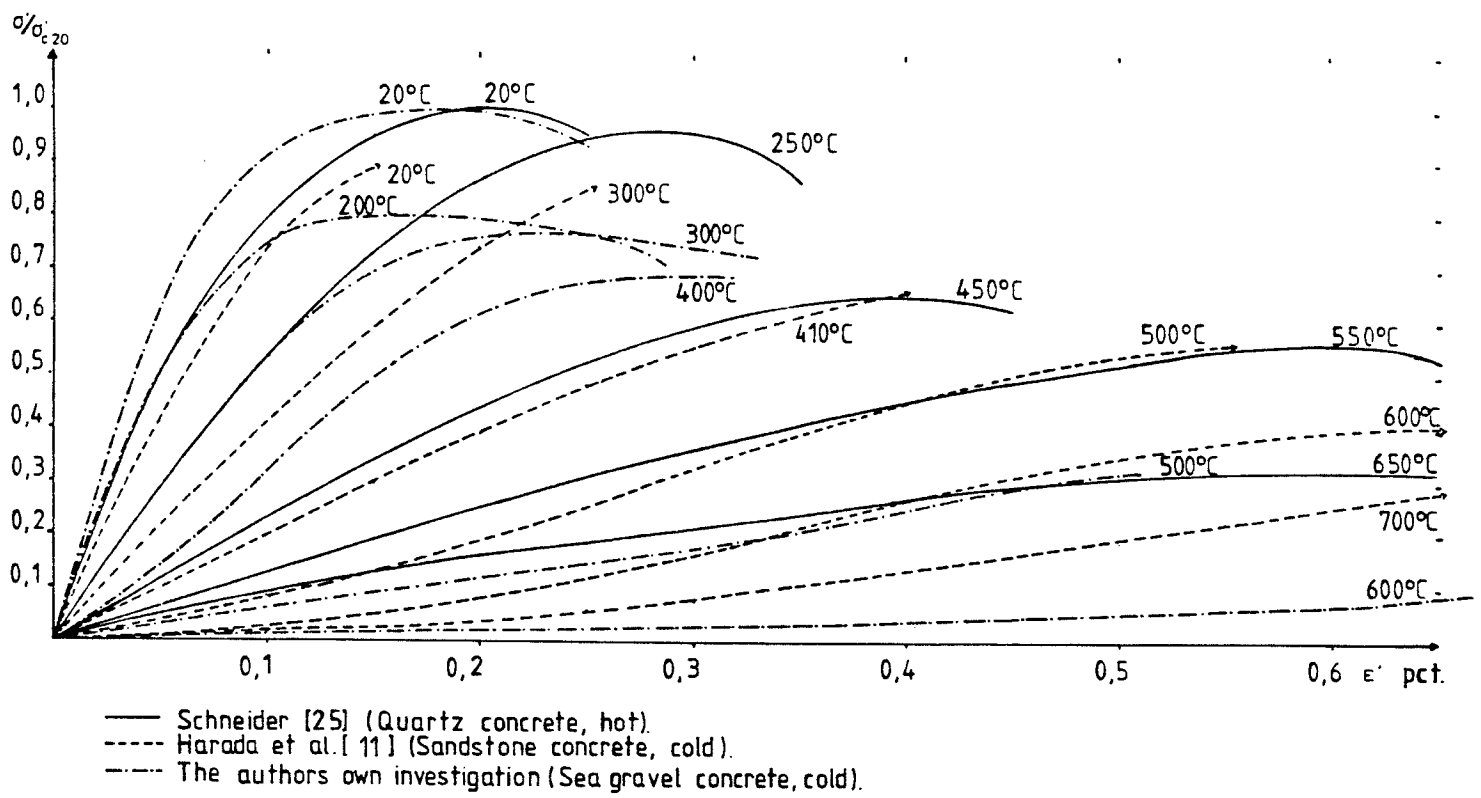
The same observation can be made from the stress-strain curves for various concretes with - or without application of load during heating and tested in a hot- or in a cold condition, as they are reported in the literature. (See for example Schneider [25], Harmathy and Berndt [12], Harada et al. [11] and Fischer [10]).

From the stress-strain curves it can also be seen that the increase in strain follows the decrease in stress, and the simple model is suggested that the product of stress and strain remains a constant for each point of the stress-strain curve while the material is weakened due to heat.

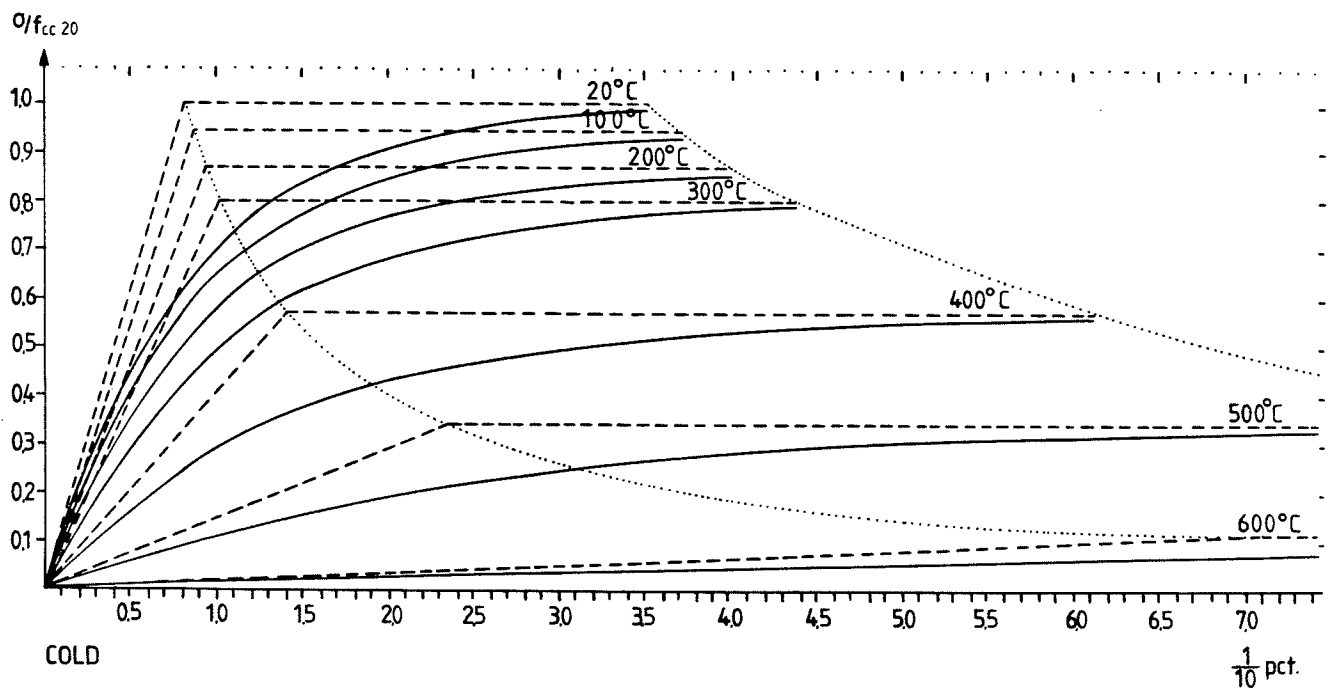
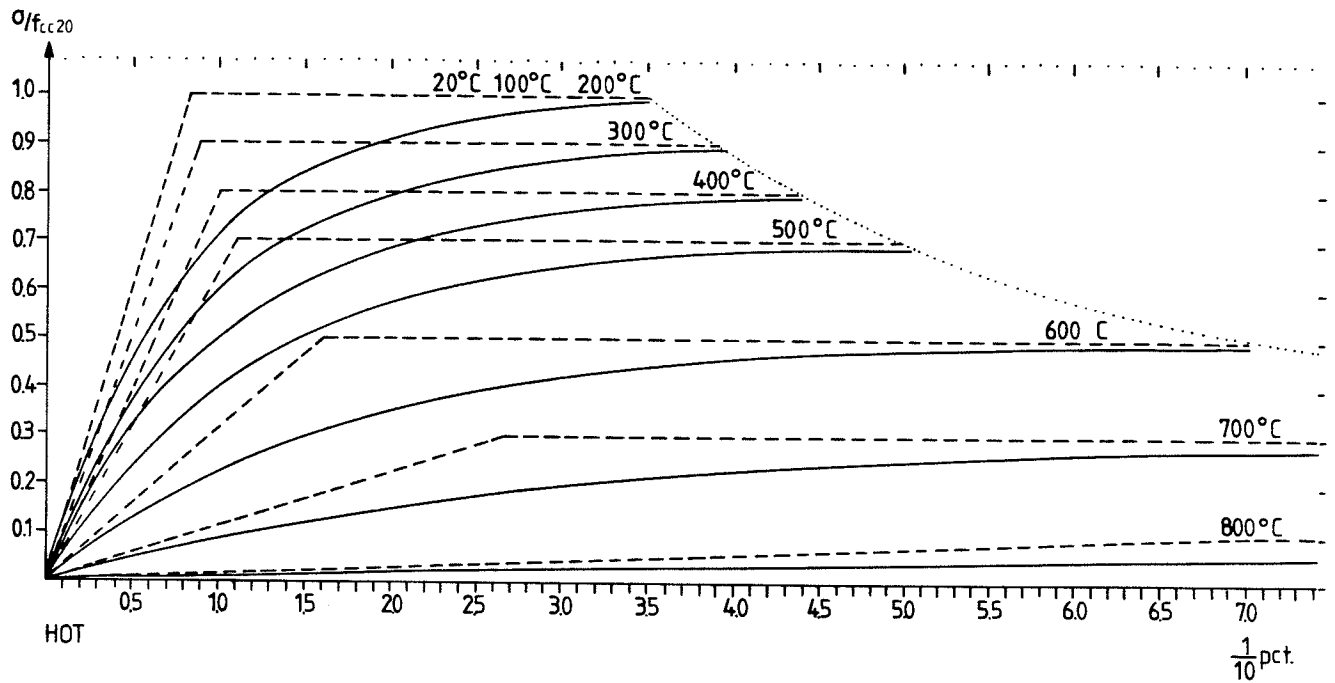
This means that

$$\sigma \epsilon = C_i$$

where C_i is a constant for each point of the stress-strain curve.



Stress-strain curves from various investigations.



Idealized stress-strain curves for concrete exposed to high temperatures in a hot condition and in a cold condition after the heat exposure.

Thus, the ultimate strain will be increased by the reciprocal reduction of the compressive strength

$$\epsilon_{cu} = \epsilon_{cu20} / \xi_c$$

which is in accordance with the test results.

For the idealized elasto-plastic stress-strain curve the point of change in gradient will be transformed from

$$(\epsilon, \sigma) = \left(\frac{f_{cc20}}{E_{co20}}, f_{cc20} \right) \text{ to } \left(\frac{1}{\xi_c} \frac{f_{cc20}}{E_{co20}}, \xi_c f_{cc20} \right)$$

and it is seen that the constant product of σ and ϵ with $f_{cc} = \xi_c f_{cc20}$ also leads to a fulfilment of the relation

$$E_{co} = \xi_c^2 E_{co20}$$

The lack of knowledge about these relationships has been a main obstacle so far to the development of simple and rationale methods for calculations of the stress-strain developments of fire exposed concrete structures.

Applying a certain variation of the single parameter ξ_c it is now possible to generate the heat induced changes of the full, idealized stress-strain curves whether the idealizations are elasto-plastic or curved lines are used.

IDEALIZED STRAIN PROPERTIES OF CONCRETE

The thermal expansion, the creep and the so called transient strain of concrete exposed to high temperatures have been analysed by a number of authors as described in Hertz [14], and a theoretical model for calculating the total strain has been developed by Anderberg and Thelandersson [2].

The total strain is assumed to be a sum of 4 contributions: the thermal strain ϵ_{th} , the instantaneous stress-related strain ϵ_{load} , the creep strain ϵ_{creep} and the so called transient strain ϵ_{tr} :

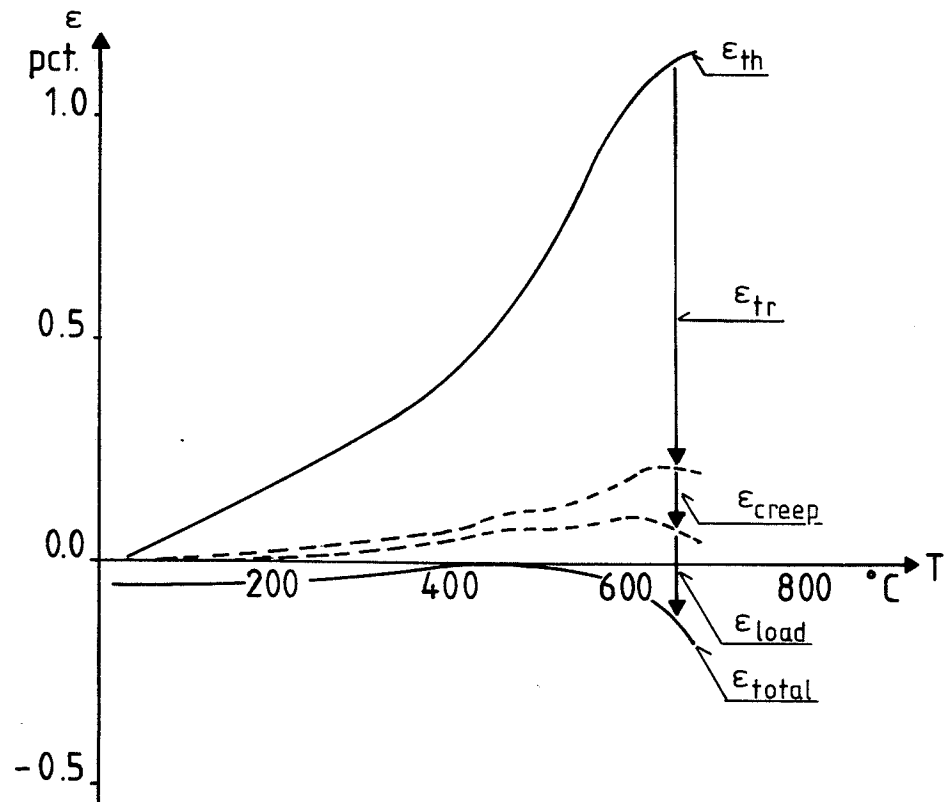
$$\epsilon = \epsilon_{th} + \epsilon_{load} + \epsilon_{creep} + \epsilon_{tr}$$

The thermal strain of the concrete depends mainly on the aggregate; yet at the temperature levels where the thermal strain may be dominant, i.e. up to 500°C, it would be a reasonable approximation to consider the thermal expansion of ordinary concrete based on quartz or limestone as linearly increasing with temperature by the coefficient $11 \times 10^{-6} \text{ } ^\circ\text{C}^{-1}$.

$$\epsilon_{th} = 11 \times 10^{-6} (T - 20^\circ\text{C}) \text{ } ^\circ\text{C}^{-1}.$$

In case an aggregate is used of less thermal expansion such as pumice or chamotte the coefficient is altered accordingly.

At temperature levels above 500°C the uncertainties of the other strain contributions become larger than the deviation of the thermal strain from the linear idealization, and the concrete becomes more plastic than concrete at temperature levels less than 500°C, these being usually present in the same cross-section.



Addition of strains according to
Anderberg and Thelandersson [2].

This means that beyond 500°C the deviation from the linear idealization increases, but the importance of a deviation decreases, and therefore it is suggested to use the simple linear idealization at all temperatures.

In order to facilitate the calculations it is also suggested to use the coefficient $11 \times 10^{-6} \text{ } ^\circ\text{C}^{-1}$ for the thermal expansion of reinforcing steel.

The instantaneous stress-related strain depends on the stress-strain curves for heated concrete, which are previously described.

The creep depends on the concrete, the load, the temperature and the time.

Anderberg and Thelandersson suggest the expression

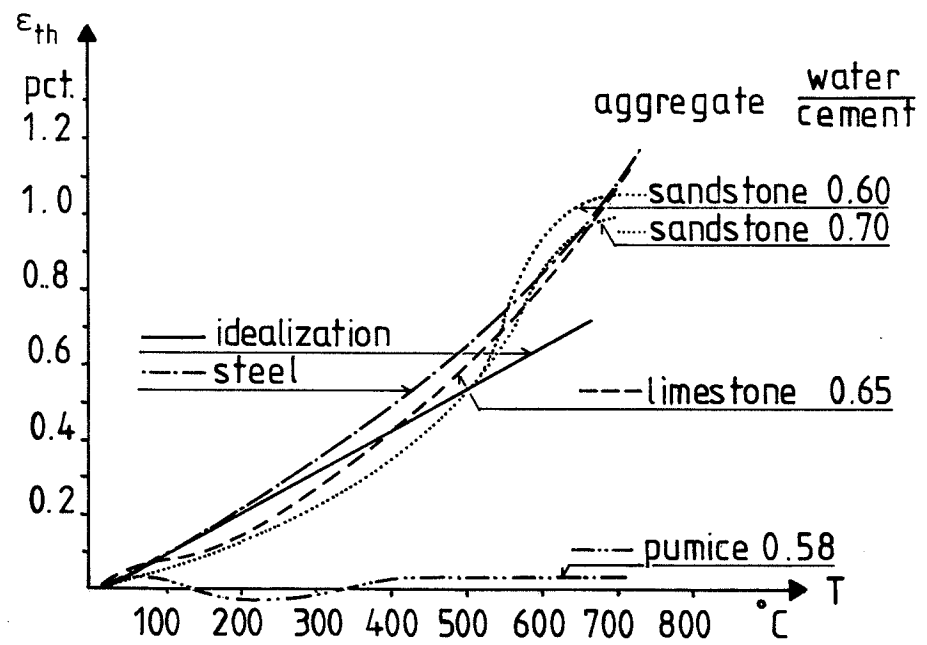
$$\epsilon_{\text{creep}} = - 530 \times 10^{-6} \frac{\sigma}{f_{cc}} \sqrt{\frac{\Delta t}{3h}} e^{3.04 \frac{(T-20^\circ\text{C})}{1000^\circ\text{C}}}$$

where σ/f_{cc} is the ratio between the actual compressive stress and the compressive strength of the concrete at the temperature T during the time Δt .

It is seen that even at a stress ratio of 1, the duration should be at least 10-20 h, if the creep strain should be comparable to the thermal strain at temperature levels below 500°C.

Creep strains therefore are important mostly for applications of concrete in industry and reactor technology, where sustained high temperatures may occur.

As regards concrete structures exposed to short-time heat-pulses from ordinary fire courses creep strains may be important for calculation of the time dependent



Thermal strain of concrete and steel from Harada et al. [11].

deflections after the fire exposure.

As regards concrete structures during the time of the fire exposures, creep strains are important mostly to structural members being close to collapse, and seldomly of importance to structural members, which are designed to resist the fully developed fire courses.

In Hertz [14] it is shown that the transient strain may be regarded as a hindered part of the thermal expansion for loaded concrete specimens exposed to heating.

The transient strain is found to be proportional to the ratio between the compressive stress and the compressive strength of the concrete at 20°C, and furthermore it is proportional to the thermal expansion.

$$\epsilon_{tr} = - 2.35 \frac{\sigma}{f_{cc20}} \epsilon_{th}$$

(Anderberg and Thelandersson [2]).

It is seen that the transient strain may become larger than the thermal strain in case the compressive stress is larger than approximately 45 pct. of the original compressive strength.

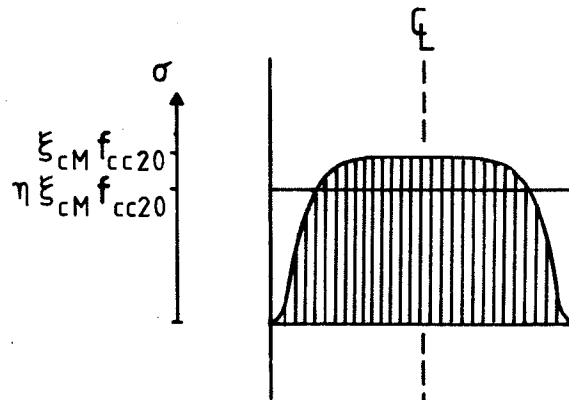
Yet it is possible to explain the phenomenon as a hindered part of the thermal expansion:

The thermal expansion is caused by the expansion of the aggregate, and by this expansion tensile stresses and cracks are developed in the surrounding hydrated cement paste.

As it is already mentioned, the hydrated cement paste of a heated concrete will decompose and shrink.

Therefore, the thermal strain of a heated concrete should be regarded as a thermal expansion due to the aggregate minus a shrinkage due to the matrix.

In case the concrete is loaded by compressive stresses, the aggregate is pretensioned, and the development of tensile stresses and cracks is hindered partly or fully in the matrix.



Definition of the stress distribution factor.

($C = 0.40 \text{ m}$, $a = 348 \times 10^{-9} \text{ m}^2/\text{s}$, $A\sqrt{h}/A_t = 0.04 \text{ m}^{-1/2}$, $q = 400 \text{ MJ/m}^2$, COLD condition).

STRESS DISTRIBUTION

One of the main hindrances for developing calculational procedures for determination of the load-bearing capacities and other mechanical properties of concrete structures has been the fact that the maximum temperature and the material properties vary considerably throughout a fire exposed cross-section.

The problems can be handled by application of finite element analyses using an appropriate computer and time for generating the in-data.

However, many of these calculations can be executed much more easily by introducing a new basic concept: the stress distribution factor.

Consider a cross-section exposed to fire at two parallel surfaces.

The isotherms will all be parallel to the surfaces at any time of the fire exposure, and the reduction of the compressive strength of the concrete ξ_c then is a function of the depth from the surface.

The maximum temperature occurring at the centre of the cross-section until the actual time is denoted T_M , and the corresponding reduction of the compressive strength of the concrete is ξ_{cM} .

The average compressive strength of the concrete in a cross-section of the thickness C is expressed as

$$\bar{f}_{cc} = \eta \xi_{cM} f_{cc20}$$

where f_{cc20} is the compressive strength at 20°C , and η is a factor called the STRESS DISTRIBUTION FACTOR.

This factor represents a very usefull concept by means of which the stress-strain conditions of a loaded and fire exposed concrete section can be calculated as a whole and almost just as easy as by the calculation of the section without fire exposure.

Considering that the alternative procedure is to split up the cross-section into a number of finite elements of the same maximum temperature and to solve the problems for the entire system of elements, the simple procedures using stress distribution factors are less laborious and just as precise as the finite element analysis.

In addition, the procedures based on stress distribution factors are identical to the procedures used for cross-sections without fire exposure in the case, when fire exposure is reduced to nil.

The stress distribution factor is determined by

$$\eta = \frac{1}{C\xi_{cM}} \int_0^C \xi_c (T(z)) dz$$

and is the ratio of the average compressive strength of the cross-section to the compressive strength at the centre of the cross-section, which is

$$f_{ccM} = \xi_{cM} f_{cc20}$$

Furthermore is utilized that if the compressive strength at any point of the cross-section is reduced by the factor ξ_c to

$$f_{cc} = \xi_c f_{cc20} ,$$

the initial modulus of elasticity of the concrete at the same point is

$$E_{co} = \xi_c^2 E_{co20}$$

and the ultimate strain is

$$\epsilon_{cu} = \epsilon_{cu20} / \xi_c$$

where ϵ_{cu20} is often considered to be 0.35 pct.

From the elasto-plastic stress-strain relations it is seen that the ultimate stress is reached at the strain ϵ_{cu20} for most of the temperature levels.

It is therefore a reasonable approximation to assume the cross-section being able to act at its ultimate stresses at every point, when compressed to a uniform strain of ϵ_{cu20} in a plastic analysis.

If ξ_{cM} is less than unity the approximation is even more valid when the entire cross-section is compressed to $\epsilon_{cuM} = \epsilon_{cu20} / \xi_{cM} > \epsilon_{cu20}$.

This means that the cross-section can be loaded to an ultimate resistance equal to the average compressive strength multiplied by the thickness of the section, before the ultimate strain is reached at the centre-line.

For applications, where the strain may vary along the centre-line, but has a constant value across the section, the material could be considered to be uniformly damaged through the section.

The stress-strain curve of the material is assessed to be the one of an impaired concrete with a compressive strength equal to the mean value through the cross-section, but with an ultimate strain not exceeding ϵ_{cuM} .

The ultimate resistance per unit length of the cross-section thus is

$$\eta \xi_{cM} f_{cc20} C$$

and the initial stiffness per unit length is

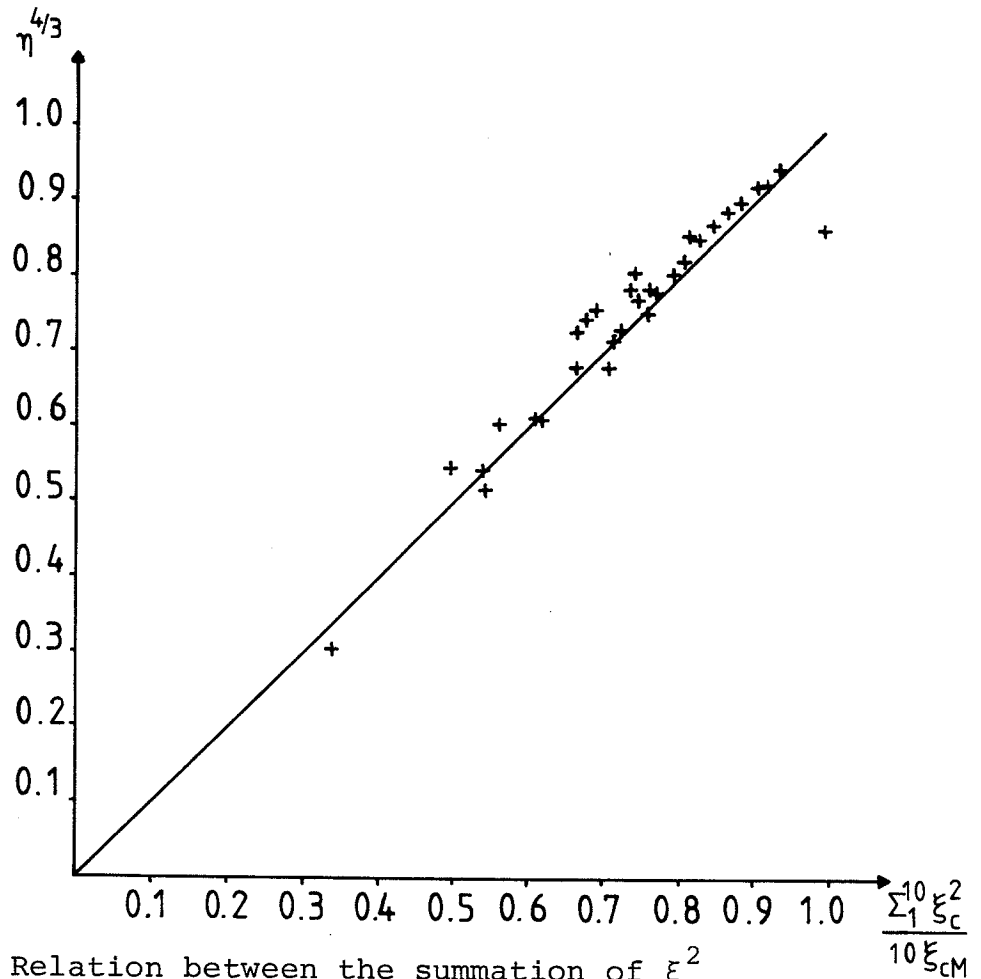
$$\int_0^C \xi_c^2 dz E_{co20}$$

In case the cross-section is assumed to consist of an uniform "average" concrete, the initial stiffness per unit length may also be

$$(\eta \xi_{cM})^2 E_{co20}$$

The factor $(\eta \xi_{cM})^2$ is smaller than the integral, and thus it would be a safe approximation to be used for calculations of instability and deflections of structural members.

However, calculations of the integral for a large

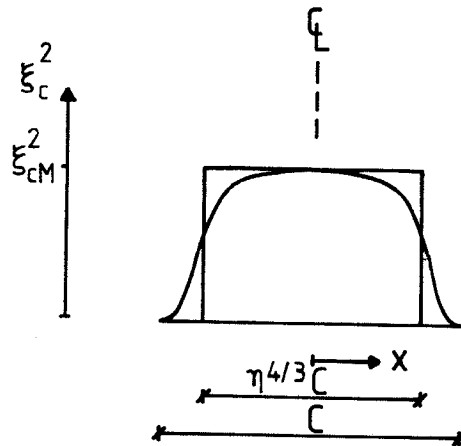


number of different fire exposures and thicknesses of the concrete cross-section show that a better approximation would be

$$\int_0^C \xi_c^2 dz \approx \eta^{\frac{4}{3}} \xi_{cM}^2 C.$$

The average deviation was less than 5 pct., and no single deviation was above 10 pct.

The distributions of the maximum temperatures and of the corresponding reductions of strength are shown in Appendix B for a hot condition, where the temperature is a maximum at 30 mm from the surface, and in the cold condition after the fire exposure for a number of fully developed fires and cross-section thicknesses.



Comparison between the model using a reduced cross-section and the actual distribution of stiffness for a typical fire development.

($C = 0.40$ m, $a = 348 \times 10^{-9} \text{ m}^2/\text{s}$, $A\sqrt{h}/A_t = 0.04 \text{ m}^{-1/2}$, $q = 400 \text{ MJ/m}^2$, COLD condition).

Thus, the initial stiffness per unit length is

$$\eta^{\frac{4}{3}} \xi_{cM}^2 E_{co20} C.$$

In case the elastic parts of the elasto-plastic stress-strain relations are used, or a more detailed analysis is made based on a stress-strain curve, the cross-section could be considered to have a fictive thickness of

$$\eta^{\frac{4}{3}} C$$

and to consist of concrete with the mechanical properties of the concrete at the centre-line, i.e.

$$f_{cc} = \xi_{cM} f_{cc20}, \quad E_{co} = \xi_{cM}^2 E_{co20}, \quad \varepsilon_{cu} = \varepsilon_{cu20} / \xi_{cM}$$

This means that the cross-section is considered to be reduced by the thickness

$$\frac{C}{2} (1 - \eta^{\frac{4}{3}})$$

from each side.

value of the moment of inertia times the E_{co} -modulus before the fire exposure.

The model using a reduced cross-section of thickness $\eta^{4/3}C$ therefore is valuable to the calculation of the load bearing capacity of a fire exposed wall or column as well as for the elastic- or curved-line analysis of a cross-section.

However, in case a plastic analysis is carried out, all parts of the cross-section will be able to act by their ultimate stresses, when they are compressed at a large uniform strain.

For this analysis the cross-section could be reduced to one of a thickness ηC having the uniform mechanical properties of the concrete at the centre-line

$$f_{cc} = \xi_{cM} f_{cc20} \quad \epsilon_{cu} = \epsilon_{cu20} / \xi_{cM}$$

In the early phases of the fire, development of large temperature gradients may occur near the surface of the cross-section.

In case the cross-section is not loaded, large thermal stresses may arise.

However, in case the cross-section is loaded the thermal strains and the transient strains should be added to the compression strain, which is assumed to be uniform through the cross-section.

If the cross-section is loaded by 30 pct. of the compression strength before the fire, a temperature difference of say 500°C between a surface layer and the core would give rise to a difference in strain of

$$\epsilon_{th} + \epsilon_{tr} = 1.1(1 - 2.35 \times 0.3) 500 / 10^3 = 0.16 \text{ pct.}$$

And the ultimate strain of the concrete in a hot condition at 500°C is increased by

$$\Delta \epsilon_{cu} = 0.35/0.7 - 0.35 = 0.15 \text{ pct.}$$

This means that in case the cross-section is loaded by 30 pct. or more of the original ultimate compression stress, the difference in thermal and transient strain between surface and core of a cross-section would approximately be within the increase of the ultimate compression strain of the hot surface layer.

Thus, a redistribution of the stresses will be possible without causing any damage to the cross-section, and in case the load is at the ultimate limit state of the heated cross-section, the stress distribution is not influenced by the thermal gradients, and the stress distribution factor η is not affected.

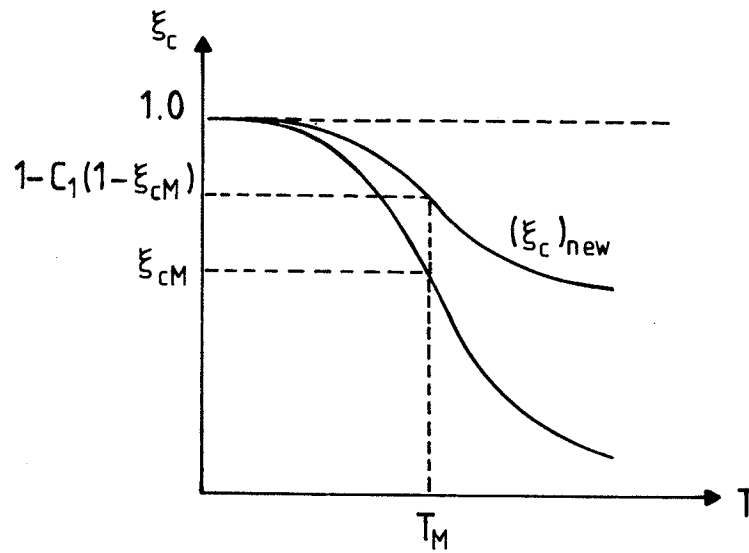
As it appears from the previous pages, the only two variables, which are necessary to know in order to describe the reduction of the mechanical properties of a fire exposed concrete section, are ξ_{CM} and η .

Their values can be calculated from the maximum temperatures, which have occurred in a number of points through the cross-section until the time considered.

Such values can also be drawn from the tables Hertz [21] for a large variety of cross-sections and fires.

These values are calculated for an unloaded concrete with Danish sea gravel aggregates, and will represent conservative estimations for most other concretes and loads.

If the reduction of the compressive strength ξ_c varies in temperature in a way, different from the one

Transformation of ξ_c .

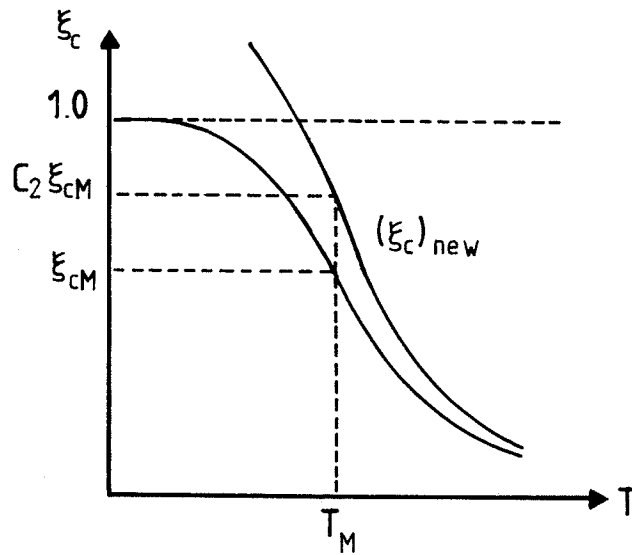
for which η and ξ_{cM} is calculated, a new calculation can always be made, but often new values can be estimated in an easy way by means of affinity considerations using the shapes of the curves of ξ_c as functions of the temperature.

Many of these curves will be almost identical by multiplication of the difference $1 - \xi_c$ by a constant C_1 , which can be done for $1 - \xi_{cM}$ and $1 - \eta$ as well.

$$(\xi_{cM})_{\text{new}} = 1 - C_1(1 - \xi_{cM}) \text{ and}$$

$$(\eta)_{\text{new}} = 1 - C_1(1 - \eta)$$

In some cases the reduction can differ for the small temperature levels, and remembering that ξ_{cM} is the largest value of ξ_c , and that only the parts of the curves are used representing temperatures larger than the temperature T_M in the middle of the cross-section, these parts may be identical by multipli-

Transformation of ξ_c .

cation of ξ_{cM} and η by a constant C_2 .

$$(\xi_{cM})_{\text{new}} = C_2 \xi_{cM} \text{ and}$$

$$(\eta)_{\text{new}} = C_2 \eta$$

where of course the value $C_2 \xi_{cM}$ must not exceed unity.

Finally the two transformations can be combined, so that

$$(\xi_{cM})_{\text{new}} = C_2 (1 - C_1 (1 - \xi_{cM})) \text{ and}$$

$$(\eta)_{\text{new}} = C_2 (1 - C_1 (1 - \eta))$$

or alternatively

$$(\xi_{cM})_{\text{new}} = 1 - C_1 (1 - C_2 \xi_{cM}) \text{ and}$$

$$(\eta)_{\text{new}} = 1 - C_1 (1 - C_2 \eta)$$

ULTIMATE LIMIT STATE ANALYSIS OF BEAMS IN BENDING

The ultimate limit state analysis has become a common tool for calculating the load bearing capacities of structures.

The simple calculations facilitates the design of the structural elements, and introducing yield hinges an acceptable approximation is often obtained for the determination of the distribution of moments and forces in hyperstatic structures.

Yet it is a precondition for genuine plastic considerations that the deformations necessary can take place to ensure the postulated distributions of forces and stresses.

However, the increased plasticity of the concrete exposed to high temperatures make the analyses even more allowable for fire exposed structures than for structures analysed for load cases without fire exposure.

In the ultimate limit state prestressed structures are generally treated like structures with slack reinforcement only, but the strain of the prestressing steel corresponding to the prestress must be taken into account calculating the strain of the reinforcement (Brøndum-Nielsen [4]).

Furthermore, the following assumptions will be made for the ultimate limit state analysis in this chapter:

Plane cross-sections are assumed to remain plane, which means that changes in strain are assumed proportional to the distance from the neutral axis.

The strain at the ultimate stress of the concrete is

$$\epsilon_{cu} = \frac{\epsilon_{cu20}}{\xi_{cm}} = \frac{0.35}{\xi_{cm}} \text{ pct.}$$

A rectangular stress block is assumed as an idealized distribution of the stresses in the compression zone of the concrete.

The depth of the stress block y is defined as

$$y = \frac{4}{5} x$$

where x is the depth of the neutral axis. (A closer discussion of the value $4/5$ is made in Appendix A).

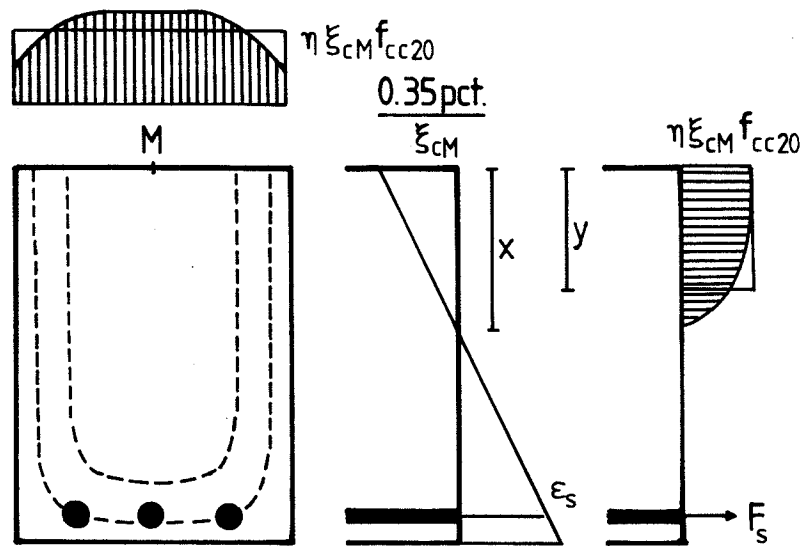
The tensile strength of the concrete is considered to be zero.

All these assumptions are even more allowable for fire exposed structures than for structures without a fire exposure.

Consider a cross-section of a beam with a compression zone of uniform width confined by a neutral axis, a compressed edge and two parallel surfaces.

At first the two parallel surfaces are considered to be fire exposed, and the compressed edge is considered to be insulated, which are the most common conditions for a rectangular cross-section subjected to a moment load.

Using these conditions the moment is defined as positive, and in the case the more compressed edge is exposed to fire the moment is defined as negative.



Beam subjected to bending.

The isotherms of the compression zone of the cross-section subjected to a positive moment are almost parallel to the two fire exposed surfaces, and the ultimate compressive force per unit length of the compression zone of width C is

$$C \eta \xi_{cM} f_{cc20}$$

according to the definition of the stress distribution factor η .

The compression zone could be considered to be of a constant width C and loaded by the average ultimate compression stress $\eta \xi_{cM} f_{cc20}$.

But just as well it could be considered to be of the reduced thickness ηC and loaded by the ultimate compression stress $\xi_{cM} f_{cc20}$.

Using this assumption the compressive strength is neglected in two surface layers of thickness

$$\frac{C}{2}(1 - \eta)$$

and the concrete in the core is considered to be of the same strength as the concrete at the centre line.

The temperature T is calculated for each reinforcing bar and the reduced strength $\xi_s(T)f_{s20}$ is determined whether f_s is defined as an yield stress, a 0.2 pct proof stress or an ultimate stress: the total ultimate force of the reinforcement is found by a summation of contributions of each bar.

$$F_{su} = \sum_i A_{si} \xi_{si} f_{s20i}$$

The force is considered to act in a depth d_s from the compressed edge of the cross-section, and the depth of the compression zone is calculated as

$$Y = \frac{F_{su}}{C \eta \xi_{cm} f_{cc20}}$$

The moment capacity is determined by

$$M_+ = F_{su} (d_s - \frac{Y}{2})$$

It is a precondition for the determination of F_{su} as the total ultimate force that a minimum strain ϵ_{smin} is reached in each reinforcing bar.

In case the steel has a well defined yield point the minimum strain would be

$$\epsilon_{smin} = \frac{\xi_s f_{s20}}{\xi_s E_{s20}} = \frac{f_{s20}}{E_{s20}}$$

i.e. ϵ_{smin} is not influenced by the temperature, be-

cause the idealized stress-strain curve of the steel is changed by a linear affinity in the strain axis.

The strain of the reinforcement is calculated as

$$\epsilon_s = \frac{d_s - \frac{5}{4}y}{\frac{5}{4}y} \frac{0.35}{\xi_{CM}} \text{ pct.}$$

and if ϵ_s is less than ϵ_{smin} the cross-section is over-reinforced.

This means that a new force of the reinforcement F must be determined in accordance with the strain distribution of the cross-section.

Usually over-reinforced cross-sections are not allowed in design, because the structure may collapse without warning by the formation of cracks in the tensile zone and the development of relatively large deflections.

The risk of emergence of over-reinforced cross-sections is often limited during the fire, as the reinforcing bars are hot and have small ultimate stresses.

But when the structure is cooled down, the ultimate stresses of the reinforcement will be regained partly or fully - depending on whether the steel is cold worked or not - while the compressive strength of the concrete is subject to a further decrease.

This may lead to over-reinforced cross-sections.

In case the structure has been designed for a standard fire exposure without a cooling phase (as for example proposed by FIP/CEB [9] and [6]), the small ultimate stresses of the hot reinforcement is often compen-

sated applying larger cross-sections of the bars.

In this case the risk of achieving a dangerous over-reinforced construction during the cooling phase of a real fire course is especially high.

The risk of achieving an over-reinforced construction is also high in case the cross-section is loaded by a negative moment.

The compression zone then is exposed to the fire at three surfaces, and the reinforcement is protected by a large part of the concrete cross-section.

In this case the strength reduction of the concrete is of a special importance for the load-bearing capacity of the cross-section.

However, the problem in estimating the ultimate moment capacity is more complex, because the isotherms of the compression zone are curved.

It will be a reasonable assumption for practical calculations that the variation in the reduction of the compressive strength of the concrete is the same, whether the original strength is reduced by heat conducted from the two parallel surfaces, or the average strength due to this variation is reduced by heat conducted from the third surface.

This assumption is in accordance with the definition of the stress distribution factor η as independent of the strength of the concrete at the centre line of the cross-section, $\xi_{cm}^f_{cc20}$.

Using the idealization that the isotherms are parallel to the two surfaces until the distance $C/2$ from the

$\eta \xi_{cM} f_{cc20}$ from a level at the distance

$$\frac{C}{2}(1 - \eta)$$

from the most compressed edge.

Using a concentrated stress block of the compressive strength at the centre line $\xi_{cM} f_{cc20}$, the simple procedure is established that the concrete strength is neglected in surface layers of the thickness

$$\frac{C}{2}(1 - \eta)$$

from all fire exposed surfaces.

The total ultimate force of the reinforcement is found by a summation of contributions of each bar with respect to the strength reductions due to their individual temperatures.

$$F_{su} = \sum_i A_{si} \xi_{si} f_{s20i}$$

The force is considered to act in the depth d'_s from the tensioned edge of the cross-section, the total depth of the cross-section is d , and the depth of the compression zone is calculated as

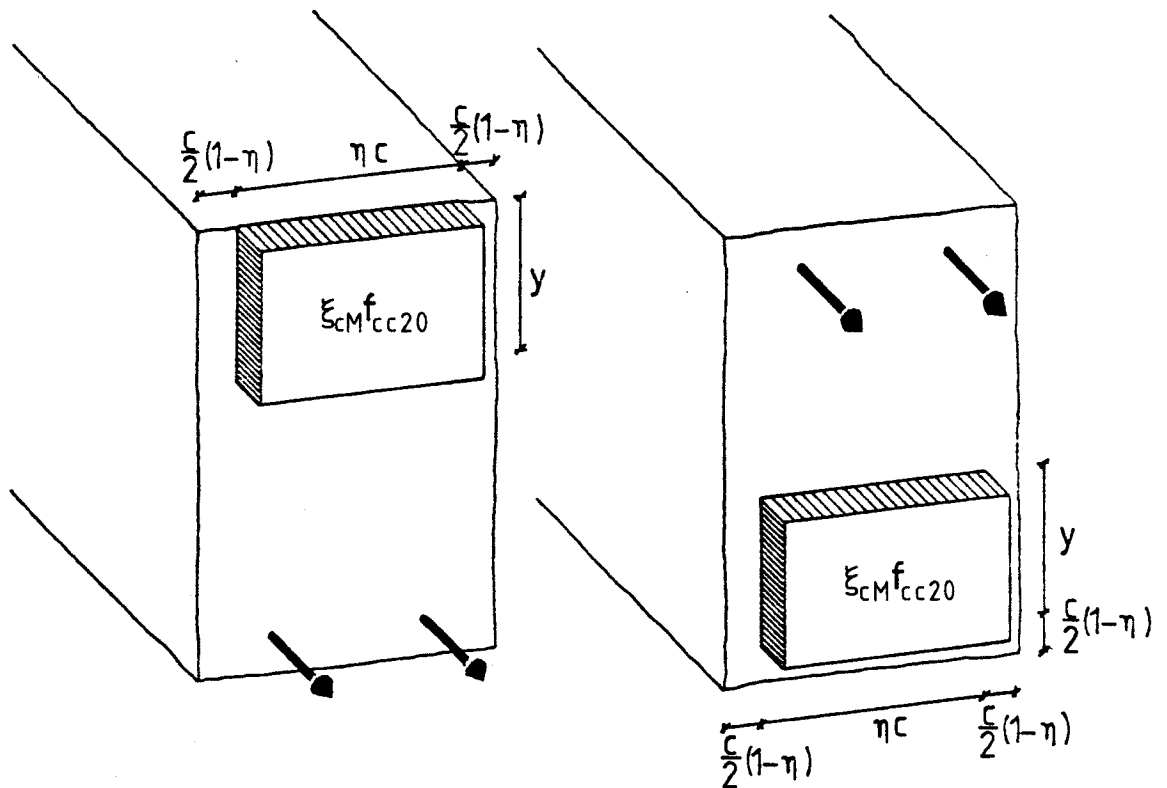
$$y = \frac{F_{su}}{\eta \xi_{cM} f_{cc20}}$$

Then, the negative moment capacity is

$$M_- = F_{su} \left(d - d'_s - \frac{C}{2}(1 - \eta) - \frac{y}{2} \right)$$

Using the model of a concentrated stress block a conservative estimate is obtained for the strain of the reinforcement

$$\epsilon_s = \frac{d - d'_s - \frac{C}{2}(1 - \eta) - \frac{5}{4}y}{\frac{5}{4}y} \frac{0.35}{\xi_{cM}} \text{ pct.}$$

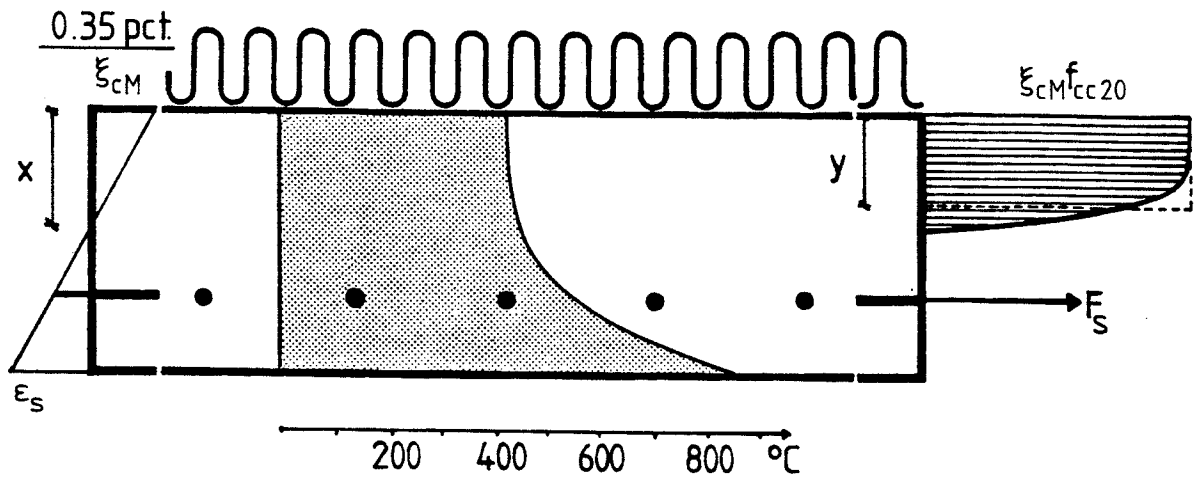


Positions of concentrated stress blocks.

which should be larger than ϵ_{smin} , if the cross-section should not be deemed to be over-reinforced.

It seems justified to use this rough and conservative estimation of ϵ_s , because the risk of achieving an over-reinforced cross-section is especially high in negative bending, and because the uncertainties of using more laborious procedures would be large anyway.

The reasons are not only uncertainties in estimating the thermal properties of the concrete, the temperature distribution of the cross-section and the precise stress-strain curve of the concrete, but also the fact, that spalling and thermal stresses at the convex corners causes a bevelling of the edges of most fire exposed concrete beams.



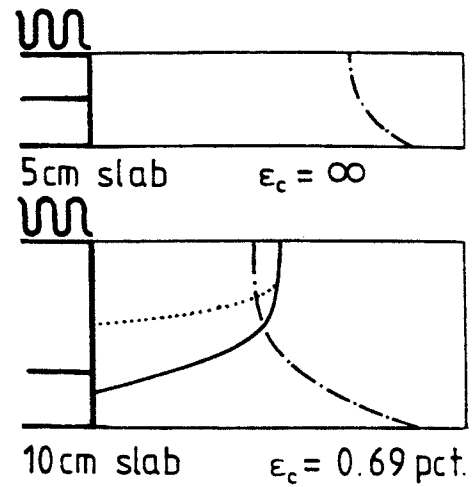
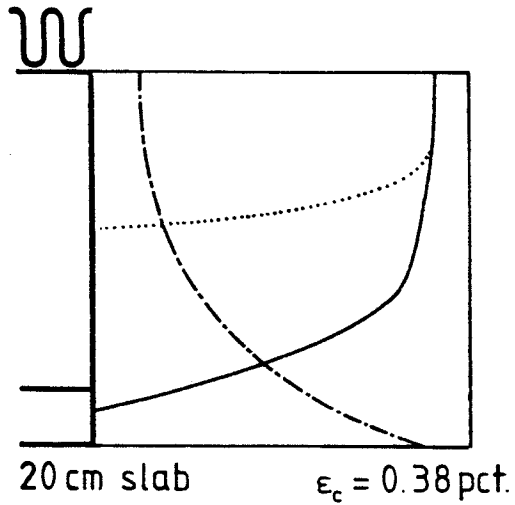
Slab with top-side insulation and subjected to bending.

SLABS AND T-SECTIONS

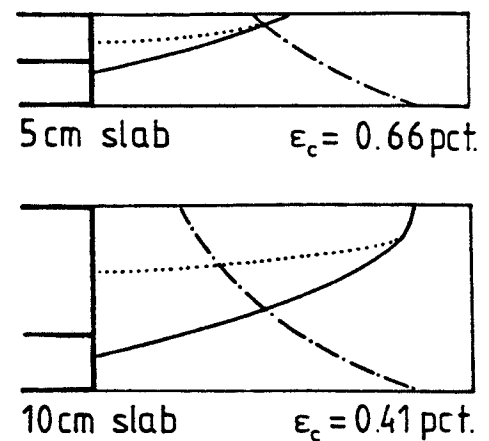
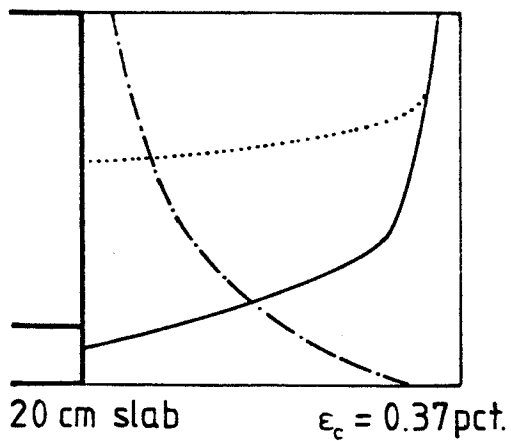
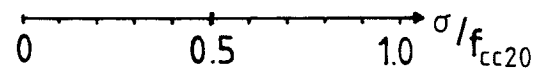
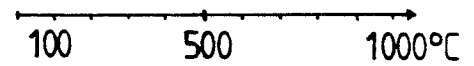
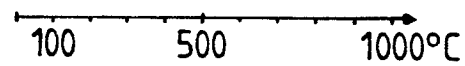
The total ultimate force of the reinforcement of a slab is in principle calculated by a summation like the one used for beams, but often the contributions of all bars are equal, because they are placed in the same depth from the fire exposed surface and hence will have the same temperature.

In estimation the stress distribution of the compression zone the problem is different from the one for beams, because the isotherms are now parallel to the neutral axis.

This means that the strain and the temperature varies simultaneously, and the stresses at different strain levels must be estimated using different stress-strain curves.



Top of slab insulated



Top of slab covered by a concrete screed

- Temperature distribution.
- Stress distribution for axial load.
- Stress distribution for moment load (0.4pct. tension of reinforcement and max. ϵ_c compression of concrete).

Temperature- and stress distributions in various slabs.

However, drawing up the stress distributions of various slabs provided with various thermal insulation it appears that the rectangular stress block of a depth equal to $4/5$ of the depth x to the neutral axis still represents a suitable idealization of the actual stress distribution with the ultimate stress at the top of the slab.

The depth of the neutral axis becomes

$$x = \frac{5}{4} y = \frac{5}{4} \frac{F_{su}}{\xi_{cm} f_{cc20}}$$

and ξ_{cm} is the reduction of the compressive strength of the concrete at the top of the slab.

However, especially in case the slab act as a compression zone of a beam, i.e. the slab is the flange of a T-shaped cross-section, the depth y of the compression zone might be so large, that the concrete is heavily damaged in a part of the compression zone near the fire exposed surface.

Therefore, the compression zone should not comprise a layer of damaged concrete of thickness

$$\frac{c}{2} (1 - \eta)$$

from the fire exposed surface of the slab.

The dimension c is a modified thickness of the slab, which is the double of the real thickness in case the top of the slab is totally insulated, and somewhat more if it is not depending on the ability of heat release from the top. (See the discussion on modified thicknesses of columns).

Also for a cross-section of a slab loaded by a ne-

gative moment the compression zone should be separated from the fire exposed edge by a surface layer of width

$$\frac{c}{2} (1 - \eta)$$

in accordance with the theory for beams with negative moment load.

Some wide and low beams approximate slabs, and for these constructions the modified thickness c is determined as the minimum of the modified slab thickness and the geometrical thickness of the beam.

The analysis in order to avoid an over-reinforced cross-section is made using the same procedure as derived for beams.

SHEAR

Consider an idealized model describing the statically function of a simply supported high beam or wall as a compression arch and a straight tensile reinforcement between the supports.

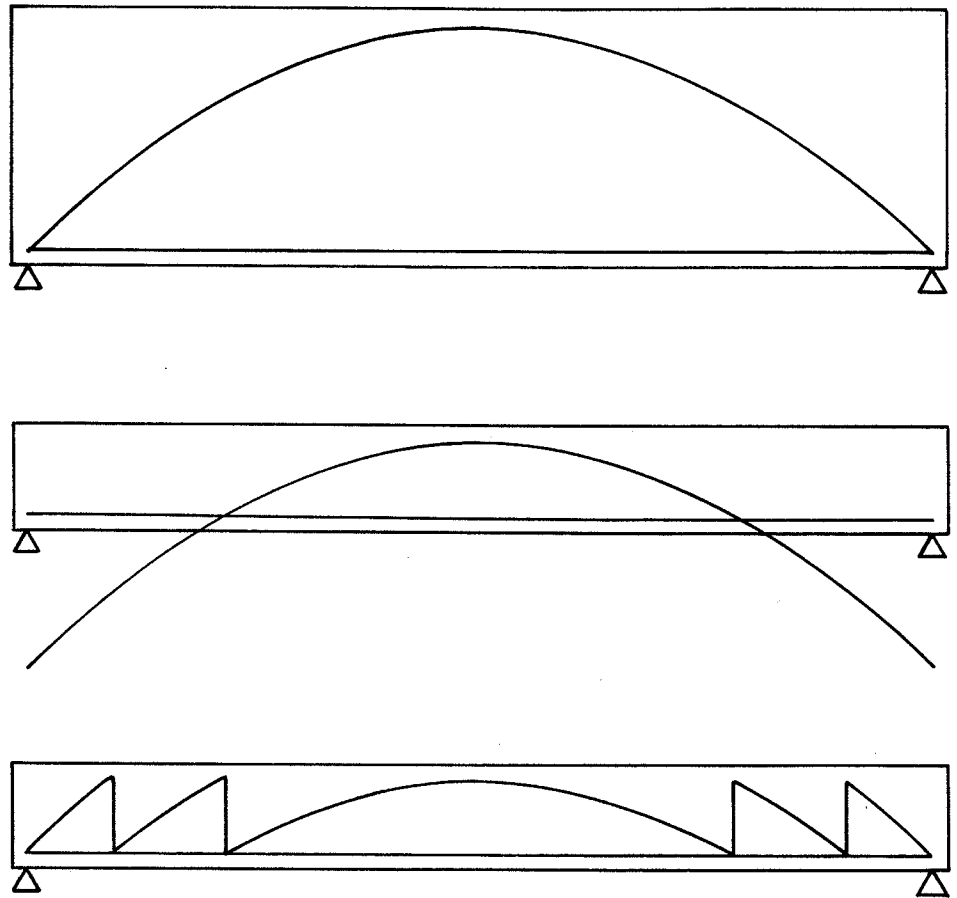
In each point the shear of the beam is represented by the vertical component of the compression force, and at the supports the horizontal components are transferred by the main reinforcement.

Decreasing the height of the beam, the horizontal component of the compression arch force increases, and if the compression zone and the tensile reinforcement are strong enough, the horizontal component might reach the anchorage capacity of the reinforcement, and a tensile shear fracture will occur.

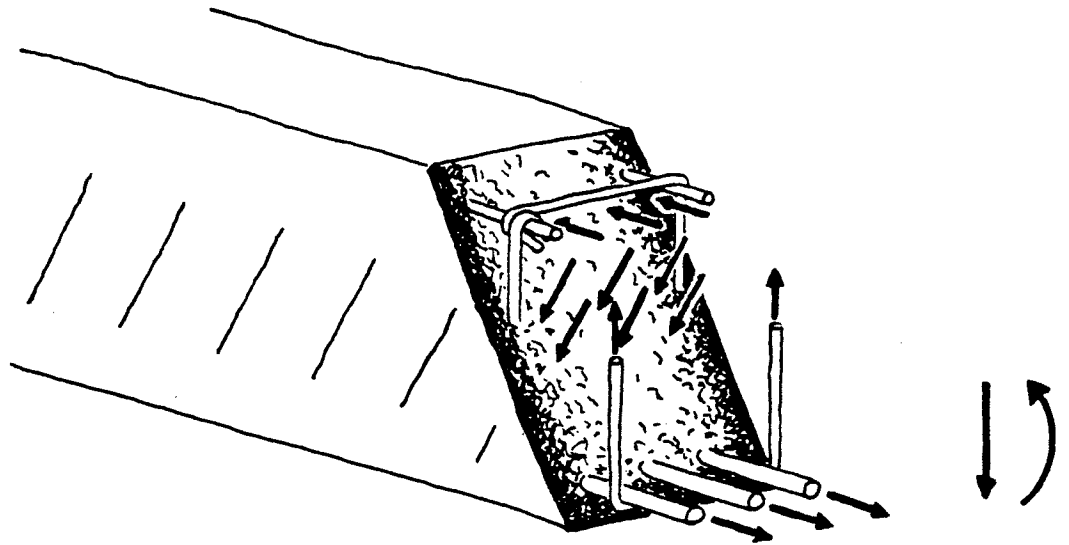
The limited anchorage capacity requires a minimum inclination of the compression arch at the supports or a minimum height of the arch.

In case a further reduction of the height of the beam is wanted, the necessary track of the compression arch would intersect the reinforcement between the supports, and additional supports may be introduced by the application of links, which are able to transfer the vertical component of the compression arch force to the top of the beam from where the arch can continue.

This simple idealized model shows that shear is not an isolated phenomenon, but it is closely related to the distribution of stresses in the compression and tension zone.



Idealized model of a compression arch in a beam.



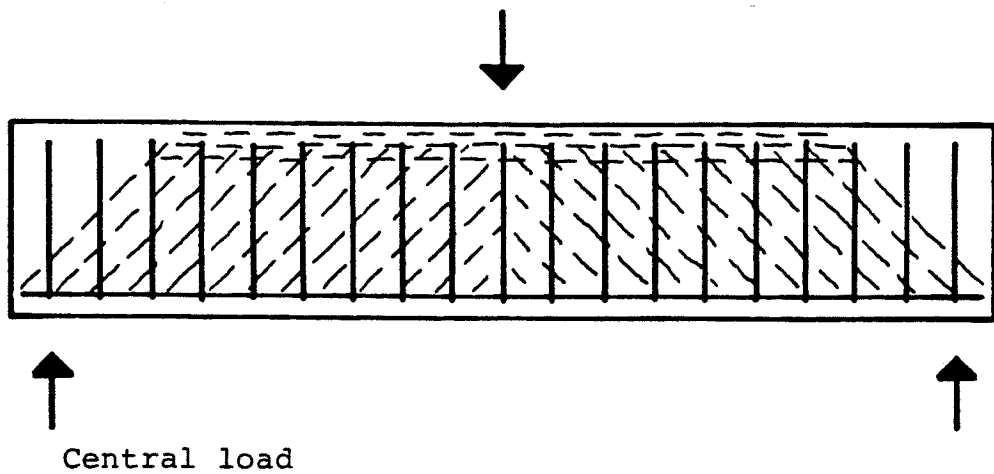
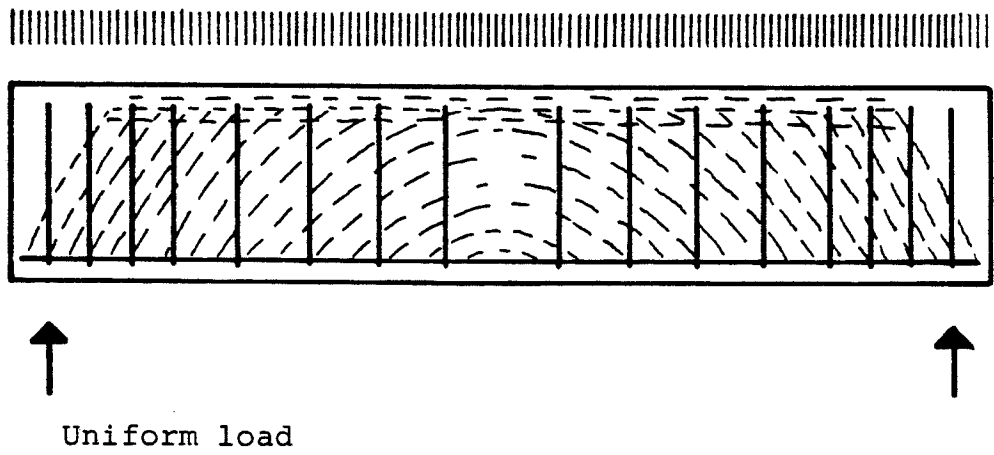
Stresses in a beam subjected to bending and shear.

In case no external loads are applied to the part of the beam or wall considered the compression arch will consist of straight sections, and the model is identical to the truss analogy.

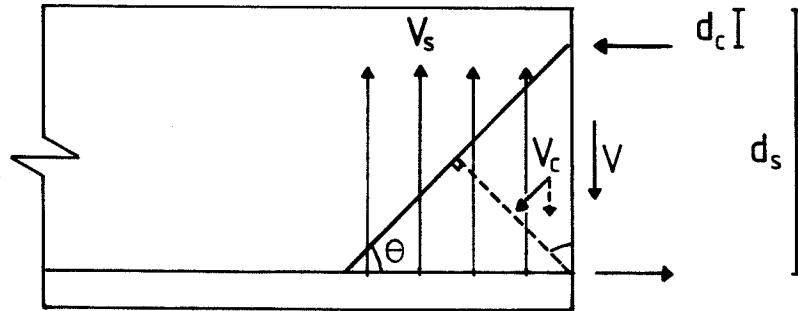
In the classical shear theory the inclination of the sections of the compression arch is assumed to be 45° , and the anchorage capacity of the main reinforcement is required to be at least equal to the reaction transverse to it at the support.

Using a variable inclination θ the anchorage capacity should vary accordingly.

With sufficiently strong links inclined 90° in a beam or a wall the shear capacity due to compression of the concrete becomes a maximum at $\theta = 45^\circ$, and if the distance between the centre lines of the tension and the compression zones is $d_s - d_c$ the capacity is



Stress distributions in beams.



Forces due to shear in a beam.

$$V_{c20} = C(d_s - d_c) \cos\theta \sin\theta f_{cc20}$$

where C is the width of the cross-section and f_{cc20} is the compression strength, which is often reduced by an empirical effectiveness factor (Nielsen [23]).

The shear capacity due to tension of the links of the total cross-section area A_s per unit length of the beam or wall is

$$V_{s20} = A_s (d_s - d_c) (\cos\theta / \sin\theta) f_{s20}$$

For the fire exposed construction the temperatures of the links are easily calculated, because they are often placed in the same depths from the surface along the entire beam or wall, and only a few reductions ξ_s of $A_s f_{s20}$ have to be determined.

The temperature distribution of the inclined compression arch in a web or a wall of thickness C is often identical to the temperature distribution of the compression zone, and the strength reduction $\eta\xi_{cM}$ is already determined at the bending analysis.

In case the main reinforcement is close to a fire exposed surface, i.e. if

$$d_s > d - C/2$$

the temperature distribution through the thickness of the compression arch near the main reinforcement can not be assumed to be equal to the temperature distribution of the compression zone.

In this case the reduction $\eta\xi_{cM}$ must be calculated according to the temperature distribution in the depth d_s .

Finally the shear capacity is determined as the minimum of the reduced capacity as to the tension of the links and the reduced capacity as to the compression of the concrete

$$V = \min \left\{ \begin{array}{l} \xi_s V_{s20} \\ \eta\xi_{cM} V_{c20} \end{array} \right.$$

For walls, beams and especially slabs without a shear reinforcement the tensile strength f_{ct} of the concrete can be taken into account, and assuming for example $\theta = 45^\circ$ the shear capacity becomes

$$V_{ct20} = \frac{1}{2} C (d_s - d_c) f_{ct20}$$

which should be reduced according to the reduction of f_{ct} , and at least by $\eta\xi_{cM}$ according to the curves of Hertz [14], and the cohesion of the construction should be estimated from the temperature distribution.

ANALYSIS OF RECTANGULAR CROSS-SECTIONS

The rectangular cross-section is by far the most common cross-section in reinforced concrete.

It therefore appears to be justified developing special methods for calculating the stress-strain distributions on cross-sections of this basical shape.

In addition such methods could also be applied in a great variety of other cross-sections such as slabs, T-shaped sections and box sections with none or only a few modifications.

In the following methods are developed for calculation of the complete stress-strain distributions on cracked and uncracked rectangular cross-sections loaded by eccentric normal forces acting in the lines of symmetry or bending moments in main axes. Curved stress-strain curves are applied and tensile stresses are neglected for the concrete, and elastoplastic stress-strain curves are applied and compression stresses are neglected for the reinforcement.

By means of the same procedure it will be possible to analyse any cross-section with constant width of the compression zone reinforced by a symmetrical slack, prestressed or partially prestressed reinforcement.

The procedure could be a part of a calculation of the deflections of a beam or a slab or the instability of a wall or a column with eccentric load, and the theoretical basis will be the same as used for calculation of instability of a centrally loaded column.

In appendix A formulas are developed for the stress-strain distribution of a rectangular cross-section of concrete loaded by an eccentric normal force acting in the line of symmetry.

Using these formulas the following procedure is made for a cross-section of constant width c and depth d loaded by the normal force N acting in the line of symmetry in a depth d_N from the compressed edge.

In case the cross-section is loaded by a bending moment only the section will be cracked.

Otherwise, the ultimate compression force of the concrete section F_{cu} and the ratio k between the normal load and F_{cu} are found.

$$F_{cu} = cdf_{cc} \quad , \quad k = N/F_{cu}$$

The calculational value a_1 and the ultimate value of the variable a called a_u are found

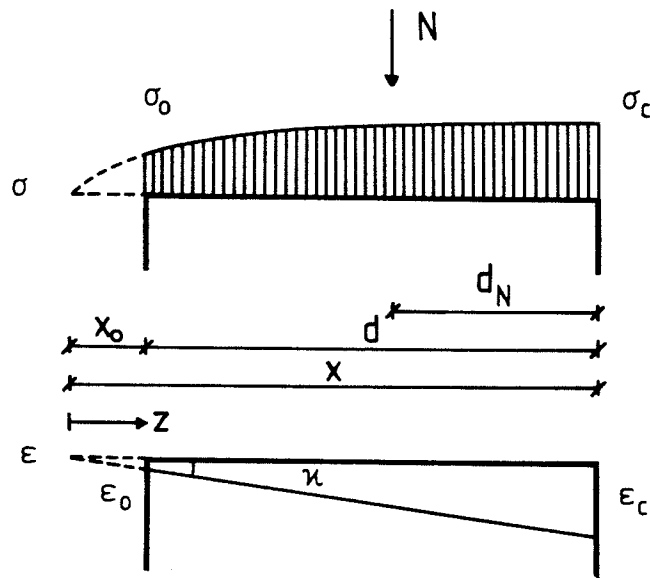
$$a_1 = \frac{dk}{\frac{d}{2} - d_N k} \quad , \quad a_u = \frac{E_{co}}{f_{cc}} \epsilon_{cu}$$

If $a_1(1 - k) > 1 - e^{-a_1}$

the the cross-section will be uncracked; if not so it will be cracked.

In case the cross-section is uncracked, the positive value y , which is at maximum a_u is found by the equation

$$\frac{d_N k}{d} = k - \frac{1}{2} + \left(\frac{1}{y} - \frac{1}{e^y - 1} \right) (1 - k)$$



Stress and strain distribution of an uncracked cross-section.

and from y the parameter a and the depth of the neutral axis $x \geq d$ is calculated by

$$a = \ln\left(\frac{e^y - 1}{y(1-k)}\right)$$

$$x = \frac{ad}{y}.$$

The maximum concrete strain ϵ_c and the curvature κ is then

$$\epsilon_c = \frac{f_{cc}}{E_{co}} a, \quad \kappa = \frac{\epsilon_c}{x}$$

and the stress as a function of the distance z from the neutral axis is

$$\sigma(z) = f_{cc} \left(1 - e^{-a \frac{z}{x}}\right).$$

In case the cross-section is cracked, it could be subjected to a bending moment M only.

Otherwise the moment is defined by

$$M = N(d_s - d_N)$$

where d_s is the depth of the main reinforcement of from the compressed edge.

The main reinforcement is considered to be represented by the total area A_s of the steel of an average E-modulus E_s .

The parameter a and the depth x of the neutral axis is found by solving the equations

$$xbcf_{cc} = N + \frac{d_s - x}{x} \frac{E_s A_s}{E_{co}} f_{cc} a$$

$$b = \frac{a - 1 + e^{-a}}{a}, \quad d_c = \frac{x}{2b} - \frac{x}{a}$$

$$xbcf_{cc}(d_s - d_c) = M$$

The tensile force of the reinforcement then is

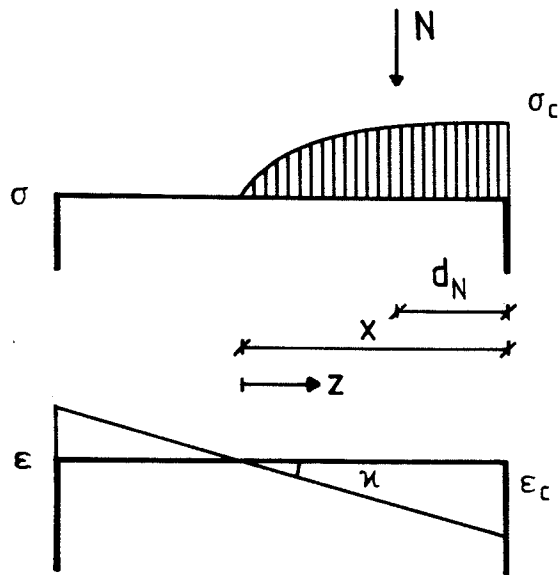
$$F_s = xbcf_{cc} - N$$

and the maximum concrete strain ϵ_c and the curvature κ can be calculated as

$$\epsilon_c = \frac{f_{cc}}{E_{co}} a, \quad \kappa = \frac{\epsilon_c}{x},$$

and the stress is a function of the distance z from the neutral axis is

$$\sigma(z) = f_{cc} \left(1 - e^{-a \frac{z}{x}}\right).$$

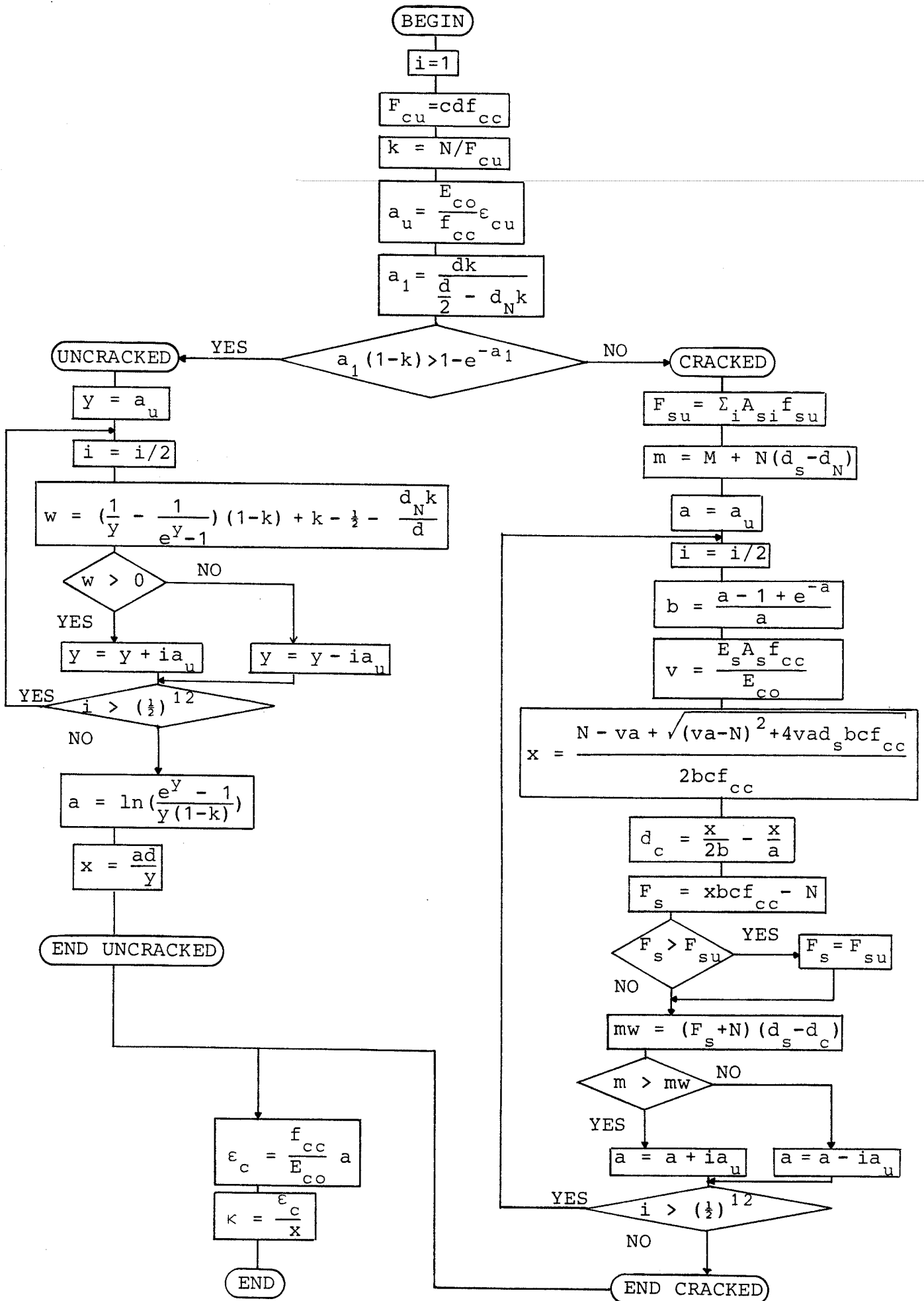


Stress and strain distribution of a cracked cross-section.

For a prestressed cross-section the prestressing is considered to be included in the normal force N , and the prestressing steel is included in the total area of the main reinforcement using an E-modulus and an ultimate stress found by the stress-strain curve from the strain at the point of prestress.

It is to be checked that the tensile force F_s of the main reinforcement is less than the maximum, whether this is defined by a yield stress, a 0.2 pct. proof stress, an ultimate stress or a combination.

In case the parameters a and x are found by an iterative process, the check could be made for each step of the iteration.



DEFLECTIONS

Large deflections of fire exposed concrete structures do often occur because of the decrease of the E-modulus and the yield strength of the reinforcement, and the decrease of the E-modulus of the concrete at any stress level and the increased plasticity.

The deflections often become so large that the structure may be deemed to be insufficient, although it still may have a sufficient load carrying capacity.

The integrity of the fire exposed structure could fail increasing the risk of the spread of fire and blocking escape routes.

In hyperstatic structures the development of deflections may cause changes in force distributions provoking collapse.

The deflections and the corresponding stress-strain distributions are important for the estimations of the possibilities of reusing fire exposed concrete structures.

This is especially important for prestressed structures, where the main reasons for using prestress are to prevent deflections and in some cases to prevent the development of cracks.

And especially these properties of the prestressed structure are most susceptible to the impact of fire, because the prestress is usually decreased or lost.

Furthermore the application of a prestressing technique often leads to relatively slender cross-sections which are heated throughout more easily than massive cross-sections.

The prestressing force is regarded as a normal force P in a certain depth d_p of the cross-section, and the resulting depth of the combined action of the prestressing force and the external normal load N in the depth d_N is denoted d_{P+N} .

Using inclined prestressing reinforcement the prestress in addition contributes to the shear force, and P is considered to be the component perpendicular to the cross-section.

In case the normal load N is present, the structure may be regarded as a centrally loaded or cross-loaded column, and the depth d_N of the normal load may often depend on the deflection.

In this case the calculation of the deflections presented in the following could be regarded as a basis of an iteration, and in case the iteration converges the actual deflection is determined; otherwise the column is not stable.

In this analysis plane cross-sections are assumed to remain plane, and the deflection of the structural member considered is assumed to depend on the distribution of the curvature only.

Previously it was found that the strain of the concrete could be regarded as superimposed by strains caused by the instantaneous application of load, the transient conditions which are the influence of load and temperature simultaneously, the thermal expansion and the creep.

Using this model the curvature of a cross-section is assumed to be superimposed by curvatures due to

the same strain contributions.

Since the integration of the curvatures' sum along the structural member is equal to the sum of integrals for each cause of curvature, the total deflection is most conveniently superimposed by contributions for each course, as it is often possible to estimate the deflection of the whole member due to a cause of curvature from calculation of the curvature of a single cross-section.

As a basic member a straight and simple supported beam of the length l is considered, and the curvature of a significant cross-section is calculated.

The cross-section chosen depends on the load distribution, but is often the one at mid-span.

The temperatures T_{si} are calculated for the reinforcing bars, and the corresponding strength reductions ξ_{si} are determined.

The average depth of the tensile reinforcement is calculated weighted by the strength reductions, which are also assumed to be the reductions of the modulus of elasticity according to the idealized model for reinforcing steel.

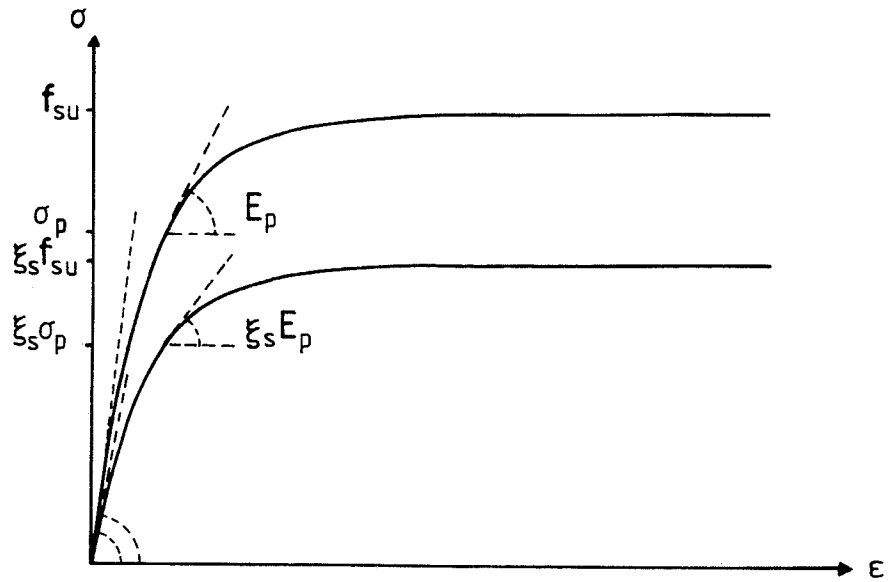
$$\bar{d}_s = \sum_i \xi_{si} E_{s20i} A_{si} d_{si} / \sum_i \xi_{si} E_{s20i} A_{si}$$

and $E_s = \sum_i \xi_{si} E_{s20i} A_{si} / A_s$ where $A_s = \sum_i A_{si}$

and $\bar{\xi}_s = \sum_i \xi_{si} f_{su20i} A_{si} / \sum_i f_{su20i} A_{si}$

The average steel temperature weighted by the E-modulus is calculated as

$$\bar{T}_s = \sum_i \xi_{si} E_{s20i} A_{si} T_{si} / A_s E_s$$



Linear affinity of the stress-strain curve of a prestressing steel.

In case a prestressing reinforcement is used with a prestress σ_p the ultimate stress increment $f_{su} - \sigma_p$ is reduced by ξ_s , and so is the tangent modulus E_p at the level of prestress.

From the previous discussion of stress distribution it is known that the elastic reaction of a fire exposed concrete section is nearly equal to the reaction of an idealized section reduced by the thickness

$$\frac{C}{2} \left(1 - \eta^{\frac{4}{3}}\right)$$

from all fire exposed surfaces and made of a concrete of a quality equal to the concrete at the centre line i.e. with

$$f_{cc} = \xi_{cm} f_{cc20}, \quad E_{co} = \xi_{cm}^2 E_{co20}, \quad \epsilon_{cu} = \epsilon_{cu20} / \xi_{cm}$$

where C is the width of the original section between

weakening through the depth from one side caused by the heat conducted from this side will be equal for all fire exposed sides of the cross-section.

Consequently, the reduced column or wall is obtained by neglecting the contributions of the concrete in surface layers of the thickness

$$\frac{C}{2}(1 - \eta^{\frac{4}{3}})$$

from all fire exposed surfaces, and by using the properties of the concrete at the centre line of a cross-section of width C equal to the smallest dimension of the column or equal to the wall thickness.

In case a concrete column with a rectangular cross-section of depth d and thickness c (where $c < d$) is exposed to fire on all four sides, the product of the moment of inertia and the modulus of elasticity becomes

$$I_c E_{co} = \frac{1}{12}(d-c(1-\eta^{\frac{4}{3}}))\eta^4 c^3 \xi_{cm}^2 E_{co20}$$

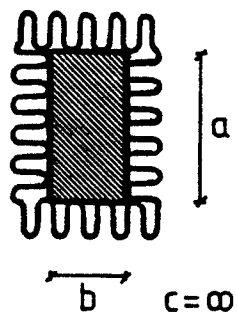
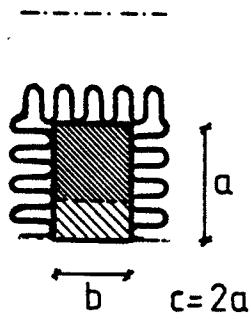
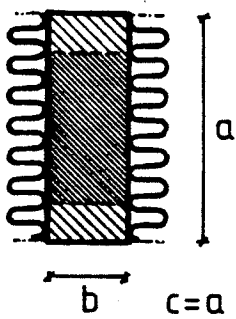
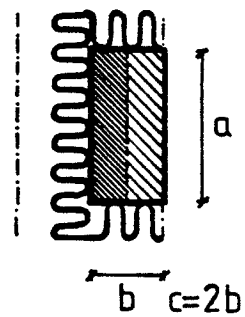
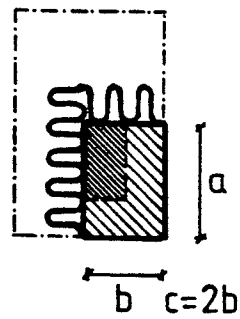
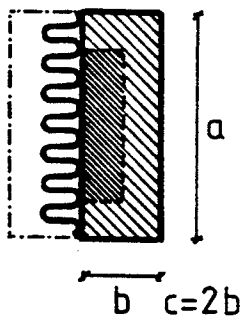
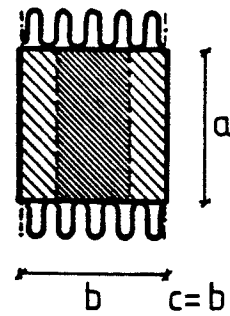
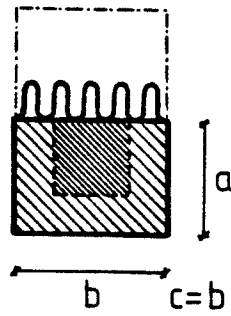
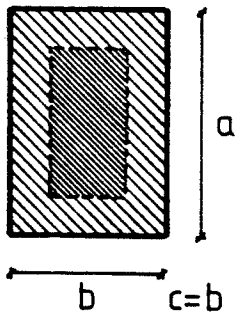
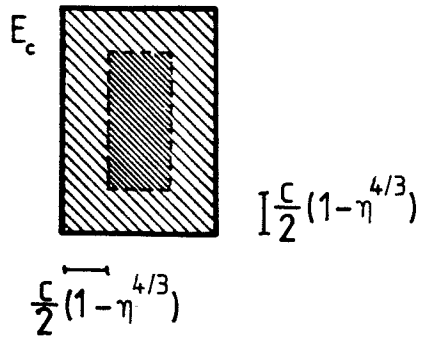
and the area of the reduced cross-section becomes

$$A_c = (d-c(1-\eta^{\frac{4}{3}}))\eta^{\frac{4}{3}} c$$

In case one or more surfaces of the column are insulated the thickness c should be modified determining the thickness of the surface layer $c/2(1 - \eta^{4/3})$.

For a rectangular column the thickness c is determined as the smaller of the two thicknesses of the column modified for the ability of heat conduction.

A modified thickness is the double of the geometrical thickness if one surface is totally insulated, it will be infinite if both surfaces are insulated totally, and if both surfaces are fire exposed it will be the geometrical thickness.



Modified thicknesses of columns.

It is the ambition to establish a total system for analysing concrete structures comprising methods for calculating deflections of beams, deflections and instability of cross-loaded columns and instability of centrally loaded columns, all methods based on the same assumptions.

This system is advantagous, because it ensures homogeneity in the calculational treatment of the structural members, which is especially required for the eccentrically loaded or cross-loaded columns.

Further it ensures continuity in the calculations of the load case Fire and other load cases, and the system offers simplicity to the every day work of the engineer, who is then able to use the same procedures or subroutines on his computer, whether he deals with a beam or a column, and whether the structure is fire exposed or not.

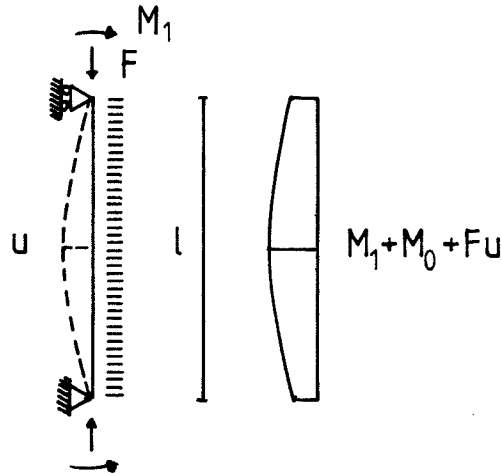
Finally the theory will fit into the procedures used for the ultimate limit state analysis of beams, because the load causing the ultimate stress-strain conditions will correspond to the load-bearing capacity obtained from the ultimate limit state procedures presented.

The calculation of the deflections of beams has been treated, and the basic assumption was the application of Ritters expression for the modulus of elasticity of concrete loaded by a compression stress σ :

$$E_c = E_{co} \left(1 - \frac{\sigma}{f_{cc}} \right)$$

and consequently the stress-strain relation:

$$\sigma = f_{cc} \left(1 - e^{-\frac{E_{co}}{f_{cc}} \epsilon} \right).$$



Cross-loaded column.

Suppose a simply supported beam, which can be pre-stressed and cross-loaded with a mid-span deflection, which has been estimated as

$$\delta_{\text{load}} = \frac{5}{48} \kappa_{\text{load}} l^2$$

in case the cross-loading is uniform, and the moment is parabolic distributed with the moment M_0 at the mid-span cross-section.

Additional deflections are calculated due to the curvature caused by thermal- and transient strains and possibly creep-strains.

In case the beam is also loaded by a constant moment M_1 , the coefficient B could be defined as

$$B = \left(\frac{5}{48} M_0 + \frac{1}{8} M_1 \right) / (M_0 + M_1)$$

and the deflection can be estimated as

$$\delta = (B(\kappa_{\text{load}} + \kappa_{\text{tr}} + \kappa_{\text{creep}}) + \frac{1}{8} \kappa_{\text{th}}) l^2$$

where κ_{load} , κ_{tr} and κ_{creep} are determined from the moment $M_o + M_1$ at the mid-span cross-section.

Now, suppose that the beam is loaded by an external normal force F centrally applied, because any eccentricity could be incorporated in the moment load M_1 .

In that a cross-loaded or eccentrically loaded column is defined.

The normal force will increase the moment load because of the deflections, and the deflections are increasing.

The total deflection curve of the column is assumed to be a sinus curve with the mid-span deflection u and a curvature of zero at the supports.

The moment distribution with respect to the column force F is sinusoidal, and the instantaneous stress-related deflection from this alone would be

$$\delta = \frac{1}{\pi^2} \kappa_{\text{load}} l^2$$

where, incidentally, $1/\pi^2$ is only 3 pct less than $5/48$.

An initial estimation of the total deflection u is made, for example as the deflection of the beam subjected to the cross-loading without the column load applied

The coefficient B is determined as

$$B = \left(\frac{5}{48} M_o + \frac{1}{8} M_1 + \frac{1}{\pi^2} uF \right) / (M_o + M_1 + uF)$$

and the total deflection δ is calculated.

In case $\delta > u$, the initial value u is increased, and if $\delta < u$, u is decreased, and a new δ is calcu-

lated.

In case the final size of $u = \delta$ is obtained from the iteration the column is stable.

In case δ is increasing infinitely the column is unstable for the column force F and the cross-load.

This analysis of a cross-loaded fire exposed column is especially suitable for the application of a personal computer and rather laborious for hand calculations.

However, for the special case of a centrally loaded column simple design procedures can be developed for the determination of the load bearing capacity.

Consider a plain simply supported concrete column or wall without reinforcement.

The cross-section is symmetrical as well as the fire exposure, and therefore the initial curvature of the column will be zero, when a central column force F_c is applied.

By the time of the fire exposure, at which the column is going to be analysed, the stability of the column is controlled by applying a sinusoidal deflection curve with an infinitesimal mid-span deflection u .

In instantaneous stress-related deflection due to the sinusoidal moment distribution is

$$\delta = \delta_{\text{load}} = \frac{1}{\pi^2} \frac{u F_c}{I_c E_c} l^2 ,$$

using the moment of inertia of the reduced concrete section and the E-modulus of the loaded concrete

$$E_c = E_{co} \left(1 - \frac{F_c}{F_{cu}} \right) , \text{ with } F_{cu} = A_c f_{cc}$$

In case $\delta < u$ the deflection will be reduced until the column is straight, and the column is stable.

In case $\delta > u$ the column is unstable, and if $\delta = u$ the applied column load is the critical load F_{crc}

$$F_{crc} = \frac{\pi^2 I_c E_{co}}{l^2} \left(1 - \frac{F_{crc}}{F_{cu}}\right) = F_{cE} \left(1 - \frac{F_{crc}}{F_{cu}}\right)$$

where F_{cE} is the Euler force of the fire exposed column. We obtain the well known Rankine formula

$$\frac{1}{F_{crc}} = \frac{1}{F_{cu}} + \frac{1}{F_{cE}} = \frac{1}{A_c \xi_{cM} f_{cc20}} + \frac{l^2}{\pi^2 I_c E_{co}}$$

and from the discussion it is seen that the formula is just as valid for a fire exposed column as for a column without a fire exposure.

This formulation divided in two contributions is advantageous, because it even indicates the failure mode of the fire exposed column.

In case $F_{cE} < F_{cu}$ the column will be subject to a buckling failure, and in case $F_{cE} > F_{cu}$ it is most likely that the failure mode will be described as a compression failure.

This is in accordance with the observations noted in the test reports for the fire exposed columns treated in the examples of Appendix C.

In case the reinforcement of a column is taken into account, the ultimate compressive yield- or 0.2 pct. proof force is summarized as

$$F_{su} = \sum_i A_{si} \xi_{si} f_{s20i}$$

In this summation only reinforcement sufficiently embedded in the column should be taken into account.

The longitudinal compression reinforcement is often placed near the surfaces of the column in order to improve the moment of inertia of the column cross-section as much as possible.

However, the positions near the surfaces will give rise to high maximum temperatures of the reinforcing bars and of the concrete surrounding them and especially of the cross reinforcement transverse to them, being placed closer to the fire exposed surfaces.

The summation of F_{su} show the reduction of the ultimate compressive force of the reinforcement; but it does not show the risk of instability of the reinforcement.

For example it may be required that the reduced ultimate tensile force of the cross reinforcement should be at least 15 pct. of the compression force taken into account for each longitudinal bar over any partial length of 15 times the diameter of the longitudinal reinforcing bar.

Furthermore it should be required that the concrete surrounding the bar is not totally damaged, and that for example at least 10 pct. of the compressive strength is left at the temperature of the longitudinal bar.

The yield point of mild steel and hot rolled bars disappears at rather low temperatures, and cold-worked bars do not have any yield point at all.

This means that the E-modulus of the reinforcement like the E-modulus of the concrete decreases, when a compression stress is applied.

Therefore, it could be proposed to use a curved-lined relation between the force and the strain of the reinforcement.

Using the same possible deflection curve as used for plain concrete columns the critical column force will be

$$F_{cr} = \frac{\pi^2 IE}{l^2}$$

and an approximative stiffness of the column cross-section is proposed to be

$$IE = I_c E_{co} \left(1 - \frac{F}{F_{cu} + F_{su}}\right) + I_s E_{so} \left(1 - \frac{F}{F_{cu} + F_{su}}\right)$$

being suitable for columns fulfilling the requirement

$$\frac{I_s}{I_c} > \frac{A_s}{A_c}$$

which most columns do, because the reinforcement usually is placed so that its moment of inertia is relatively large.

In case the reinforcement has a yield point, the strain of the column might be more than the yield strain; in this case, however, it must be remembered that the strain will decrease for almost half of the reinforcing bars if the loaded column deflects, and these bars will act with their full E-modulus at the occurring large column forces for which

$$F_c = F - F_{su} > \frac{1}{2} (F_{cu} - F_{su}) \Leftrightarrow$$

$$\left(1 - \frac{F}{F_{cu} + F_{su}}\right) < \frac{1}{2} ,$$

thus the reduction of the stiffness of the reinforcement is safe.

For the concrete we obtain using $F = F_c + F_{su}$:

$$F_c F_{cu} + F_{su} F_{cu} > F_c F_{cu} + F_c F_{su} \Leftrightarrow$$

$$(1 - \frac{F}{F_{cu} + F_{su}}) < (1 - \frac{F_c}{F_{cu}})$$

and the reduction of the concrete stiffness is safe as well.

In case the column strain is less than the yield strain all bars are in elastic state, and for small values of the critical column force and relatively small values of I_s the reduction of the concrete stiffness might be too small, and the approximation of IE might be slightly unsafe; but if $I_s/I_c \geq A_s/A_c$ the deviation is found to be within 5 pct.

So, the approximation is acceptable provided that $I_s/I_c \geq A_s/A_c$.

Defining the Euler forces of concrete and reinforcement as

$$F_{cE} = \frac{\pi^2 I_c E_{co}}{l^2} \text{ and } F_{sE} = \frac{\pi^2 I_s E_{so}}{l^2}$$

the stiffness of the reinforcement is calculated by summation for the same bars taken into account when calculating the ultimate compression force of the reinforcement F_{su}

$$I_s E_{so} = \sum_i z_i^2 A_{si} \xi_{si} E_{so20i}$$

where z_i is the lever arm of bar number i .

The critical column force becomes

$$F_{cr} = (F_{cE} + F_{sE}) (1 - \frac{F_{cr}}{F_{cu} + F_{su}})$$

and an extended Rankine formula can be derived as

$$\frac{1}{F_{cr}} = \frac{1}{F_{cu} + F_{su}} + \frac{1}{F_{cE} + F_{sE}} \quad \text{if } \frac{I_s}{I_c} \geq \frac{A_s}{A_c}$$

The formula appears to be the simplest possible extension of the Rankine formula for plain concrete columns and is just as advantageous in use.

The examples of Appendix C show that the critical column force estimated by means of the formula is very close to the load-bearing capacities found by fire testings and slightly on the safe side.

THE FULLY DEVELOPED FIRE COURSE

Using the calculational models presented in this context the time at which the load-bearing capacity, the stability or the deflection is calculated can be chosen freely.

However, usually the minimum load-bearing capacity of the fire exposed construction is the important parameter in estimating the fire safety of the total structure.

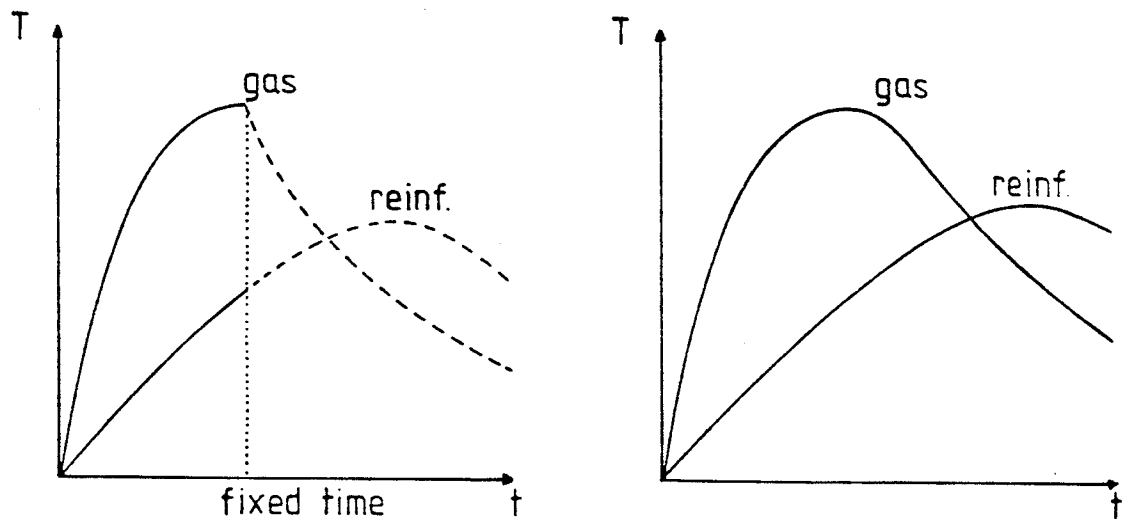
When designing a structure the requirements concerning the fire resistance must be clarified.

In case the traditional requirement is applied that the structure should be able to carry its load within a certain time of a standard fire course of steadily increasing temperature, the investigation is reduced to comprise this time only.

An investigation like that still does not show, whether the structure will be able to carry the load throughout a complete fire course.

The reason is that the time of the largest reduction of the load-bearing capacity always is beyond the time of the maximum gas temperature, as it takes time for the heat to be conducted into the cross-section. See "Design Philosophy for Fire Exposed Concrete Structures".

In case it is required that the structure should be able to carry a certain load throughout a complete fire course, the investigation must comprise the conditions for which the structure is at the weakest.



Temperature-time developments of a gas and a reinforcement embedded in concrete.

In general this implies that the load-bearing capacity should be calculated at the time, when the reinforcement is at the weakest, and at the time, when the concrete is at the weakest.

The time of the weakest condition of the reinforcement is always later than the time of the maximum gas temperature, and mostly the delay is from about 15 minutes to several hours.

The time of the weakest reinforcement is found by an optimization based on calculations of the temperatures of the single reinforcing bars and their strength reductions weighted by their cross-section areas.

In this "HOT" condition the strength reduction of the concrete η and ξ_{CM} should be calculated for the same time as is the maximum reduced force of the reinforcement.

ment.

The calculation for the hot condition is usually much less sensitive to variations in time for the concrete than for the reinforcement.

Stress distribution factors η and strength reductions ξ_{CM} therefore are tabulated at the times of maximum temperatures in a fixed depth of 30 mm from the surface of an infinite specimen (Hertz [21]).

When calculating the stress distribution factor in a hot condition it must be remembered that until a certain depth from the surface the concrete has attained its maximum temperature prior to the time called for.

In this layer the maximum temperatures must be used, and in the remainder of the cross-section the temperature distribution at the time called for has to be used.

The second part of the investigation deals with the time, at which the concrete is at the weakest.

This time is usually about a week after the fire, and the calculation therefore also estimates the residual load-bearing capacity of the structure.

In this "COLD" condition the residual strength of each reinforcing bar is calculated using the maximum temperatures of the bars, and the values of η and ξ_{CM} of the concrete are calculated from the distribution of maximum temperatures through the cross-section.

These values have also been tabulated for a large variety of cross-sections and fires in Hertz [21].

The values are calculated using material properties of an unloaded concrete with Danish sea gravel and will be conservative for most other concretes and loads.

REFERENCES

- [1] ANDERBERG, Y.:
Behaviour of Steel
at High Temperatures.
RILEM-Committee 44-PHT
Report 114 p.
February 1983.

- [2] ANDERBERG, Y. THELANDERSSON, S.:
Stress and Deformation Characteristics
of Concrete at High Temperatures.
2. Experimental Investigation and
Material Behaviour Model.
Bulletin 54
Lund Institute of Technology
Lund 1976.

- [3] BRANSON, D.E.:
Design Procedures for
Computing Deflections
ACI Journal, pp. 730-742
September 1968.

- [4] BRØNDUM-NIELSEN, T.:
Structural Concrete.
Polyteknisk Forlag 136 p.
Copenhagen, January 1973.

- [5] CAHILL, T.:
The Behaviour of Prestressing Wire
at Elevated Temperatures.
Proc. of Symposium on Fire Resistance
of Prestressed Concrete
Braunschweig 1965.

- [6] CEB:
Design of Concrete Structures
for Fire Resistance
(Draft of an Appendix to the CEB/FIP
Model Code on Concrete Structures).
Bulletin d'information No. 145
Comité Euro-International du Béton
Paris, January 1982.
- [7] DS 412
Norm for stålkonstruktioner
Danish Code of Practice for
Steel Structures.
2. Edition. 106 p.
Danish Standardisation Organisation
Danish Society of Civil Engineers
Copenhagen 1983.
- [8] DANNENBERG, J.:
Festigkeitsuntersuchung
Bewehrungsstahls bis 600⁰C
Deutscher Ausschuss für
Stahlbeton, Heft 132.
Wilhelm Ernst und Sohn
Berlin 1959.
- [9] FIP/CEB:
Report on Methods of Assessment of
the Fire Resistance of Concrete
Structural Members.
Cement and Concrete Association. 91 p.
Wexham Springs 1978.

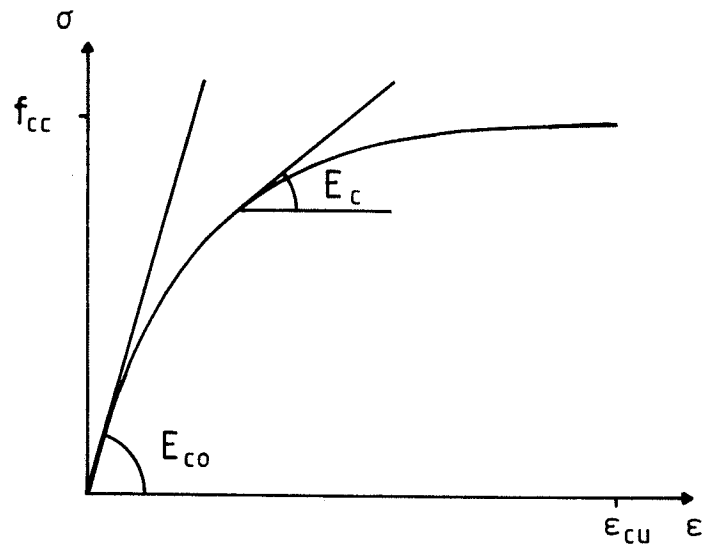
- [10] FISCHER; R.:
Über das Verhalten von Zementmörtel
und Beton bei höheren Temperaturen
Deutscher Ausschuss für Stahlbeton,
Heft 214, pp. 61-128
Berlin 1970.
- [11] HARADA, T. TAKEDA. J.
YAMANE, S. FUTUMURA, F.:
Strength, Elasticity and Thermal
Properties of Concrete Subjected
to Elevated Temperatures.
ACI, SP-34, pp. 377-406.
Detroit 1972.
- [12] HARMATHY, T.Z. BERNDT, J.E.:
Hydrated Portland Cement and Light weight
Concrete at Elevated Temperatures.
Journal of the ACI Vol.63, No.1, pp. 93-112
Research Paper No. 280.
Division of Building Research.
Ottawa 1966.
- [13] HARMATHY, T.Z. STANZAK, W.W.:
Elevated Temperatures Tensile and Creep
Properties of some Structural
and Prestressing Steels.
Nat. Research Council of Canada.
Research Paper No. 424. NCR 11163.
Division of Building Research.
Ottawa 1970.

- [14] HERTZ, K.D.:
Betonkonstruktioners
brandtekniske egenskaber
(Properties of Fire Exposed Concrete
Structures. Part 1 and 2 of Ph.D. Thesis)
Report No. 140. 210 p. (In Danish).
Institute of Building Design,
Technical University of Denmark.
Lyngby, July 1980.
- [15] HERTZ, K.D.:
Design of Fire Exposed
Concrete Structures.
Report No. 160. 49 p.
Institute of Building Design,
Technical University of Denmark.
Lyngby, September 1981.
CIB W14/81/20 (DK).
- [16] HERTZ, K.D.:
Heat-Induced Explosion of
Dense Concretes.
Report No. 166. 20 p.
Institute of Building Design,
Technical University of Denmark.
Lyngby, February 1984.
CIB W14/84/33 (DK)
- [17] HERTZ, K.D.:
Microwave Heating for Fire
Material Testing of Concrete
- A Theoretical Study.
Report No. 144. 24 p.
Institute of Building Design.
Technical University of Denmark.
Lyngby, March 1981.
CIB W14/81/3 (DK).

- [18] HERTZ, K.D.:
Microwave Heating for Fire
Material Testing of Concrete
- An Experimental Study.
Report No. 164. 38 p.
Institute of Building Design,
Technical University of Denmark.
Lyngby, August 1983.
CIB W14/83/19 (DK).
- [19] HERTZ, K.D.:
Reference List on Concrete Construc-
tions Exposed to High Temperatures.
Report No. 141. 63 p. (Approx. 500 Ref.)
Institute of Building Design,
Technical University of Denmark.
Lyngby, May 1980.
- [20] HERTZ, K.D.:
Simple Temperature Calculations of
Fire Exposed Concrete Constructions.
Report No. 159. 54 p.
Institute of Building Design,
Technical University of Denmark.
Lyngby, June 1981.
CIB W14/81/13 (DK).
- [21] HERTZ, K.D.:
Stress Distribution Factors.
Report No. 158. 60 p.
Institute of Building Design,
Technical University of Denmark.
Lyngby, July 1981.
CIB W14/81/14 (DK).

- [22] MUFF, M.:
Brandbestandig beton baseret på molér.
(Fire Resistant Concrete Based on Mo-clay
Graduation work in Danish) 138 p.
Institute of Building Design,
Technical University of Denmark.
Lyngby 1983.
- [23] NIELSEN, M.P.:
Limit Analysis and Concrete Plasticity.
Prentice-Hall Inc. 420 p.
New Jersey 1984.
- [24] RUGE, J. LINNEMANN, R.:
Festigkeits- und Verformungsverhalten
von Bau-, Beton- und Spannstählen
bei hohen Temperaturen.
Sonderforschungsbereich 148, B4. p.159-211.
Technische Universität
Braunschweig, Maj 1983.
- [25] SCHNEIDER, U.:
Festigkeits- und Verformungsverhalten
von Beton unter stationär und
instationärer Temperaturbeanspruchung.
Die Bautechnik heft 4. pp. 123-132.
Wilhelm Ernst und Sohn.
Berlin 1977.
- [26] SKINNER, D.H.:
Measurement of High Temperature
Properties of Steel.
Melbourne Research Laboratories.
MRL 6/10.
May 1972.

- [27] SKJØDT, P.:
Nedbøjning af brandpåvirkede
betonkonstruktioner.
(Deflection of Fire Exposed
Concrete Structures
Graduation work in Danish) 131 p.
Institute of Building Design,
Technical University of Denmark.
Lyngby 1984.
- [28] VOVES, B.:
Behaviour of Prestressed Concrete
Structures during Fire.
Czechoslovakian Technical University
Prauge 1978.
- [29] НЕКРАСОВ, К.Д. ТАРАСОВА, А.П.:
Жаростойкий бетон на портландцементе.
(Fire Resistant Concrete on Portland Cement.
In Russian). 192 p.
Издательство литературы по строительству.
Москва 1969.



Stress-strain curve for concrete.

A rectangular cross-section is considered of thickness c and loaded by an eccentric compression force F_c .

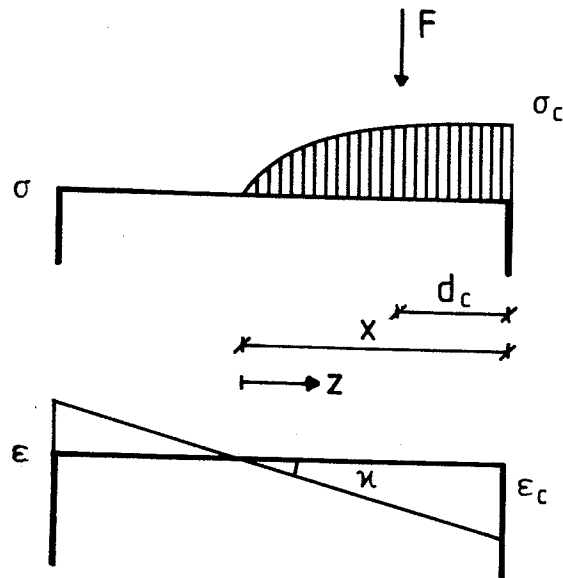
The force acts in the distance d_c from the most compressed edge, and as a first case, the cross-section is supposed to be cracked to the distance x from the compressed edge, and the coordinate z is counted from the neutral axis.

Introducing the parameter a as

$$(3) \quad a = \frac{E_{co}}{f_{cc}} \epsilon_c$$

where ϵ_c is the maximum compressive strain occurring in the cross-section, and assuming a linear strain distribution, the stress distribution is described by

$$(4) \quad \sigma(z) = f_{cc} \left(1 - e^{-a \frac{z}{x}} \right)$$



Stress and strain distribution of a cracked cross-section.

By integration of the expression the force is found

$$F_c = \int_0^x \sigma(z) dz \quad \text{leading to}$$

$$(5) \quad \underline{F_c = b x c f_{cc}}, \text{ where } \underline{b = \frac{a - 1 + e^{-a}}{a}}$$

Calculating the moment from the neutral axis

$$(x - d_c) F_c = c \int_0^x z \sigma(z) dz = c f_{cc} \int_0^x (z - z e^{-a \frac{z}{x}}) dz$$

$$\text{using } \int_0^x z e^{-a \frac{z}{x}} dz = \left[z \left(-\frac{x}{a} \right) e^{-\frac{a}{x} z} \right]_0^x - \int_0^x \left(-\frac{x}{a} \right) e^{-\frac{a}{x} z} dz$$

$$= \left[-\frac{x}{a} e^{-\frac{a}{x} z} \left(z + \frac{x}{a} \right) \right]_0^x = -\frac{x}{a} e^{-a} \left(x + \frac{x}{a} \right) + \left(\frac{x}{a} \right)^2, \text{ we have}$$

$$(x - d_c) F_c = \left(\frac{1}{2} - \frac{1}{a^2} (1 - e^{-a} (a + 1)) \right) x^2 c f_{cc}$$

and introducing F_c as found above (5)

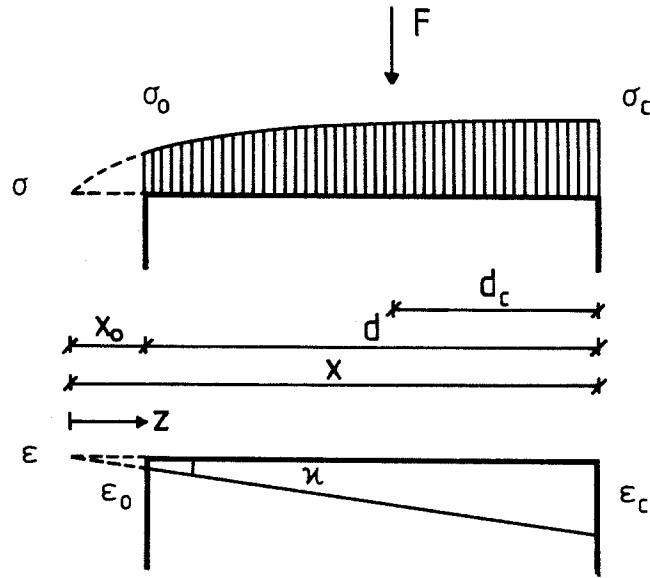
$$x - d_c = x \frac{\frac{1}{2}a^2 - 1 + ae^{-a} + e^{-a}}{a(a-1+e^{-a})} = x \frac{a-1+e^{-a}+a^2-a+ae^{-a}-\frac{1}{2}a^2}{a(a-1+e^{-a})}$$

$$x - d_c = x \left(\frac{1}{a} + 1 - \frac{1}{2b} \right)$$

$$(6) \quad \underline{d_c = \frac{x}{2b} - \frac{x}{a}}$$

(For a concrete of compressive strength $f_{cc} = 23$ MPa, modulus of elasticity $E_{co} = 32.8$ GPa and ultimate compression strain $\epsilon_c = \epsilon_{cu} = 0.35$ pct. the value of a and b become $a = 4.99$ and $b = 0.801$. This means that $F_c = 0.8cx f_{cc}$. The same expression is often used for plastic design. $d_c = 0.424x$, where $0.4x$ is used for plastic design.

Variation of f_{cc} only affects this good agreement a little. For $f_{cc} = 15$ MPa, $E_{co} = 27$ GPa we become $a = 6.30$, $b = 0.842$ and $d_c = 0.435x$, and for $f_{cc} = 40$ MPa, $E_{co} = 38$ GPa we become $a = 3.33$, $b = 0.710$ and $d_c = 0.403x$, so the fixed values seem to be justified as reasonable alternatives for a simple plastic design procedure).



Stress and strain distribution of an uncracked cross-section.

As the second case the rectangular cross-section is considered to be uncracked, and the neutral axis is outside the cross-section, i.e. x is greater than the depth of the cross-section d .

The minimum compressive stress on the cross-section is called σ_0 , the corresponding strain ϵ_0 , and the difference $\sigma_c - \sigma_0 = \Delta\sigma$.

The following values are introduced: $x_0 = x - d$,

$$(7) \quad \underline{F_{cu} = c d f_{cc}}, \quad \epsilon_0 = \epsilon_c \frac{x-d}{x}, \quad a_0 = \frac{E_{co}}{f_{cc}} \epsilon_0, \quad b_0 = \frac{a_0 - 1 + e^{-a_0}}{a_0}$$

and the relation between the compressive force and the ultimate compressive force of the cross-section is called k

$$(8) \quad \underline{k = \frac{F_c}{F_{cu}}}$$

For $x \leq d$ we have

$$(17) \quad b = \frac{a-1+e^{-a}}{a} = \frac{F}{x c f_{cc}} \geq \frac{F}{d c f_{cc}} = k \text{ and from that}$$

$$\frac{1}{2k} - \frac{1}{a} \geq \frac{d_c}{x} = \frac{1}{2b} - \frac{1}{a} \geq \frac{d_c}{d} \text{ and from that}$$

$$\frac{1}{a} \leq \frac{1}{2k} - \frac{d_c}{x} \leq \frac{1}{2k} - \frac{d_c}{d} \text{ and further}$$

$$(18) \quad a = \frac{x b}{\frac{x}{2} - d_c b} \geq \frac{x k}{\frac{x}{2} - d_c k} \geq \frac{d k}{\frac{d}{2} - d_c k} = a_1 \text{ defining } a_1$$

For $x \leq d$ we now consider k to be fixed and varies d_c untill the value d_{c1} , where $x=d$ and

$$(19) \quad a = a_{11} = \frac{d k}{\frac{d}{2} - d_{c1} k} \geq \frac{d k}{\frac{d}{2} - d_c k} = a_1$$

We now know that

$$a \geq a_{11} \geq a_1 \text{ and } a(1-k) \geq 1-e^{-a} \text{ and } a_{11}(1-k) = 1-e^{-a_{11}}$$

and therefore we also know that

$$(20) \quad \underline{a_1(1-k) \leq 1-e^{-a_1}}$$

The procedure is then as follows:

$$\text{calculate } a_1 = \frac{d k}{\frac{d}{2} - d_c k}$$

$$\text{If } \underline{a_1(1-k) < 1-e^{-a_1}},$$

the cross-section is cracked, and $x < d$.

Elsewise the cross-section is uncracked and $x \geq d$.

APPENDIX B

STRENGTH- AND TEMPERATURE DISTRIBUTIONS

In the chapter on stress distribution conclusions are made based on a variety of cases with different fire exposures and thickness of the concrete cross-section.

The strength and temperature distributions of these cases are illustrated in this appendix, and the stress distribution factors are calculated using a simple formula comprising the strength reduction ξ_{ci} in 11 points from $i = 0$ at the surface to $i = 10$ at the centre line of the cross-section.

$$\eta = \frac{1}{10\xi_{cM}} ((\xi_{c0} + \xi_{cM})/2 + \sum_1^9 \xi_{ci})$$

In addition the average reduction of the E-modulus through the cross-section is calculated using the same strength reductions

$$\frac{\bar{E}_c}{E_{c20}} = \frac{1}{10\xi_{cM}^2} ((\xi_{c0}^2 + \xi_{cM}^2) + \sum_1^9 \xi_{ci}^2)$$

and the reduction of the stiffness of the cross-section is calculated as

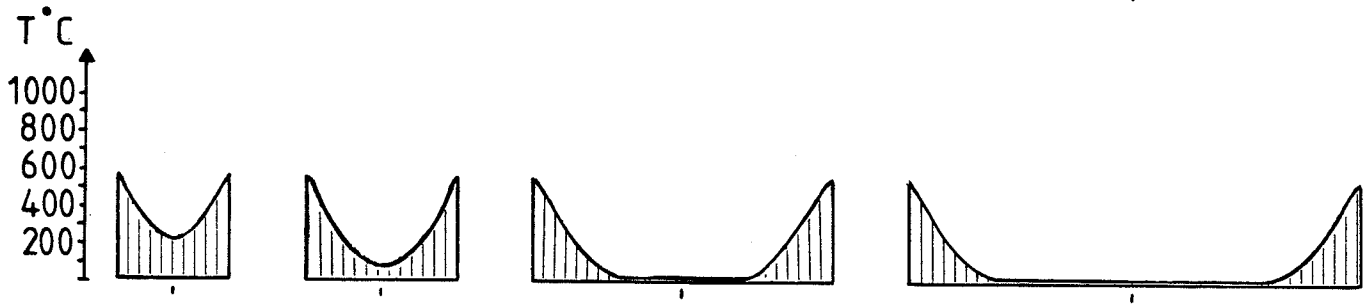
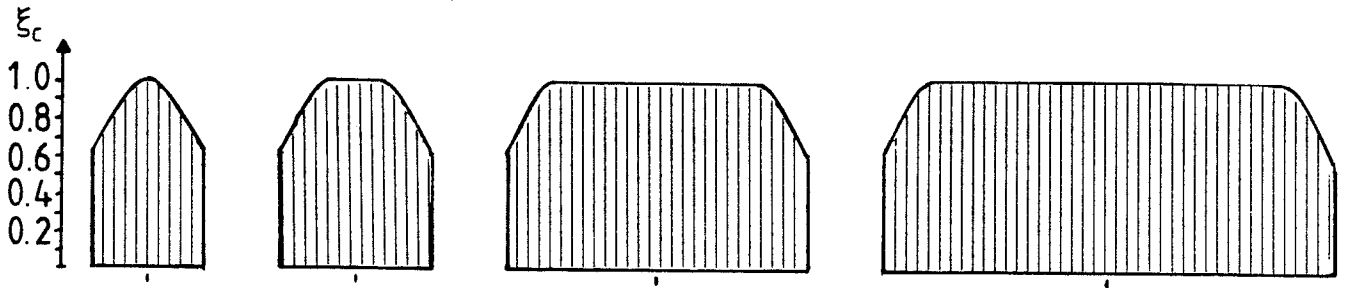
$$\frac{I_c E_c}{I_c E_{c20}} = \frac{3}{10} (\frac{1}{2}\xi_{c0}^2 + \sum_1^9 ((1 - \frac{i}{10})\xi_{ci})^2)$$

Furthermore, the illustrations offer an impression of the importance of the fire data and the cross-section thickness for the distribution of temperature and strength in a HOT and a COLD condition and for the approximation in using an idealized model of a reduced cross-section.

Thermal diffusivity $3.48 \times 10^7 \text{ m}^2/\text{s}$. $C = 1.2$. $D = 180$. $E = 540$.

$q = 200 \text{ MJ/m}^2$. $A\sqrt{h}/A_c = 0.04 \text{ m}^2$.

HOT



$C = 150\text{mm}$

200mm

400mm

600mm

$\eta = 0.8529$

0.8918

0.9448

0.9624

$\frac{1}{10\xi_{cm}^2} \sum_{10\xi_c} \xi_c^2 = 0.7424$

0.8119

0.9048

0.9358

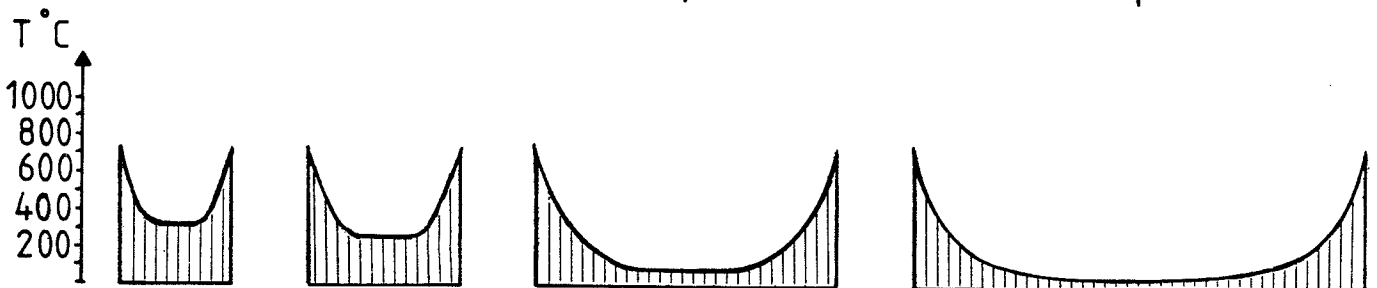
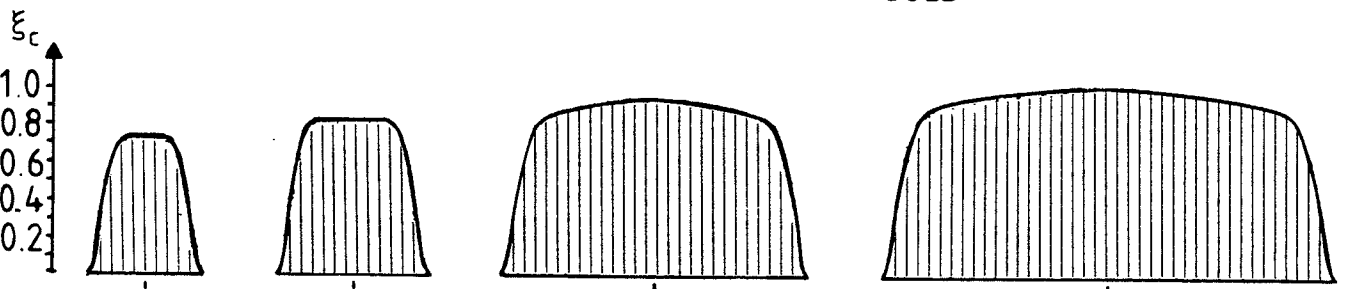
$I_c/I_{c20} = 0.5542$

0.6225

0.7657

0.8309

COLD



$C = 150\text{mm}$

200mm

400mm

600mm

$\eta = 0.7504$

0.8116

0.8533

0.8671

$\frac{1}{10\xi_{cm}^2} \sum_{10\xi_c} \xi_c^2 = 0.6694$

0.7601

0.7911

0.8029

$I_c/I_{c20} = 0.1785$

0.2784

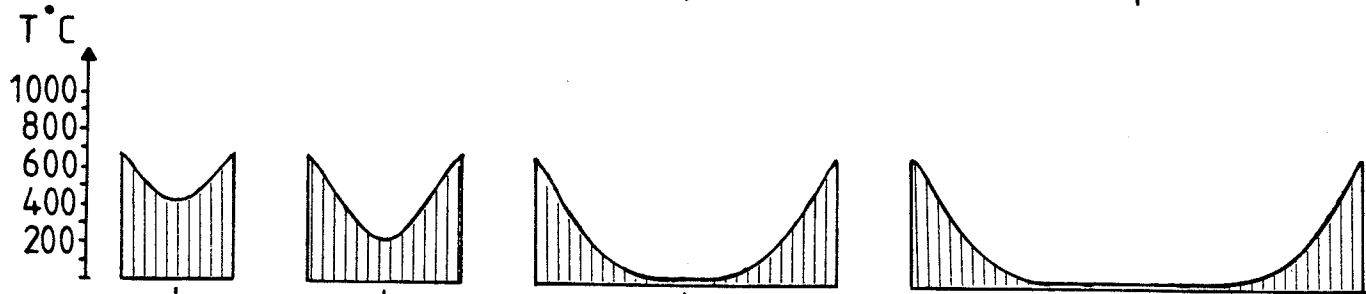
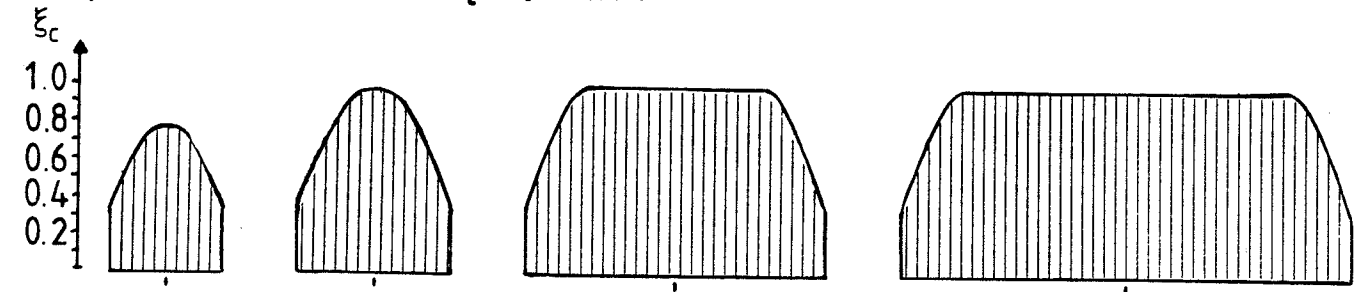
0.4894

0.5944

Thermal diffusivity $3.48 \times 10^{-7} \text{ m}^2/\text{s}$. $C = 2.8$. $D = 240$. $E = 540$.

$q = 400 \text{ MJ/m}^2$. $A\sqrt{h}/A_c = 0.04 \text{ m}^{3/2}$.

HOT



$C = 150\text{mm}$

200mm

400mm

600mm

$\eta = 0.8128$

0.7912

0.8916

0.9273

$\frac{1}{10\xi_{cm}^2} \sum_{10\xi_c}^2 = 0.6933$

0.6645

0.8294

0.8862

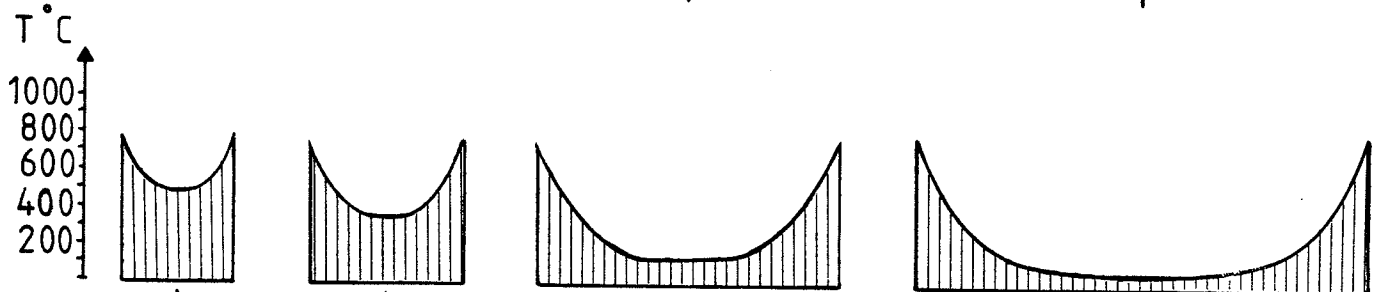
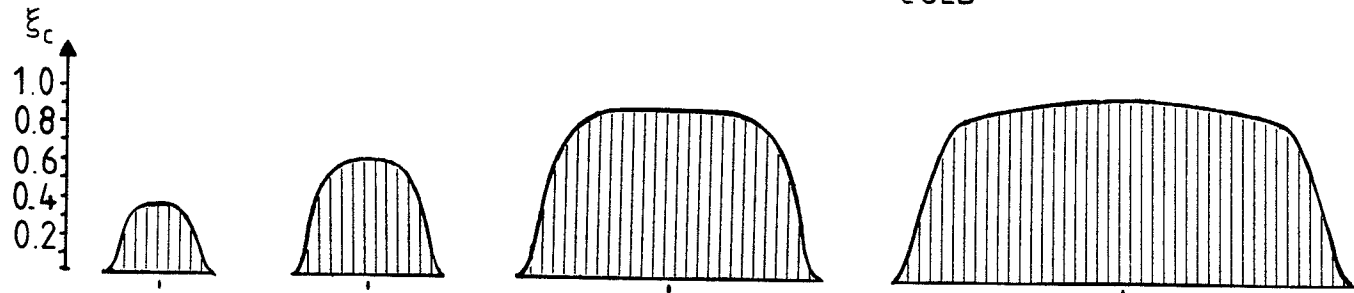
$I_c/I_{c20} = 0.2664$

0.3899

0.6041

0.7131

COLD



$C = 150\text{mm}$

200mm

400mm

600mm

$\eta = 0.6328$

0.6964

0.7938

0.8241

$\frac{1}{10\xi_{cm}^2} \sum_{10\xi_c}^2 = 0.5390$

0.6164

0.7258

0.7487

$I_c/I_{c20} = 0.0269$

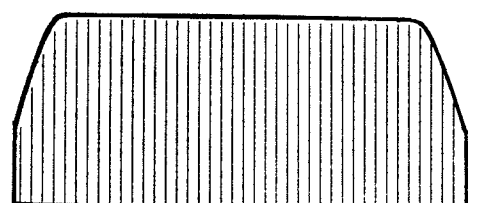
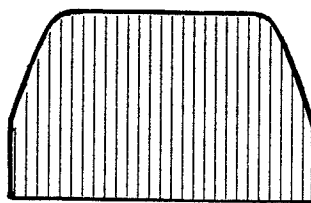
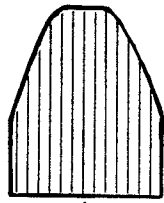
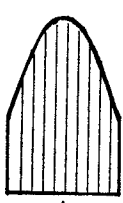
0.1009

0.3371

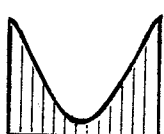
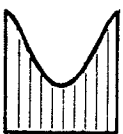
0.4686

Thermal diffusivity $3.48 \times 10^7 \text{ m}^2/\text{s}$. $C = 1.2$. $D = 180$. $E = 650$.
 $q = 400 \text{ MJ/m}^2$. $A\sqrt{h}/A_c = 0.08 \text{ m}^2$. HOT

ξ_c
1.0
0.8
0.6
0.4
0.2



$T^\circ\text{C}$
1000
800
600
400
200



$C = 150\text{mm}$

200mm

400mm

600mm

$\eta = 0.8040$

0.8366

0.9181

0.9445

$\frac{1}{10\xi_{CM}^2} \sum_{10\xi_c} \xi_c^2 = 0.6785$

0.7363

0.8687

0.9128

$l_c/l_{c20} = 0.3942$

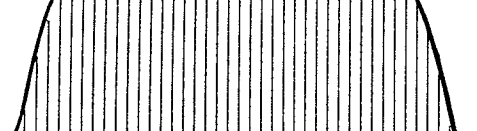
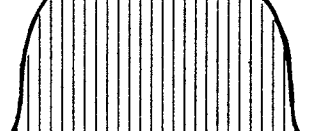
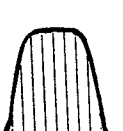
0.4818

0.6797

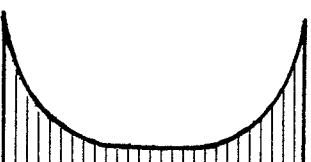
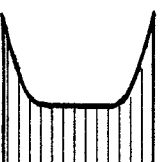
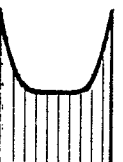
0.7706

COLD

ξ_c
1.0
0.8
0.6
0.4
0.2



$T^\circ\text{C}$
1000
800
600
400
200



$C = 150\text{mm}$

200mm

400mm

600mm

$\eta = 0.6925$

0.8972

0.8312

0.8284

$\frac{1}{10\xi_{CM}^2} \sum_{10\xi_c} \xi_c^2 = 0.6201$

0.9946

0.7725

0.7439

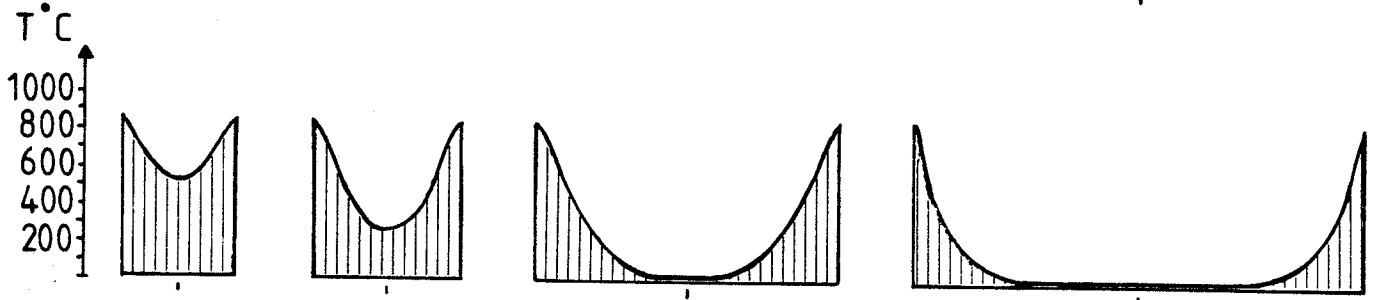
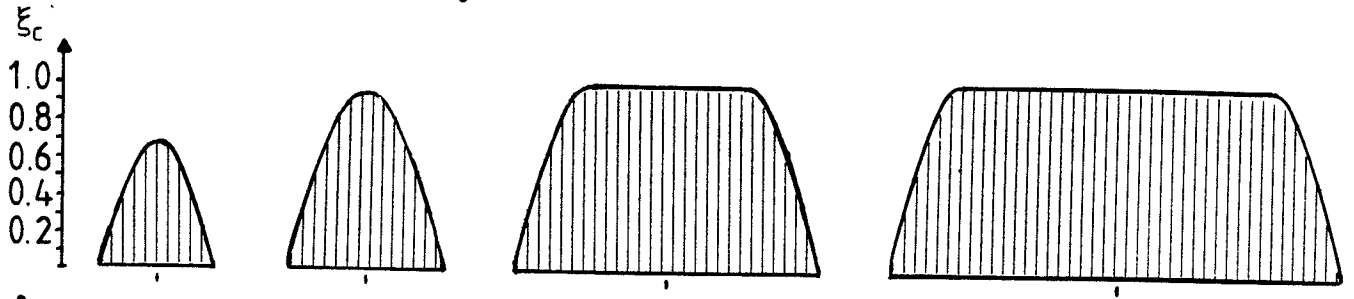
$l_c/l_{c20} = 0.0895$

0.1624

0.3885

0.5065

Thermal diffusivity $3.48 \times 10^7 \text{ m}^2/\text{s}$. $C = 2.4$. $D = 245$. $E = 720$.
 $q = 800 \text{ MJ/m}^2$. $A\sqrt{h}/A_c = 0.08 \text{ m}^2$. HOT



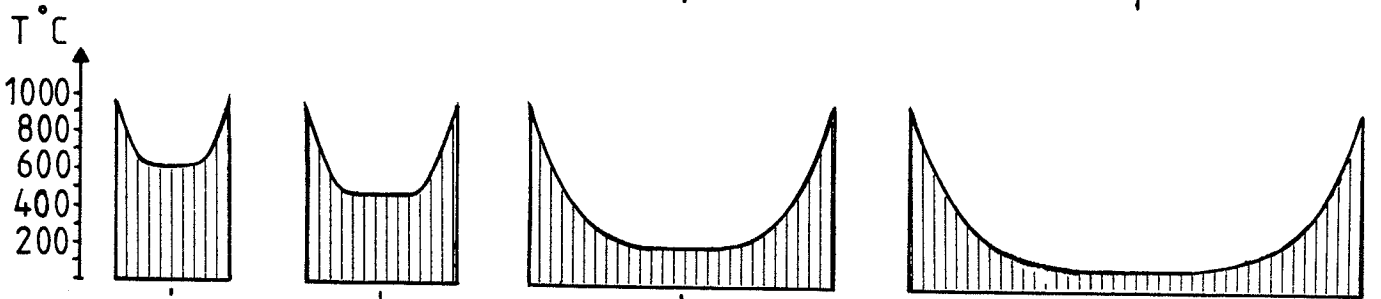
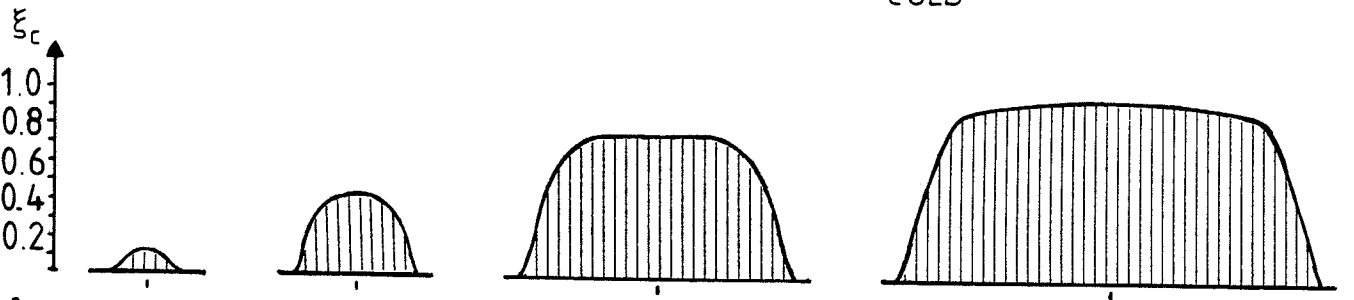
$C = 150\text{mm}$ 200mm 400mm 600mm

$\eta = 0.6374$. 0.6853 . 0.8322 . 0.8855 .

$\frac{1}{10\xi_{CM}^2} \sum_{10\xi_c}^2 = 0.4972$. 0.5619 . 0.7694 . 0.8451 .

$I_c/I_{c20} = 0.0873$. 0.2192 . 0.4814 . 0.6154 .

COLD



$C = 150\text{mm}$ 200mm 400mm 600mm

$\eta = 0.4085$. 0.6124 . 0.7521 . 0.7859 .

$\frac{1}{10\xi_{CM}^2} \sum_{10\xi_c}^2 = 0.3366$. 0.5445 . 0.7070 . 0.7188 .

$I_c/I_{c20} = 0.0009$. 0.0328 . 0.2466 . 0.3743 .

APPENDIX C

EXAMPLES

A number of structural elements has been analysed by means of the procedures presented in the main text, and the main data and results are shown in standardized schedules.

In addition each schedule is provided with two illustrations showing the structural element in question and the development in time of the load bearing capacity and for beams also that of the deflection.

The data of the examples are chosen in accordance with the data of testings reported in the literature, and the test results are for comparison shown with the results of the calculations.

In general the calculations of the load bearing capacities are slightly on the safe side due to the conservative idealizations made in the theory and estimating the material properties.

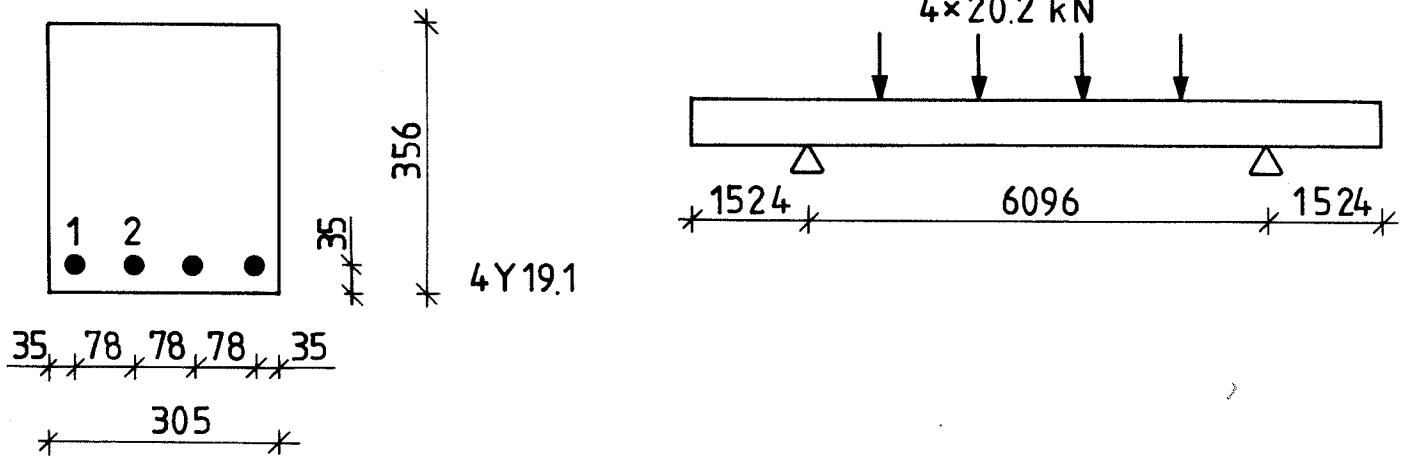
Also the calculated deflections appear to be in a reasonable agreement with the observations.

Yet, some differences are seen immediately before collapse of the structural elements, mainly caused by a plastic behaviour of the reinforcement at this stage of the test and the neglect of creep strains.

The calculational procedures could be extended to take these effects into account, but structural elements, having been so close to collapse, would be of almost no use after the fire, and the contributions to the deflections calculated are found to be clearly unacceptable for most purposes.

EXAMPLE

member: BEAM



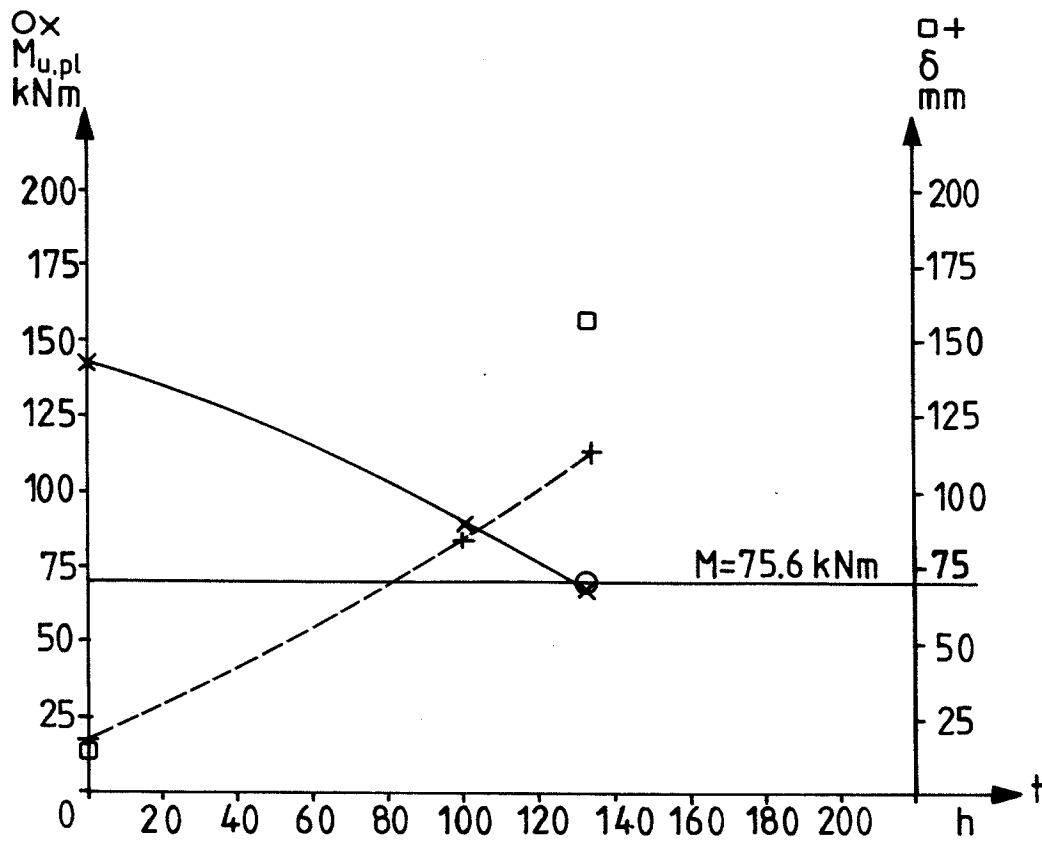
Cross-section and structural system. (All measures in mm).

FIRE DATA: Standard 1.33h

LOAD: $M = 70.6$ kNm, $N =$ kN, $d_N =$ m

REFERENCE: Note 59 (PCA), CRSI [C 1]

t (h)	0.00	1.00	1.33				
C' (h)		2.00	2.66				
$D'_w/D' (^{\circ}\text{C})$	/	195,	268,	/	/	/	/
$E'_w/E' (^{\circ}\text{C})$	/	540,	540,	/	/	/	/
$T_T/T_B (^{\circ}\text{C})$	/	/	/	/	/	/	/
$T_M (^{\circ}\text{C})$		20	20				
$T_{s1} (^{\circ}\text{C})$		502	592				
$T_{s2} (^{\circ}\text{C})$		322	399				
$T_s (^{\circ}\text{C})$		392	458				
ξ_s		0.614	0.468				
ξ_{cm}		1.0000	1.0000				
η		0.9052	0.8695				
f_{cc} (MPa)	35	35	35				
E_{c0} (GPa)	37	37	37				
ϵ_{cu} (/1000)	3.5	3.5	3.5				
f_{su} (MPa)	420	258	197				
$f_{su-\sigma_p}$ (MPa)							
E_s (GPa)	210	129	98				



Comparison of test: O and calculation: X.

CROSS SECTION: $C = 0.305 \text{ m}$ C_{slab} m $A_s = 1146 \text{ mm}^2$

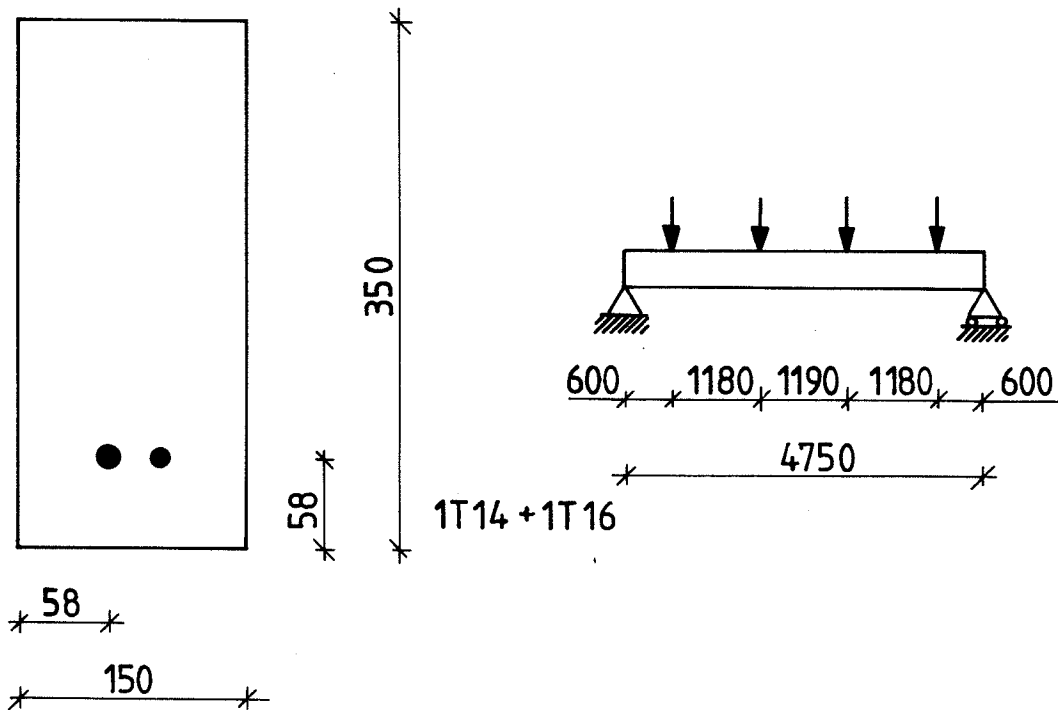
$d_{s1} = 0.321 \text{ m}$ d_{s2} m d_{s3} m

CONCRETE: $a = 0.348 \text{ mm}^2/\text{s}$ aggregate: Elgin gravel age:

t (h)	0.00	1.00	1.33				
\bar{d}_s (m)	0.321	0.321	0.321				
\bar{C} (m)	0.305	0.267	0.253				
P (kN)							
d_{P+N} (m)							
$M_{u,pl}$ (kNm)	143.7	90.4	69.8				
F_{cu} (kN)							
F_{cE} (kN)							
F_{sE} (kN)							
F_{cr} (kN)							
x (m)	0.105	0.092	0.077				
σ_c (MPa)	14.3	17.8	21.3				
κ_{load} (/km)	4.7596	7.2434	11.5073				
δ_{load} (mm)	18.2	28.0	44.5				
δ_{tr} (mm)		0.1	0.2				
δ_{th} (mm)		58.8	69.1				
$\Sigma \delta$ (mm)	18.2	86.9	113.8				
δ_{obs} (mm)	17.8	-	157.5				

EXAMPLE

member: BEAM



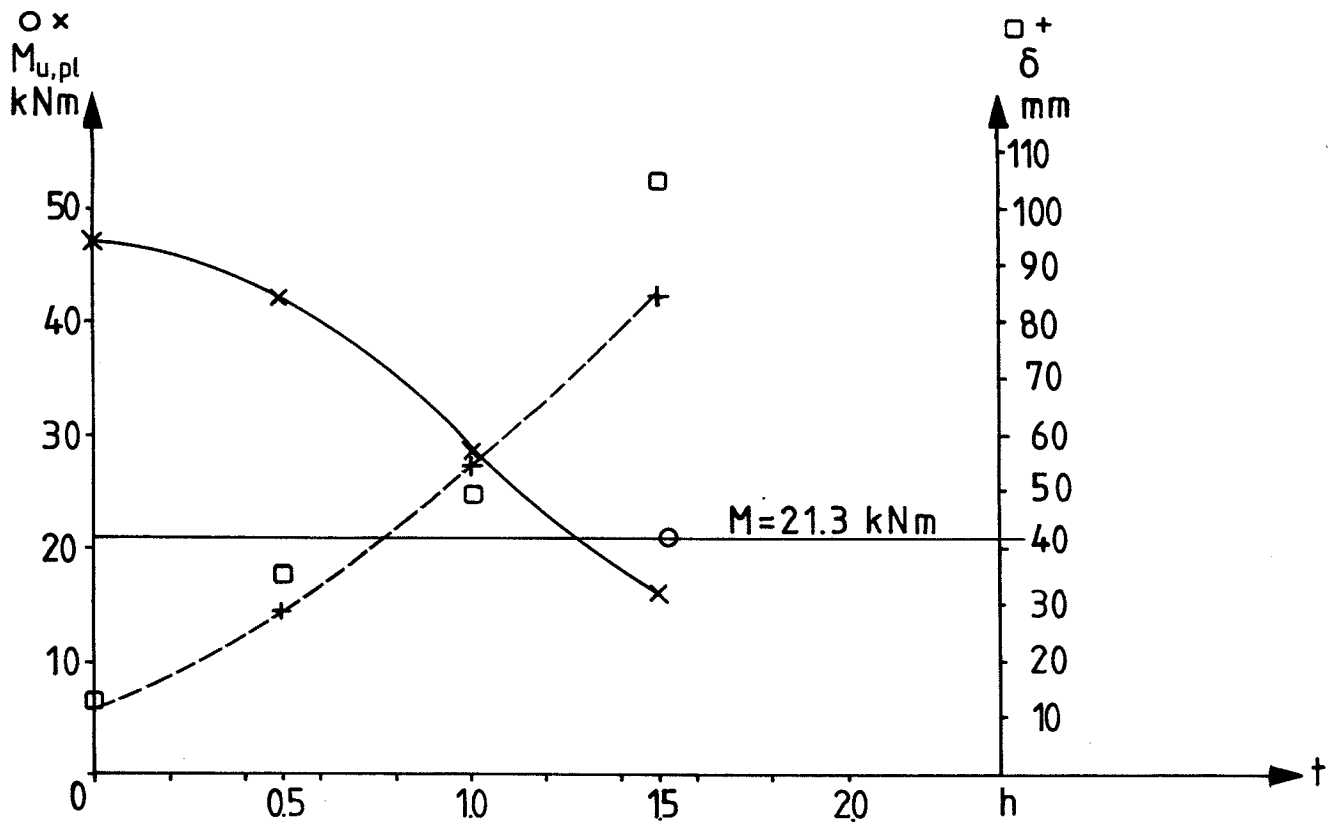
Cross-section and structural system. (All measures in mm).

FIRE DATA: Standard 1.63h

LOAD: $M = 21.3$ kNm, $N =$ kN, $d_N =$ m

REFERENCE: Beam 2, von Postel [C 2]

t (h)	0.00	0.50	1.00	1.50	1.53		
C' (h)		1.00	2.00	3.00			
$D'_w/D' (^{\circ}\text{C})$	/	135,	195,	280,	/	/	/
$E'_w/E' (^{\circ}\text{C})$	/	540,	540,	540,	/	/	/
$T_T/T_B (^{\circ}\text{C})$	/	/	/	/	/	/	/
$T_M (^{\circ}\text{C})$		79	256	405			
$T_{s1} (^{\circ}\text{C})$		195	422	573			
$T_{s2} (^{\circ}\text{C})$							
$T_{s3} (^{\circ}\text{C})$							
ξ_s		0.884	0.613	0.331			
ξ_{cm}		1.0000	0.9435	0.7947			
η		0.8629	0.7829	0.7128			
f_{cc} (MPa)	44	44	41.5	35.0			
E_{c0} (GPa)	39	39	34.7	24.6			
ϵ_{cu} (/1000)	3.5	3.5	3.7	4.4			
f_{su} (MPa)	480	424	294	159			
$f_{su-\sigma_p}$ (MPa)							
E_s (GPa)	210	186	129	69.5			



Comparison of test: O and calculation: X.

CROSS SECTION: $C = 0.150$ m C_{slab} m $A_s = 355$ mm²

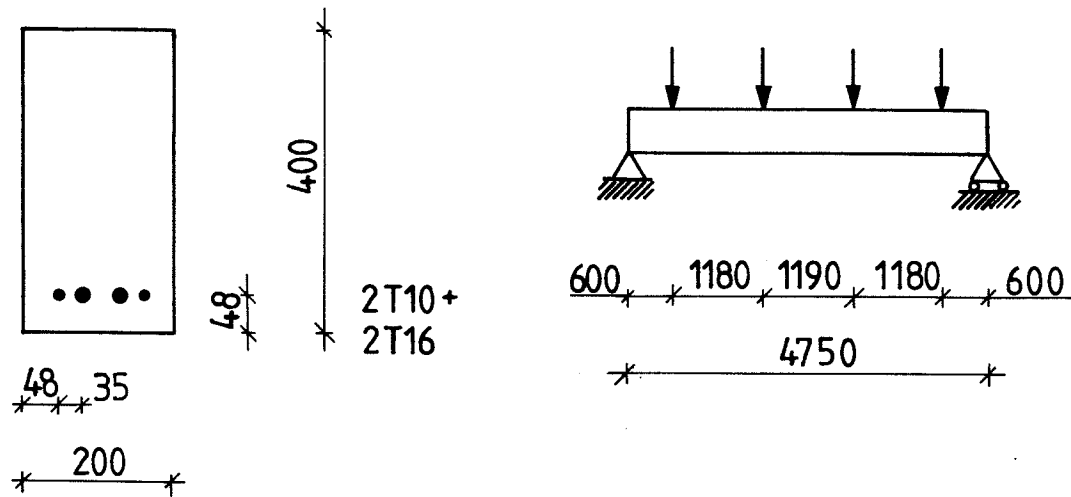
$d_{s1} = 0.292$ m d_{s2} m d_{s3} m

CONCRETE: $a = 0.520$ mm²/s aggregate: Siliceous age: 89 days

t (h)	0.00	0.50	1.00	1.50	1.53		
\bar{d}_s (m)	0.292	0.292	0.292	0.292			
\bar{C} (m)	0.150	0.123	0.108	0.096			
P (kN)							
d_{P+N} (m)							
$M_{u,pl}$ (kNm)	47.6	42.0	29.4	16.1			
F_{cu} (kN)							
F_{cE} (kN)							
F_{sE} (kN)							
F_{cr} (kN)							
x (m)	0.078	0.081	0.079	0.076			
σ_c (MPa)	13.1	15.1	17.4	19.4			
κ_{load} (/km)	5.0368	5.8048	8.2410	15.0941			
δ_{load} (mm)	11.8	13.6	19.4	35.5			
δ_{tr} (mm)		5.4	27.6	56.6			
δ_{th} (mm)		10.5	7.1	- 6.7			
$\Sigma \delta$ (mm)	11.8	29.5	54.1	85.4			
δ_{obs} (mm)	12	34	49	104	failure		

EXAMPLE

member: BEAM



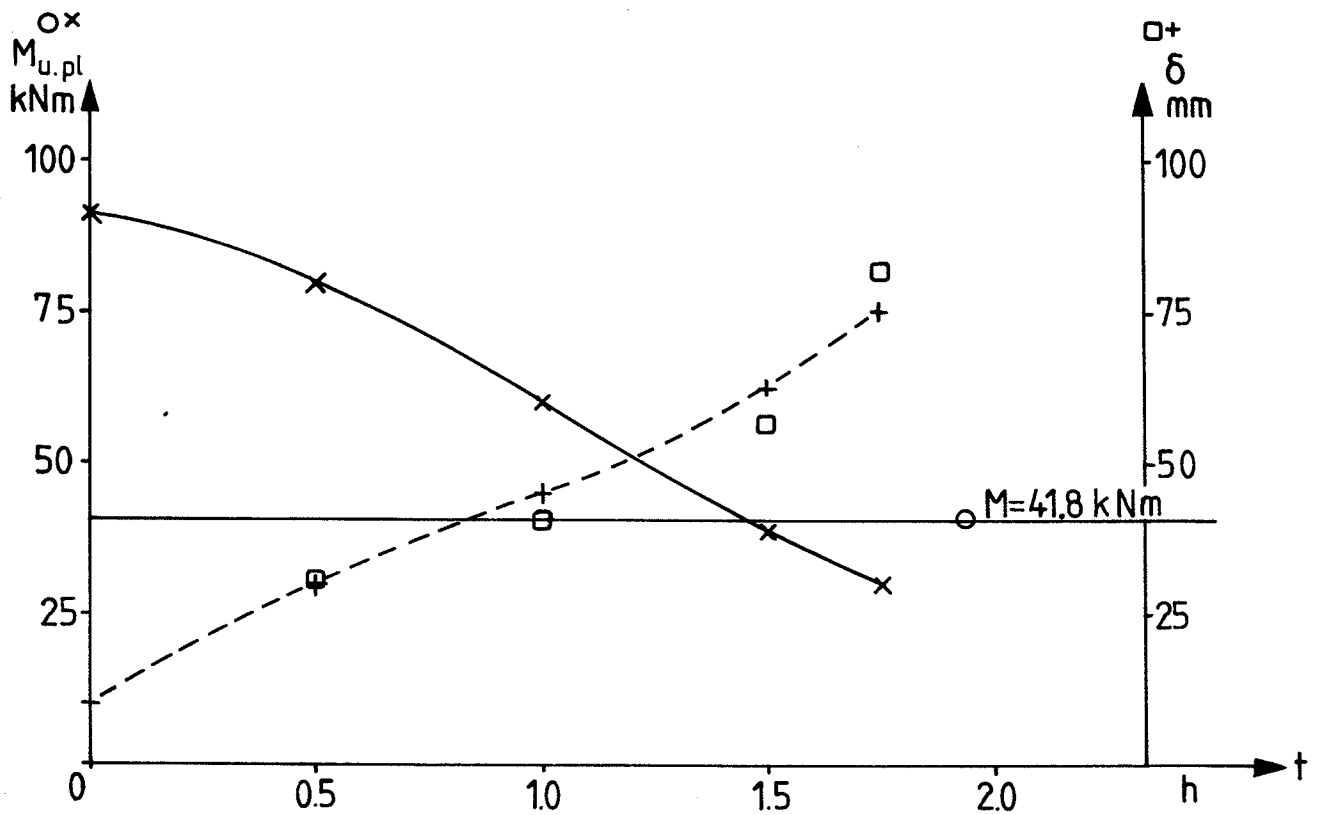
Cross-section and structural system. (All measures in mm).

FIRE DATA: Standard 1.93h

LOAD: $M = 41.8 \text{ kNm}$, $N =$ kN, $d_N =$ m

REFERENCE: Beam 3, von Postel [C 2]

t (h)	0.00	0.50	1.00	1.50	1.75	1.93	
C' (h)		1.00	2.00	3.00	3.50		
$D'_w/D' (^{\circ}\text{C})$	/	135	195	280	306	/	/
$E'_w/E' (^{\circ}\text{C})$	/	540	540	540	540	/	/
$T_T/T_B (^{\circ}\text{C})$	/	/	/	/	/	/	/
$T_M (^{\circ}\text{C})$		20	106	208	252		
$T_{s1} (^{\circ}\text{C})$		282	457	585	635		
$T_{s2} (^{\circ}\text{C})$		175	357	500	556		
$T_s (^{\circ}\text{C})$		225	401	533	584		
ξ_s		0.872	0.665	0.430	0.321		
ξ_{cm}		1.0000	1.0000	0.9920	0.9478		
η		0.8961	0.8282	0.7318	0.7072		
f_{cc} (MPa)	52	52	52	51.6	49.3		
E_{c0} (GPa)	40	40	40	39.4	35.9		
ϵ_{cu} (/1000)	3.5	3.5	3.5	3.5	3.7		
f_{su} (MPa)	480	419	319	206	154		
$f_{su} - \sigma_p$ (MPa)							
E_s (GPa)	210	183	140	90.3	67.4		



Comparison of test: O and calculation: X.

CROSS SECTION: $C = 0.200$ m C_{slab} m $A_s = 559$ mm²

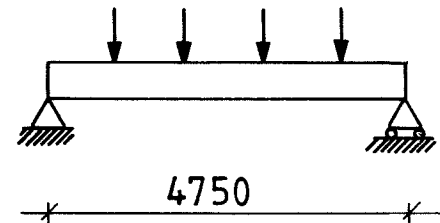
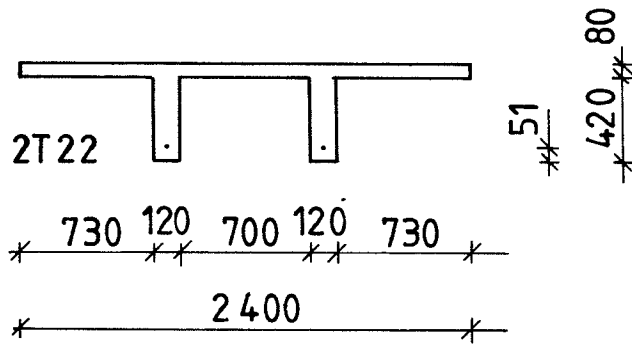
$d_{s1} = 0.352$ m d_{s2} m d_{s3} m

CONCRETE: $a = 0.520$ mm²/s aggregate: Siliceous age: 160 days

t (h)	0.00	0.50	1.00	1.50	1.75	1.93	
\bar{d}_s (m)	0.352	0.352	0.352	0.352	0.352		
\bar{C} (m)	0.200	0.173	0.156	0.132	0.126		
P (kN)							
d_{P+N} (m)							
$M_{u,pl}$ (kNm)	91.0	79.5	60.9	39.7	29.8		
F_{cu} (kN)							
F_{cE} (kN)							
F_{sE} (kN)							
F_{cr} (kN)							
x (m)	0.092	0.093	0.087	0.080	0.076		
σ_c (MPa)	13.5	15.4	17.8	22.4	24.3		
K_{load} (/km)	4.2673	4.9206	6.2653	9.3157	12.329		
δ_{load} (mm)	10.0	11.6	14.7	22.0	29.0		
δ_{tr} (mm)		0.2	6.9	22.0	30.7		
δ_{th} (mm)		17.8	23.3	19.2	16.2		
$\Sigma \delta$ (mm)	10.0	29.6	44.9	63.2	75.9		
δ_{obs} (mm)	-	30.2	40.4	57.6	82.0	failure	

EXAMPLE

member: TT-BEAM



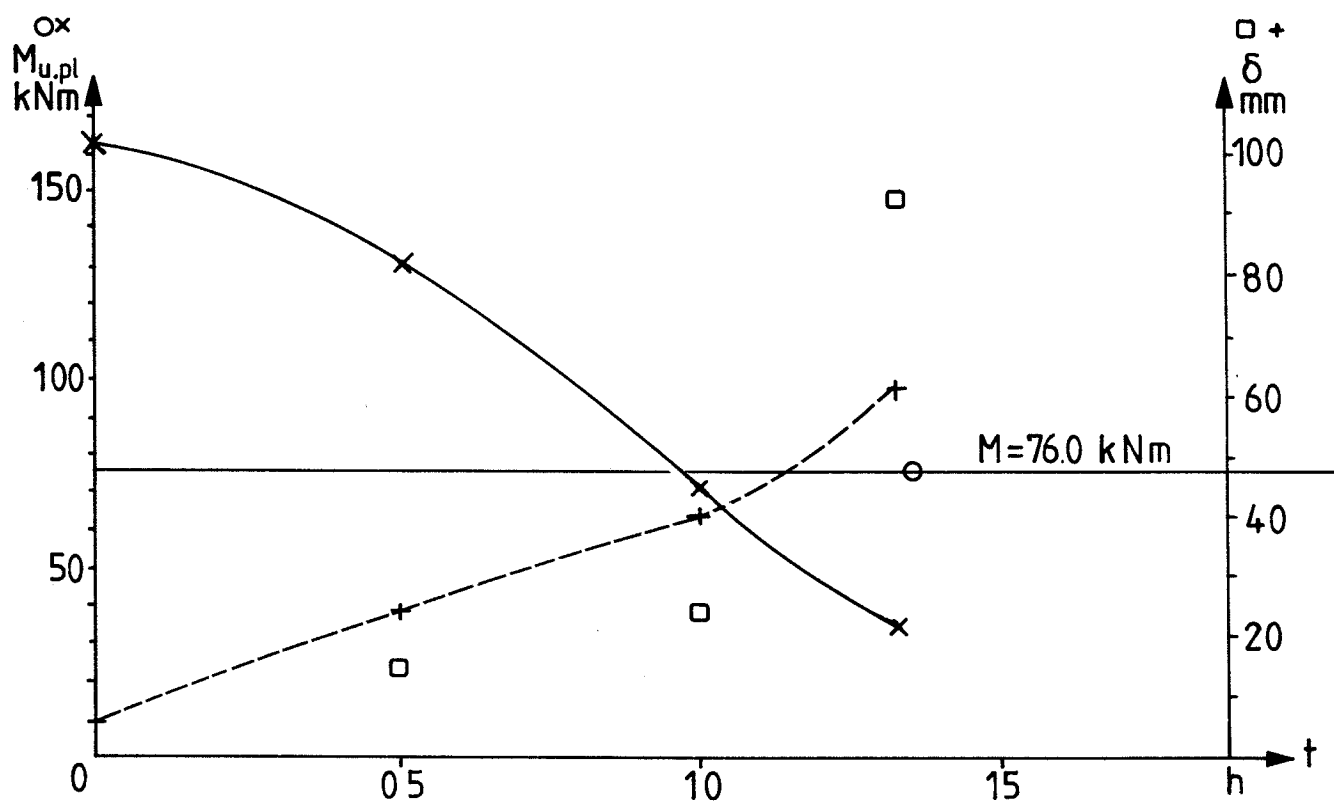
Cross-section and structural system. (All measures in mm).

FIRE DATA: Standard 1.38h

LOAD: $M = 76.0$ kNm, $N =$ kN, $d_N =$ m

REFERENCE: Beam 6, von Postel [C 2]

t (h)	0.00	0.50	1.00	1.33	1.38		
C' (h)		1.00	2.00	2.66			
$D'_w/D' (^{\circ}C)$	/	135 / 150	195 / 220	268 / 295	/	/	/
$E'_w/E' (^{\circ}C)$	/	540 / 600	540 / 600	540 / 600	/	/	/
$T_{T/T_B} (^{\circ}C)$	/	30 / 750	122 / 820	175 / 895	/	/	/
$T_M (^{\circ}C)$		289	521	630			
$T_{s1} (^{\circ}C)$							
$T_{s2} (^{\circ}C)$							
$T_{s3} (^{\circ}C)$							
ξ_s		0.791	0.439	0.210			
ξ_{CM}		1.0000	1.0000	1.0000			
η							
f_{cc} (MPa)	47	47	47	47			
E_{c0} (GPa)	39	39	39	39			
ϵ_{cu} (/1000)	3.5	3.5	3.5	3.5			
f_{su} (MPa)	480	380	211	101			
$f_{su-\sigma_p}$ (MPa)							
E_s (GPa)	210	166	92.3	44.2			



Comparison of test: O and calculation: X.

CROSS SECTION: $C = 0.120 \text{ m}$ $C_{\text{slab}} = 0.320 \text{ m}$ $A_s = 760 \text{ mm}^2$

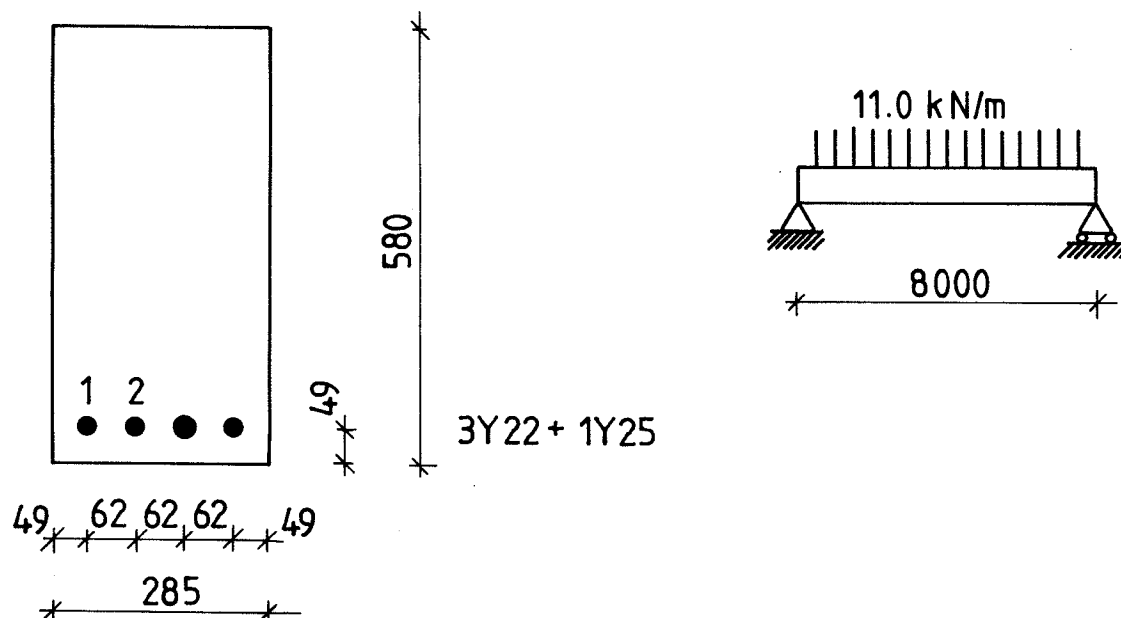
$d_{s1} = 0.449 \text{ m}$ $d_{s2} = \text{m}$ $d_{s3} = \text{m}$

CONCRETE: $a = 0.520 \text{ mm}^2/\text{s}$ aggregate: Siliceous age: 106 days

t (h)	0.00	0.50	1.00	1.33	1.38		
\bar{d}_s (m)	0.449	0.449	0.449	0.449			
\bar{C} (m)	2.400	2.400	2.400	2.400			
P (kN)							
d_{P+N} (m)							
$M_{u,pl}$ (kNm)	163.2	129.3	71.9	34.4			
F_{cu} (kN)							
F_{cE} (kN)							
F_{sE} (kN)							
F_{cr} (kN)							
x (m)	0.038	0.034	0.026	0.018			
σ_c (MPa)	3.8	4.2	5.5	7.7			
κ_{load} (/km)	2.6555	3.3170	5.8127	11.8556			
δ_{load} (mm)	6.2	7.8	13.7	27.9			
δ_{tr} (mm)		0.1	1.6	3.4			
δ_{th} (mm)		16.1	24.8	31.4			
$\Sigma \delta$ (mm)	6.2	24.0	40.1	62.7			
δ_{obs} (mm)	-	14.2	23.2	92.2	failure		

EXAMPLE

member: BEAM



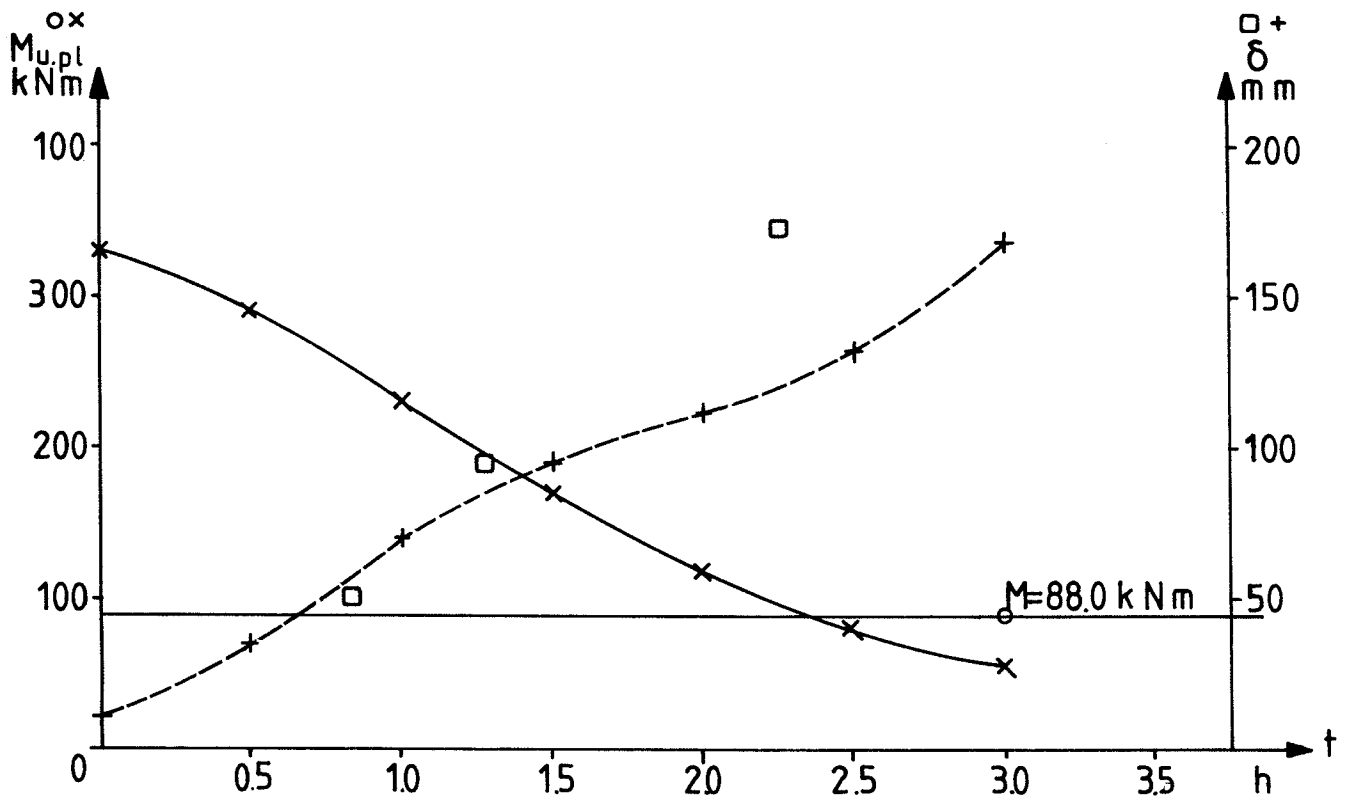
Cross-section and structural system. (All measures in mm).

FIRE DATA: Standard 3.00h

LOAD: $M = 88.0 \text{ kNm}$, $N =$ kN, $d_N =$ m

REFERENCE: Beam M.2, Deutschmann [C 3]

t (h)	0.00	0.50	1.00	1.50	2.00	2.50	3.00
C' (h)		1.00	2.00	3.00	4.00	5.00	6.00
$D'_w/D' (^{\circ}\text{C})$	/	135,	195,	280,	325,	348,	370,
$E'_w/E' (^{\circ}\text{C})$	/	540,	540,	540,	540,	540,	540,
$T_T/T_B (^{\circ}\text{C})$	/	/	/	/	/	/	/
$T_M (^{\circ}\text{C})$		20	20	43	102	156	204
$T_{s1} (^{\circ}\text{C})$		271	448	571	651	703	747
$T_{s2} (^{\circ}\text{C})$		153	295	441	498	596	628
$\bar{T}_s (^{\circ}\text{C})$		204	354	484	535	626	660
$\bar{\xi}_s$		0.868	0.685	0.493	0.341	0.238	0.156
ξ_{cm}		1.0000	1.0000	1.0000	1.0000	0.9287	0.8642
η		0.9196	0.8599	0.7870	0.7180	0.6996	0.6748
$f_{cc} \text{ (MPa)}$	25	25	25	25	25	23.2	21.6
$E_{c0} \text{ (GPa)}$	31	31	31	31	31	26.7	23.2
$\epsilon_{cu} \text{ (/1000)}$	3.5	3.5	3.5	3.5	3.5	3.8	4.1
$f_{su} \text{ (MPa)}$	420	365	288	207	143	100	65.5
$f_{su-\sigma_p} \text{ (MPa)}$							
$E_s \text{ (GPa)}$	210	182	144	103	71.7	50.0	32.7



Comparison of test: O and calculation: X.

CROSS SECTION: $C = 0.285 \text{ m}$ $C_{\text{slab}} = \text{m}$ $A_s = 1631 \text{ mm}^2$

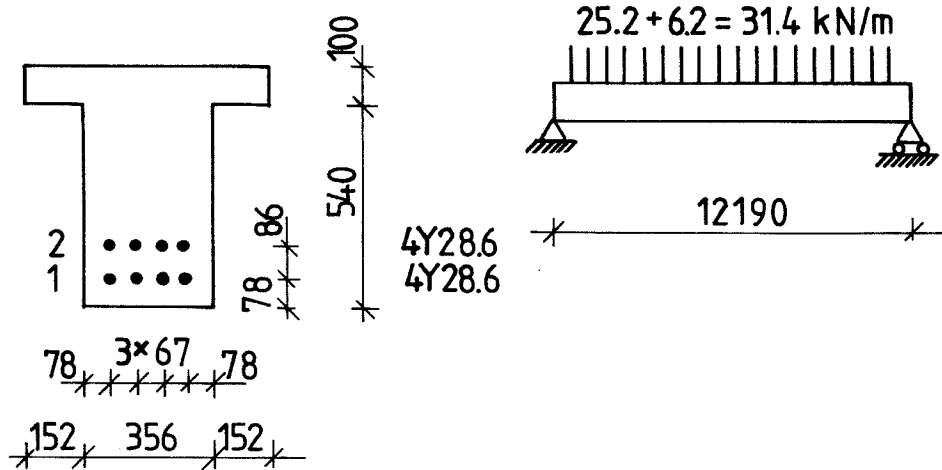
$d_{s1} = 0.531 \text{ m}$ $d_{s2} = \text{m}$ $d_{s3} = \text{m}$

CONCRETE: $a = 0.520 \text{ mm}^2/\text{s}$ aggregate: age:

t (h)	0.00	0.50	1.00	1.50	2.00	2.50	3.00
\bar{d}_s (m)	0.531	0.531	0.531	0.531	0.531	0.531	0.531
\bar{C} (m)	0.285	0.255	0.233	0.207	0.183	0.177	0.169
P (kN)							
d_{P+N} (m)							
$M_{u,pl}$ (kNm)	331	289	231	169	118.5	83.7	55.4
F_{cu} (kN)							
F_{cE} (kN)							
F_{sE} (kN)							
F_{cr} (kN)							
x (m)	0.175	0.174	0.166	0.154	0.142	0.134	0.125
σ_c (MPa)	7.1	7.9	9.0	10.6	12.6	13.4	14.5
K_{load} (/km)	1.5336	1.7629	2.1638	2.9059	4.0157	5.6223	8.3563
δ_{load} (mm)	10.2	11.8	14.4	19.4	26.8	37.5	55.7
δ_{tr} (mm)		0.2	0.5	5.4	22.7	40.3	61.2
δ_{th} (mm)		30.1	54.6	70.4	62.4	62.1	52.3
$\Sigma \delta$ (mm)	10.2	42.1	69.5	95.2	111.9	139.9	169.2
δ_{obs} (mm)			50	90		170	failure

EXAMPLE

member: BEAM



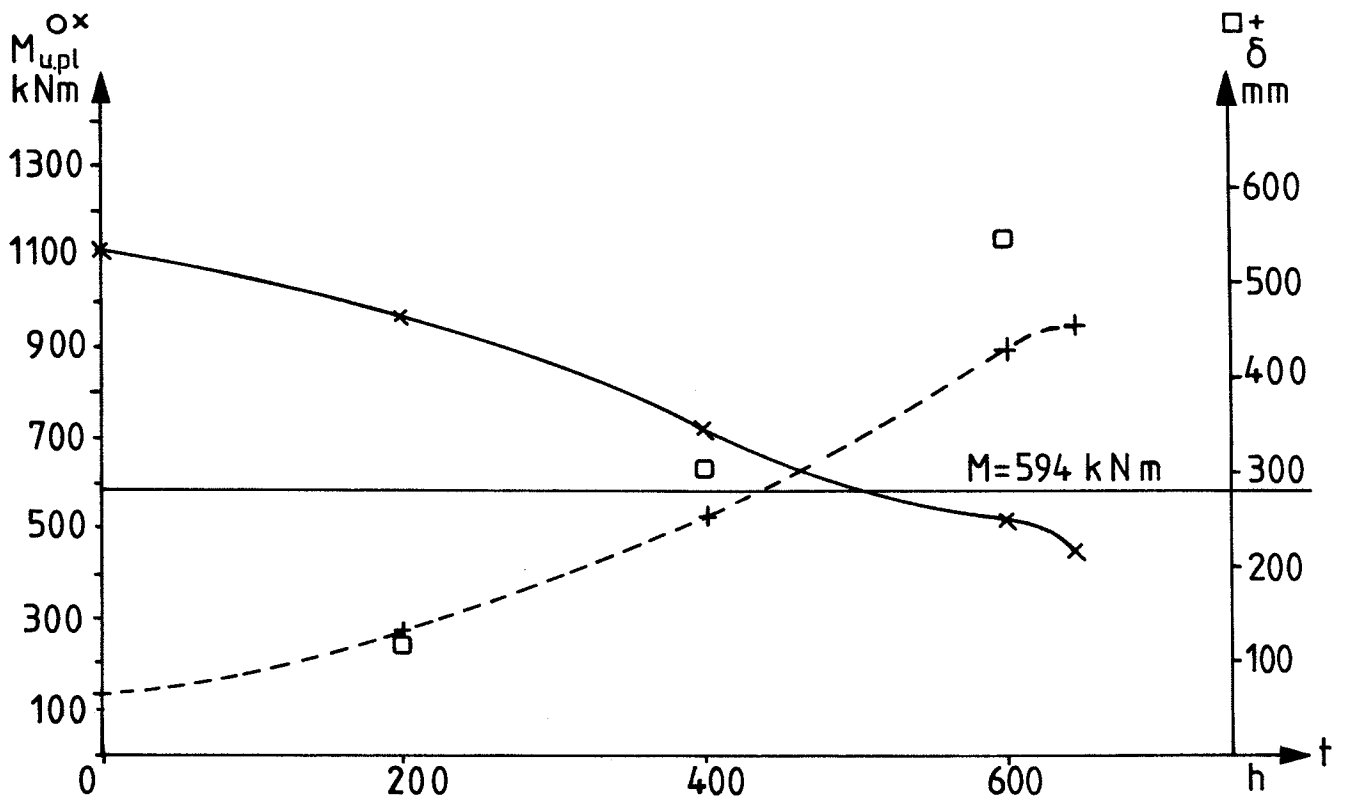
Cross-section and structural system. (All measures in mm).

FIRE DATA: Standard 6.22 h

LOAD: $M = 594$ kNm, $N =$ kN, $d_N =$ m

REFERENCE: Beam 85, Gustaferro et al, [C 4]

t (h)	0.00	2.00	4.00	6.00	6.22		
C' (h)		4.00	8.00	12.00	12.44		
$D'_w/D' (^{\circ}C)$	/	325,360	410,460	478,513	483,519	/	/
$E'_w/E' (^{\circ}C)$	/	540,600	540,600	540,600	540,600	/	/
$T_T/T_B (^{\circ}C)$	/	99,960	243,1060	355,1113	366,1119	/	/
$T_M (^{\circ}C)$		20	69	164	173		
$T_{s1} (^{\circ}C)$		308/179	546/389	691/546	703/562		
$T_{s2} (^{\circ}C)$		171/31	365/137	500/272	512/287		
$T_s (^{\circ}C)$		164	318	422	432		
ξ_s		0.890	0.669	0.453	0.432		
ξ_{CM}		1.0000	1.0000	1.0000	1.0000		
η		0.9133	0.7549	0.6647	0.6562		
f_{cc} (MPa)	40.7	40.7	40.7	40.7	40.7		
E_{c0} (GPa)	38	38	38	38	38		
ϵ_{cu} (/1000)	3.5	3.5	3.5	3.5	3.5		
f_{su} (MPa)	455	397	292	192	185		
$f_{su-\sigma_p}$ (MPa)							
E_s (GPa)	210	183	135	89	85		



Comparison of test: O and calculation: X.

CROSS SECTION: $C = 0.356 \text{ m}$ $C_{\text{slab}} = 0.400 \text{ m}$ $A_s = 5130 \text{ mm}^2$

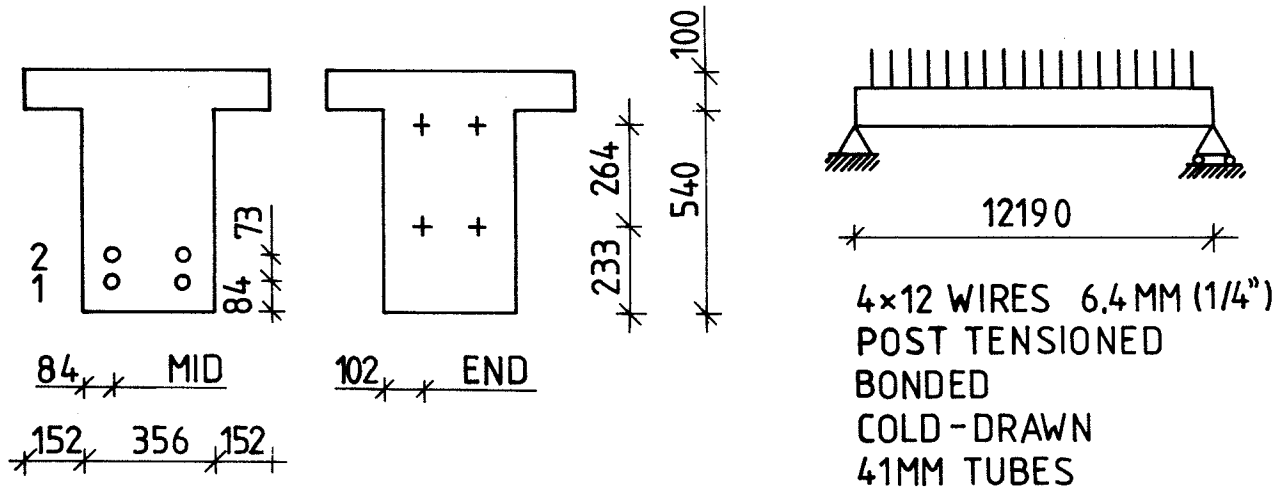
$d_{s1} = 0.562 \text{ m}$ $d_{s2} = 0.476 \text{ m}$ $d_{s3} = \text{m}$

CONCRETE: $a = 0.348 \text{ mm/s}$ aggregate: Elgin gravel age: 903 days

t (h)	0.00	2.00	4.00	6.00	6.22		
\bar{d}_s (m)	0.519	0.516	0.510	0.501	0.499	(fact	1.22)
C (m)	0.434	0.386	0.299	0.253	0.248		
P (kN)							
d_{P+N} (m)							
$M_{u,pl}$ (kNm)	1110	974	721	513	455		
F_{cu} (kN)							
F_{cE} (kN)							
F_{sE} (kN)							
F_{cr} (kN)							
x (m)	0.225	0.227	0.232	0.225	0.225		
σ_c (MPa)	24.2	26.7	32.3	37.0	37.5		
κ_{load} (/km)	4.2777	5.0314	7.2795	11.389	12.080		
δ_{load} (mm)	66.2	77.9	112.7	176.3	187.0		
δ_{tr} (mm)		1.3	50.1	191.1	209.8		
δ_{th} (mm)		56.0	87.2	56.8	52.7		
$\Sigma \delta$ (mm)	66.2	135.2	250.0	424.2	449.5		
δ_{obs} (mm)	-	132	302	574	failure		

EXAMPLE

member: BEAM, PRESTRESSED



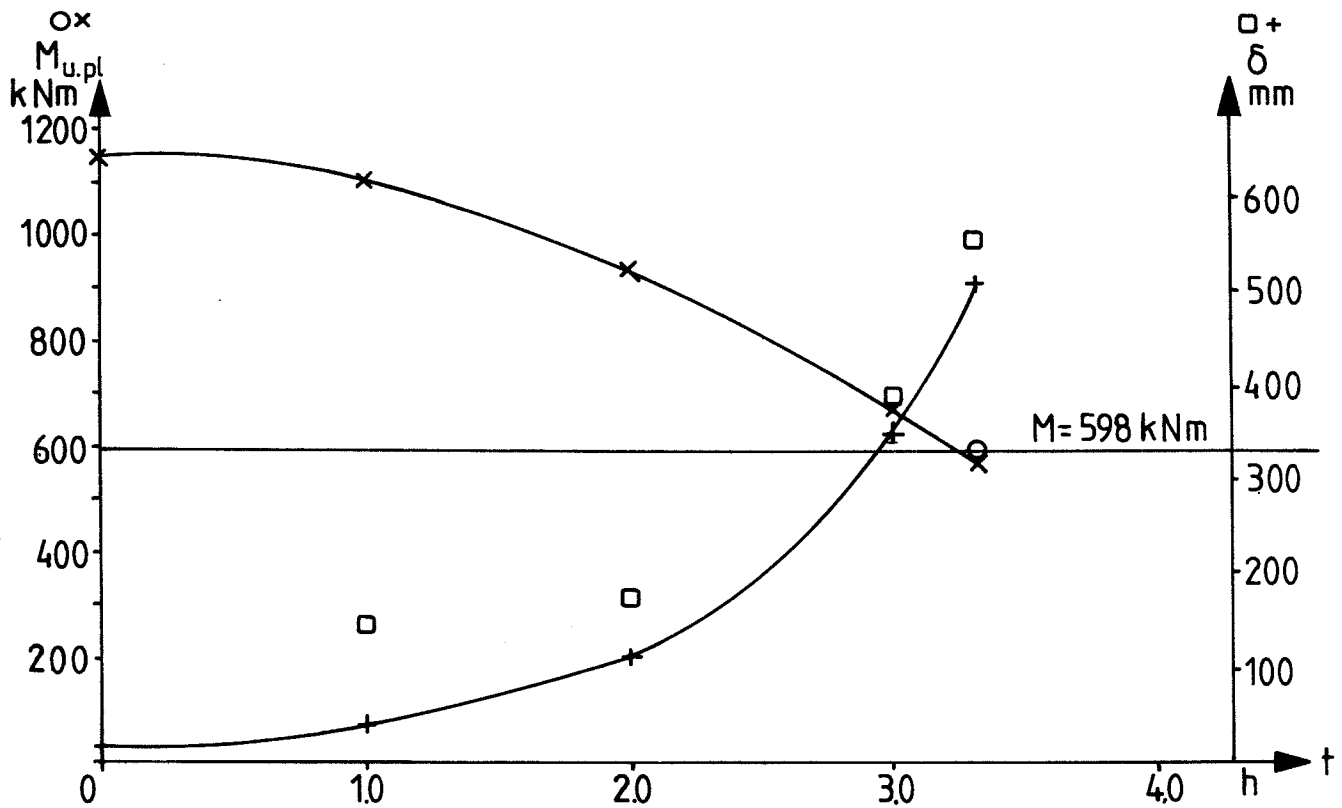
Cross-section and structural system. (All measures in mm).

FIRE DATA: Standard 3.33 m

LOAD: $M = 598$ kNm, $N =$ kN, $d_N =$ m

REFERENCE: Beam 78, Gustaferro et al, [C 4]

t (h)	0.00	1.00	2.00	3.00	3.33		
C' (h)		2.00	4.00	6.00	6.66		
$D'_w/D' (^{\circ}C)$	/	195,220	325,360	370,410	396,428	/	/
$E'_w/E' (^{\circ}C)$	/	540,600	540,600	540,600	540,600	/	/
$T_{T_B}/T_B (^{\circ}C)$	/	20,820	99,960	171,1010	196,1028	/	/
$T_M (^{\circ}C)$		20	20	20	35		
$T_{s1} (^{\circ}C)$		91	260	399	439		
$T_{s2} (^{\circ}C)$		47	144	251	284		
$T_s (^{\circ}C)$		69	196	305	332		
ξ_s		0.958	0.804	0.577	0.490		
ξ_{cm}		1.0000	1.0000	1.0000	1.0000		
η		0.9193	0.8476	0.7999	0.7799		
f_{cc} (MPa)	43.4	43.4	43.4	43.4	43.4		
E_{c0} (GPa)	39	39	39	39	39		
ϵ_{cu} (/1000)	3.5	3.5	3.5	3.5	3.5		
f_{su} (MPa)	1579	1513	1270	911	774		
$f_{su-\sigma_p}$ (MPa)	417	400	336	241	205		
E_s (GPa)	69.5	66.6	56.0	40.1	34.1		



Comparison of test: O and calculation: X.

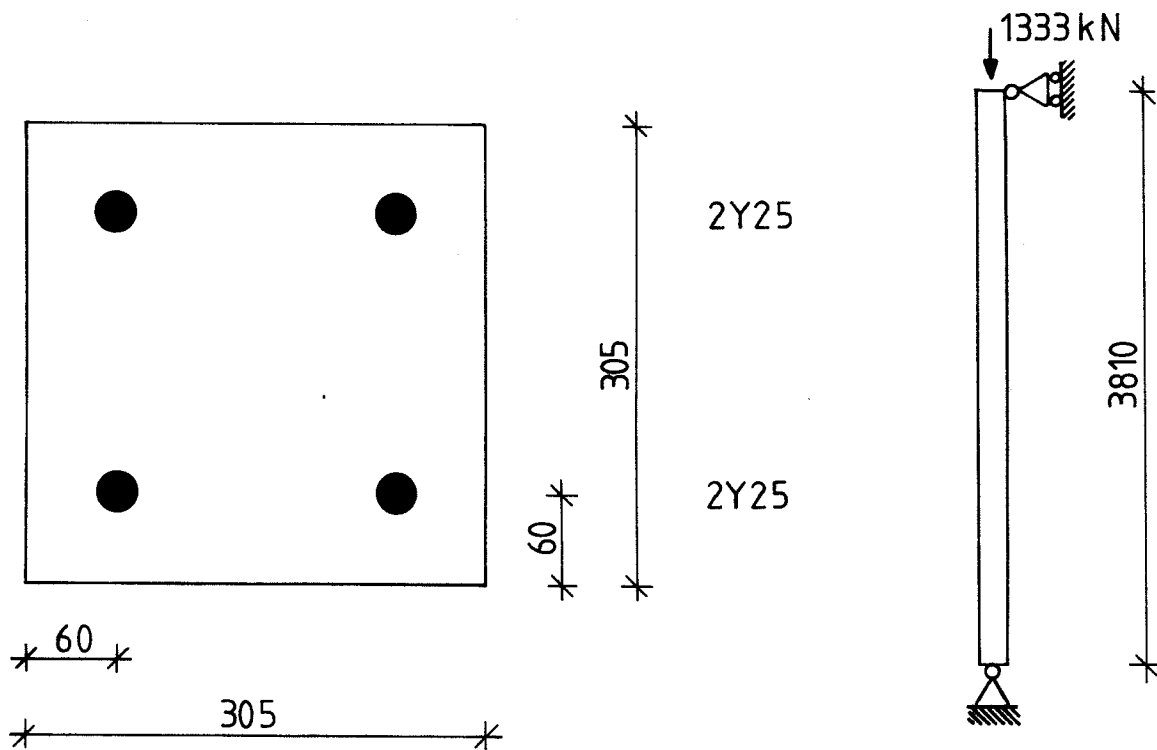
CROSS SECTION: $C = 0.356 \text{ m}$ $C_{\text{slab}} = 0.400 \text{ m}$ $A_s = 1520 \text{ mm}^2$
 $d_{s1} = 0.556 \text{ m}$ $d_{s2} = 0.483 \text{ m}$ $d_{s3} = \text{m}$

CONCRETE: $a = 0.348 \text{ mm}^2/\text{s}$ aggregate: Elgin gravel age: 910 days

t (h)	0.00	1.00	2.00	3.00	3.33		
\bar{d}_s (m)	0.520	0.519	0.516	0.509	0.506	(fact	1.22)
\bar{C} (m)	0.434	0.388	0.346	0.322	0.312		
P (kN)	1766	1692	1420	1019	865		
d_{P+N} (m)	0.181	0.166	0.095	-0.078	-0.185		
$M_{u,pl}$ (kNm)	1148	1101	931	671	571		
F_{cu} (kN)							
F_{cE} (kN)							
F_{sE} (kN)							
F_{cr} (kN)							
x (m)	0.525	0.482	0.310	0.161	0.142		
σ_c (MPa)	14.5	16.7	24.2	38.5	41.5		
κ_{load} (/km)	0.8616	0.1300	2.9375	15.060	24.619		
δ_{load} (mm)	13.3	17.5	45.5	233.1	381.1		
δ_{tr} (mm)		0.7	2.1	4.8	21.8		
δ_{th} (mm)		18.4	67.7	111.6	114.4		
$\Sigma \delta$ (mm)	13.3	36.6	115.3	349.5	517.3		
δ_{obs} (mm)	-	142	170	381	559		

EXAMPLE

member: COLUMN



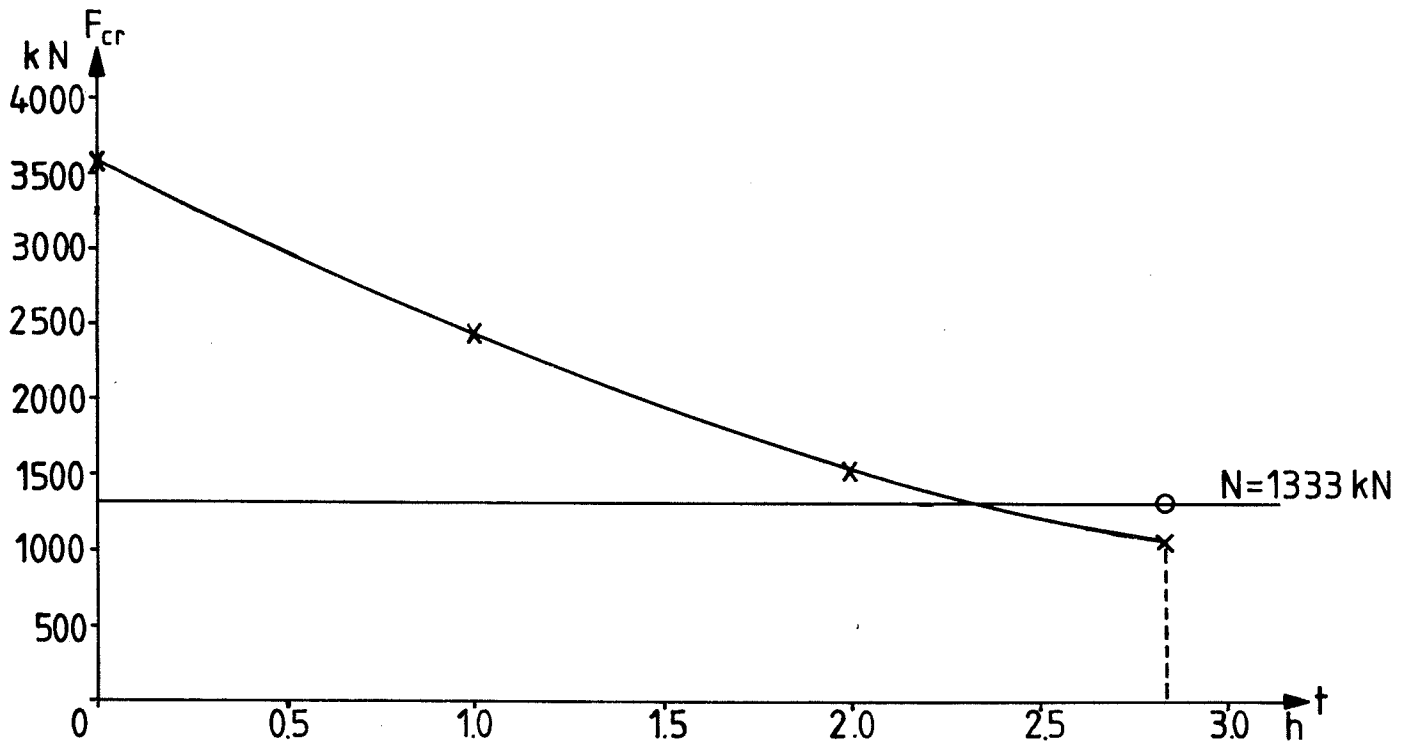
Cross-section and structural system. (All measures in mm).

FIRE DATA: Standard 2.83h

LOAD: $M =$ kNm, $N = 1333$ kN, $d_N = 0.153$ m

REFERENCE: Column 2, Lie, Allen and Abrams [C 5]

t (h)	0.00	1.00	2.00	2.83			
C' (h)		2.00	4.00	5.66			
$D'_w/D' (^{\circ}\text{C})$	/	195,	325,	370,	/	/	/
$E'_w/E' (^{\circ}\text{C})$	/	540,	540,	540,	/	/	/
$T_T/T_B (^{\circ}\text{C})$	/	/	/	/	/	/	/
$T_M (^{\circ}\text{C})$		20	106	217			
$T_{s1} (^{\circ}\text{C})$		354	569	668			
$T_{s2} (^{\circ}\text{C})$							
$T_s (^{\circ}\text{C})$							
ξ_s		0.711	0.340	0.157			
ξ_{cm}		1.0000	1.0000	1.0000			
η		0.8857	0.7831	0.7197			
f_{cc} (MPa)	37	37	37	37			
E_{c0} (GPa)	37	37	37	37			
ϵ_{cu} (/1000)	3.5	3.5	3.5	3.5			
f_{su} (MPa)	444	316	151	69.8			
$f_{su-\sigma_p}$ (MPa)							
E_s (GPa)	210	149	71.3	33.0			



Comparison of test: O and calculation: X.

CROSS SECTION: $C = 0.305$ m $C_{\text{slab}} =$ m $A_s = 1963$ mm²

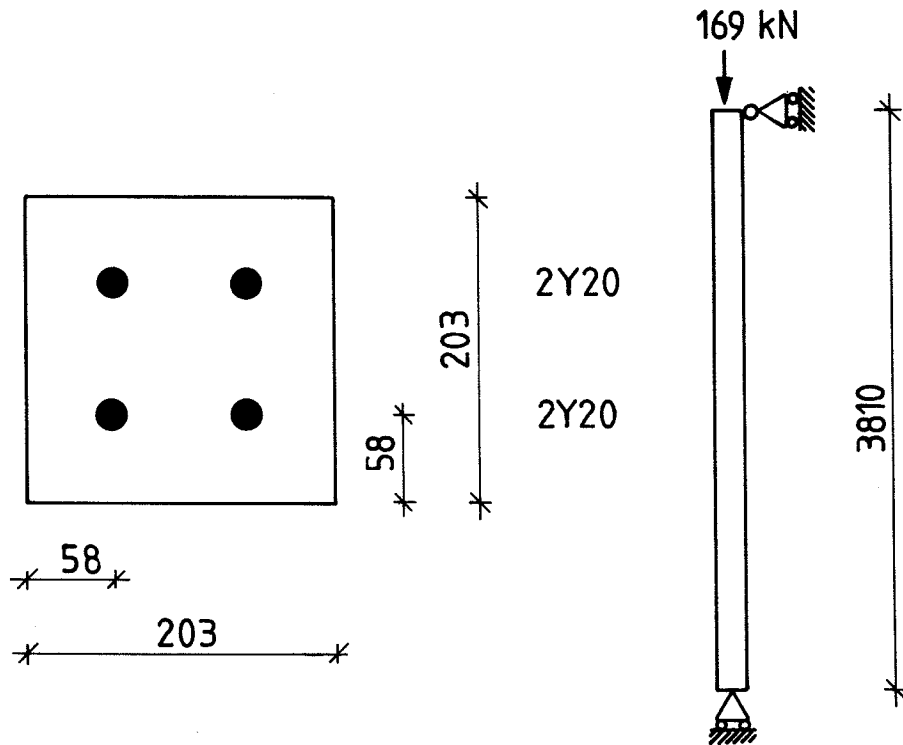
$d_{s1} = 0.245$ m $d_{s2} =$ m $d_{s3} =$ m

CONCRETE: $a = 0.520$ mm²/s aggregate: Siliceous age:

t (h)	0.00	1.00	2.00	2.83			
\bar{d}_s (m)							
\bar{C} (m)	0.305	0.259	0.220	0.197			
P (kN)							
d_{P+N} (m)							
$M_{u,pl}$ (kNm)							
F_{cu} (kN)	3442	2490	1793	1432			
F_{ce} (kN)	18141	9496	4925	3139			
F_{se} (kN)	2398	1702	814	377			
F_{cr} (kN)	3565	2434	1532	1085			
x (m)							
σ_c (MPa)							
K_{load} (/km)							
δ_{load} (mm)							
δ_{tr} (mm)							
δ_{th} (mm)							
$\Sigma \delta$ (mm)				Compr. failure			
δ_{obs} (mm)							

EXAMPLE

member: COLUMN



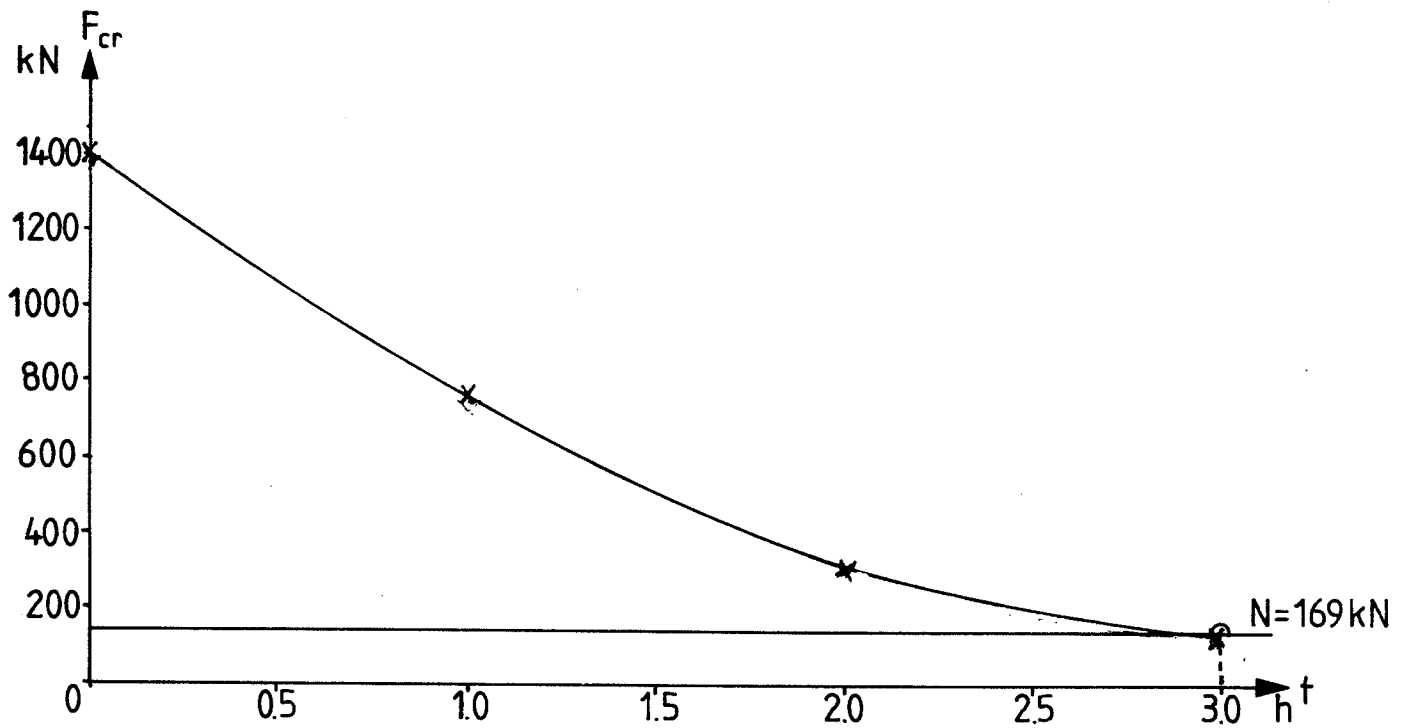
Cross-section and structural system. (All measures in mm).

FIRE DATA: Standard 3.00h

LOAD: $M =$ kNm, $N = 169$ kN, $d_N = 0.102$ m

REFERENCE: Colomn 6, Lie, Allen and Abrams [C 5]

t (h)	0.00	1.00	2.00	3.00			
C' (h)		2.00	4.00	6.00			
$D'_w/D' (^{\circ}\text{C})$	/	195,	325,	370,	/	/	/
$E'_w/E' (^{\circ}\text{C})$	/	540,	540,	540,	/	/	/
$T_T/T_B (^{\circ}\text{C})$	/	/	/	/	/	/	/
$T_M (^{\circ}\text{C})$		142	389	572			
$T_{s1} (^{\circ}\text{C})$		371	611	733			
$T_{s2} (^{\circ}\text{C})$							
$T_s (^{\circ}\text{C})$							
ξ_s		0.688	0.246	0.098			
ξ_{cm}		1.0000	0.9077	0.7443			
η		0.8310	0.6917	0.6231			
f_{cc} (MPa)	42	42	38.1	31.3			
E_{c0} (GPa)	39	39	32.1	21.6			
ϵ_{cu} (/1000)	3.5	3.5	3.86	4.7			
f_{su} (MPa)	442	304	108.6	43.5			
$f_{su} - \sigma_p$ (MPa)							
E_s (GPa)	210	145	51.6	20.7			



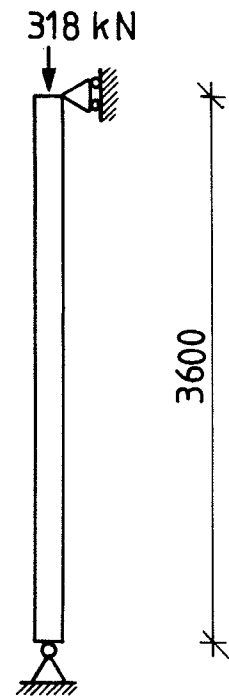
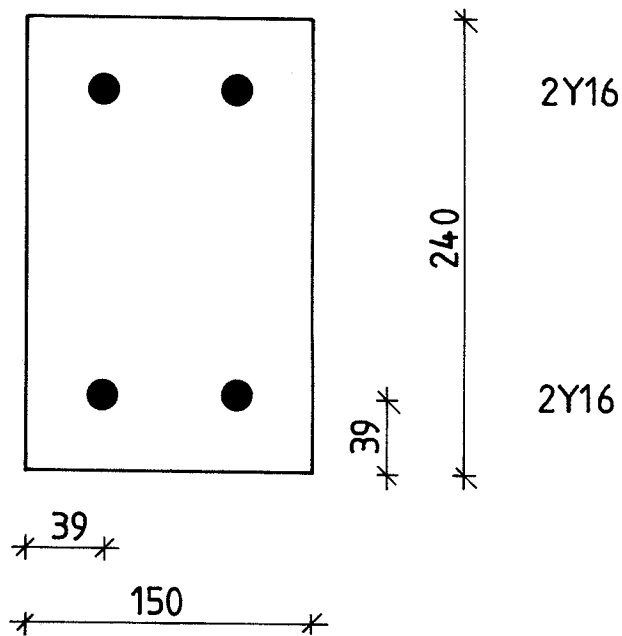
Comparison of test: O and calculation: X.

CROSS SECTION: $C = 0.203$ m $C_{slab} =$ m $A_s = 1257$ mm²

$d_{s1} = 0.145$ m $d_{s2} =$ m $d_{s3} =$ m

CONCRETE: $a = 0.520$ mm/s aggregate: Siliceous age:

t (h)	0.00	1.00	2.00	3.00			
\bar{d}_s (m)							
\bar{C} (m)	0.203	0.159	0.124	0.108			
P (kN)							
d_{P+N} (m)							
$M_{u,pl}$ (kNm)							
F_{cu} (kN)	1731	1056	588	365			
F_{cE} (kN)	3753	1398	433	167			
F_{sE} (kN)	340	234	83.4	33.5			
F_{cr} (kN)	1467	764	302	136			
x (m)							
σ_c (MPa)							
κ_{load} (/km)							
δ_{load} (mm)							
δ_{tr} (mm)							
δ_{th} (mm)							
$\Sigma \delta$ (mm)							
δ_{obs} (mm)				Buckl. failure			



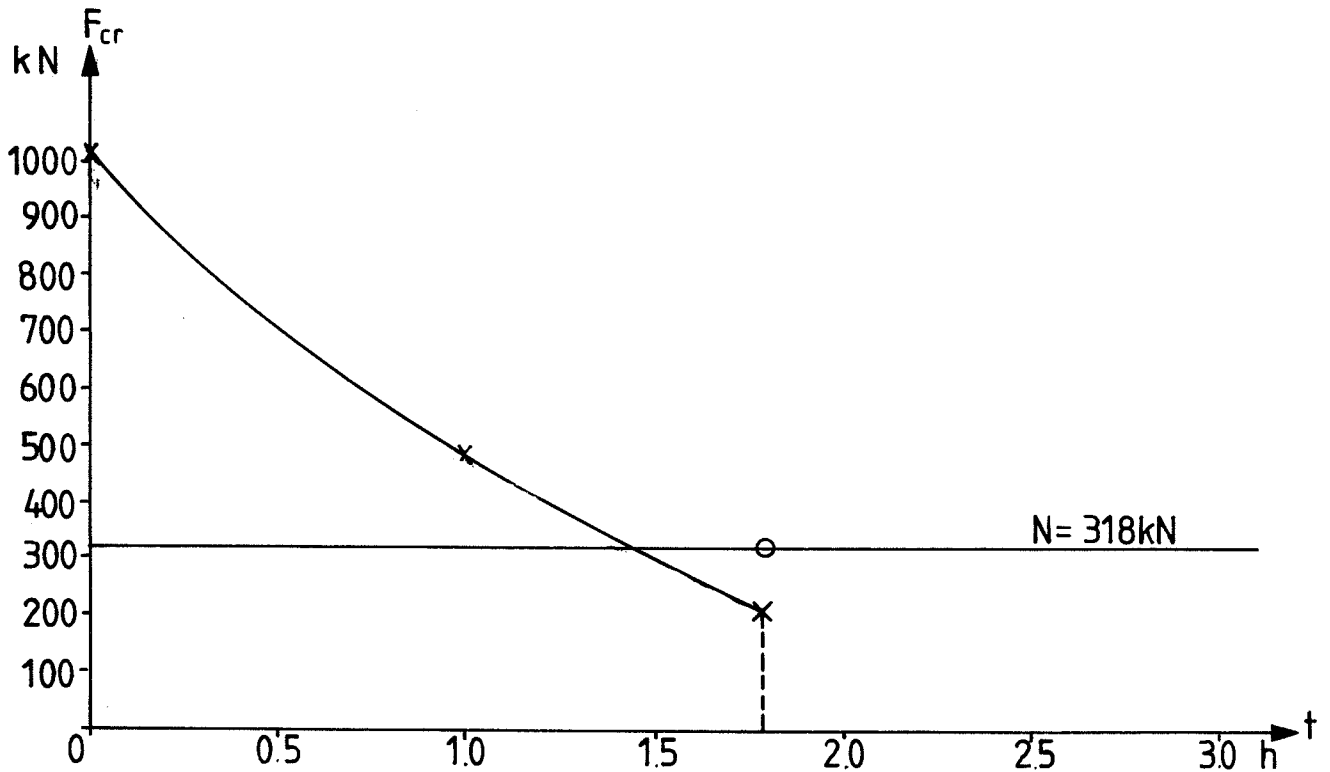
Cross-section and structural system. (All measures in mm).

FIRE DATA: Standard 1.78h

LOAD: $M =$ kNm, $N = 318$ kN, $d_N =$ m

REFERENCE: Column 5, Seekamp, Becker, Struck [C 6]

t (h)	0.00	1.00	1.78				
C' (h)		2.00	3.56				
D _w '/D' (°C)	/	195,	309,	/	/	/	/
E _w '/E' (°C)	/	540,	540,	/	/	/	/
T _T /T _B (°C)	/	/	/	/	/	/	/
T _M (°C)		148	346				
T _{s1} (°C)		461	655				
T _{s2} (°C)							
T _s (°C)							
ξ _s		0.549	0.173				
ξ _{cm}		1.0000	0.8742				
η		0.8113	0.6986				
f _{cc} (MPa)	42.7	42,7	37.3				
E _{c0} (GPa)	39	39	29.8				
ε _{cu} (/1000)	3.5	3.5	4.0				
f _{su} (MPa)	480	264	83.0				
f _{su} - σ _p (MPa)							
E _s (GPa)	210	115	36.3				



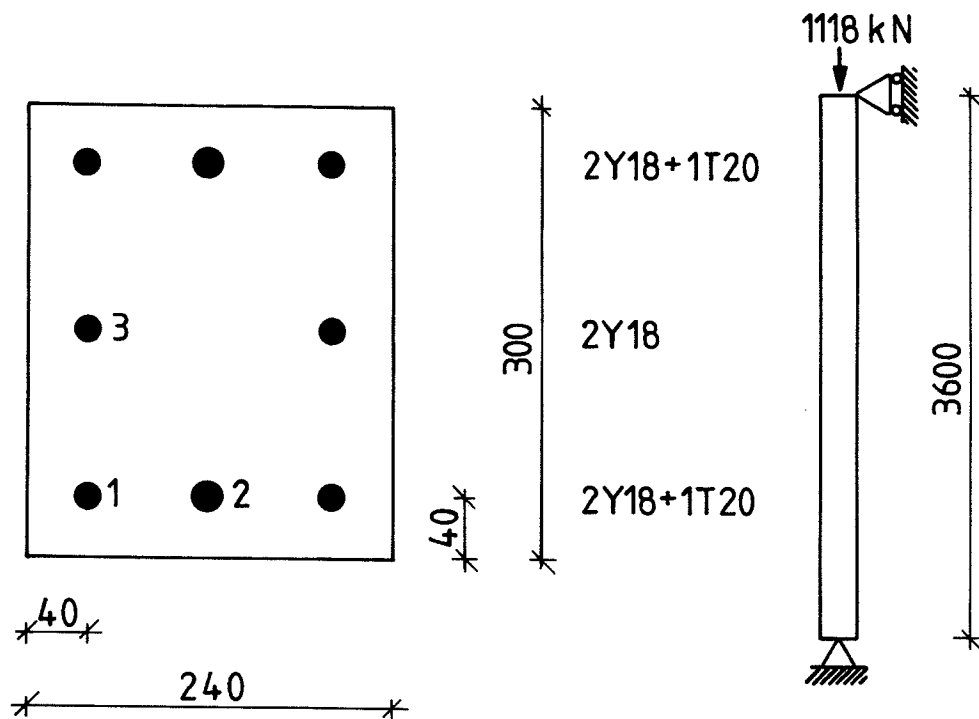
Comparison of test: O and calculation: X.

CROSS SECTION: $C =$ m $C_{slab} =$ m $A_s = 804$ mm²

$d_{s1} =$ m $d_{s2} =$ m $d_{s3} =$ m

CONCRETE: $a = 0.348$ mm²/s aggregate: Limestone age: 14 months

t (h)	0.00	1.00	1.78				
\bar{d}_s (m)							
\bar{C} (m)	0.150	0.114	0.093				
P (kN)							
d_{P+N} (m)							
$M_{u,pl}$ (kNm)							
F_{cu} (kN)	1537	986	635				
F_{cE} (kN)	2005	736	278				
F_{sE} (kN)	167	91.3	28.8				
F_{cr} (kN)	1020	489	213				
x (m)							
σ_c (MPa)							
κ_{load} (/km)							
δ_{load} (mm)							
δ_{tr} (mm)							
δ_{th} (mm)							
$\Sigma \delta$ (mm)							
$\delta_{obs.}$ (mm)							



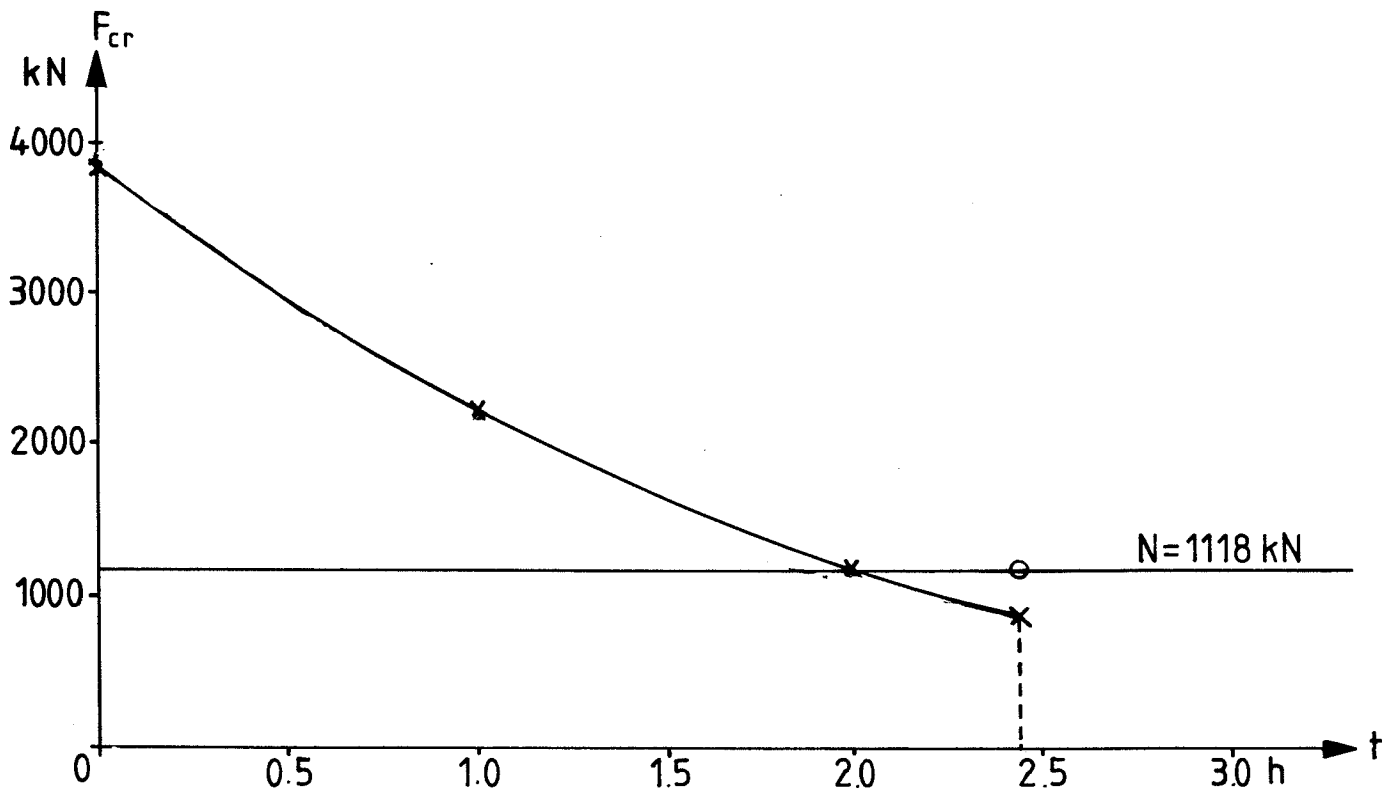
Cross-section and structural system. (All measures in mm).

FIRE DATA: Standard 2.45h

LOAD: $M =$ kNm, $N = 1118$ kN, $d_N =$ m

REFERENCE: Column 20, Seekamp, Becker, Struck [C 6]

t (h)	0.00	1.00	2.00	2.45			
C' (h)		2.00	4.00	4.90			
$D'_w/D' (^{\circ}\text{C})$	/	195,	325,	353,	/	/	/
$E'_w/E' (^{\circ}\text{C})$	/	540,	540,	540,	/	/	/
$T_T/T_B (^{\circ}\text{C})$	/	/	/	/	/	/	/
$T_M (^{\circ}\text{C})$		33	219	288			
$T_{s1} (^{\circ}\text{C})$		525	714	763			
$T_{s2} (^{\circ}\text{C})$		360	581	642			
$T_{s3} (^{\circ}\text{C})$		343	520	580			
ξ_s		0.580	0.249	0.168			
ξ_{cm}		1.0000	1.0000	0.9582			
η		0.8565	0.7173	0.6800			
f_{cc} (MPa)	62.0	62.0	62.0	59.4			
E_{c0} (GPa)	41	41	41	37.6			
ϵ_{cu} (/1000)	3.5	3.5	3.5	3.7			
f_{su} (MPa)	480	278	120	80.6			
$f_{su-\sigma_p}$ (MPa)							
E_{s1+3} (GPa)	210	111	46.6	33.2			



Comparison of test: O and calculation: X.

CROSS SECTION: $C = 0.240$ m $C_{\text{slab}} =$ m $A_s = 2155$ mm²

$d_{s1} =$ m $d_{s2} =$ m $d_{s3} =$ m

CONCRETE: $a = 0.520$ mm²/s aggregate: Quartz age: 19 months

t (h)	0.00	1.00	2.00	2.45			
\bar{d}_s (m)							
\bar{C} (m)	0.240	0.195	0.154	0.144			
P (kN)							
d_{P+N} (m)							
$M_{u,pl}$ (kNm)							
F_{cu} (kN)	4464	3089	2046	1735			
F_{ce} (kN)	10791	4940	2039	1435			
F_{se} (kN)	1563	826	347	247			
F_{cr} (kN)	3805	2250	1172	894			
x (m)							
σ_c (MPa)							
κ_{load} (/km)							
δ_{load} (mm)							
δ_{tr} (mm)							
δ_{th} (mm)							
$\Sigma \delta$ (mm)							
δ_{obs} (mm)							

ERRATA

for Report 174,

'Analyses of Prestressed Concrete Structures Exposed to Fire'.

Page 17 line 17:

$$\zeta_s = \frac{0.108(750 - T)}{T - 440} \quad \text{for } 600 < T \leq 1000^\circ\text{C}$$

should be

$$\zeta_s = \frac{0.108(1000 - T)}{T - 440} \quad \text{for } 600 < T \leq 1000^\circ\text{C}$$

Page 22 line 26: 'exploding' should be 'explosion'

Page 42 line 23:

'...of the same maximum temperature...' should be
'...each of uniform maximum temperature...'

Page 45 line 1 (axis): $\sum \frac{10\zeta^2}{1\zeta_C}$ should be $\frac{\sum 10\zeta^2}{10\zeta_{CM}}$

Page 54 line 4: '....af the stresses...' should be '....of the stresses...'

Page 58 line 5: '....over-reinforced...' should be '.... over-reinforced....'

Page 60 line 19:

$$y = \frac{F_{su}}{\eta \zeta_{cm} f_{cc20}} \quad \text{should be}$$

$$y = \frac{F_{su}}{C \eta \zeta_{cm} f_{cc20}}$$

Page 65 line 9:

$$x = \frac{5}{4} y = \frac{5}{4} \frac{F_{su}}{\zeta_{cm} f_{cc20}} \quad \text{should be}$$

$$x = \frac{5}{4} y = \frac{5}{4} \frac{F_{su}}{C \zeta_{cm} f_{cc20}}$$

Page 67 line 16: '...anchorage apacity...' should be '...anchorage capacity...'

Page 74 line 19: 'the the...' should be 'then the...'

Page 86 line 5:

$$\sigma_{load} = \frac{5}{48} \kappa_{load12} \quad \text{should be}$$

$$\delta_{load} = \frac{5}{48} \kappa_{load12}$$

Page 87 line 14:

$$\sigma_{tr} = \frac{5}{48} \kappa_{tr12} \quad \text{should be}$$

$$\delta_{tr} = \frac{5}{48} \kappa_{tr12}$$

Page 95 line 27: '....E-modolus...' should be '....E-modulus...'

Page 115 line 4:

$$F_c = \int_0^x \sigma(z) dz \quad \text{should be}$$

$$F_c = c \int_0^x \sigma(z) dz$$

Page 118 line 11: '....Fcc...' should be '....Fcu...'

Page 129 Figure: 'M=75.6 kNm' should be 'M=70.6 kNm'

REFERENCES TO THE EXAMPLES

- [C 1] CONCRETE REINFORCING STEEL INSTITUTE:
Reinforced Concrete Fire Resistance.
CRSI Engineering Practice Committee, 238 p.
Chicago, 1980.
- [C 2] POSTEL, R. VON:
Brandversuche an statisch bestimmt
aufgelagerten Stahlbetonplatten und
- balken mit Rechteck- und
Plattenbalkenquerschnitt.
Deutscher Ausschuss für Stahlbeton
Heft 230, Teil 3, pp. 95 - 118.
Wilhelm Ernst und Sohn.
Berlin 1975.
- [C 3] DEUTSCHMANN, H.:
Brandprüfungen an vorgespannten
Betonbauteilen.
Deutscher Ausschuss für Stahlbeton
Heft 162, Teil 4, 18 p.
Wilhelm Ernst und Sohn.
Berlin 1964.
- [C 4] GUSTAFERRO, A.H. ABRAMS, M.S. SALSE, E.A.B.:
Fire Resistance of Prestressed
Concrete Beams.
Study C: Structural Behaviour
During Fire Tests.
Research and Development Bulletin RD009,01B
Portland Cement Association.
Skokie 1971.

- [C 5] LIE, T.T. ALLEN, D.E. ABRAMS; M.S.:
Fire Resistance of
Reinforced Concrete Columns.
DBR Paper No. 1167. 54 p.
National Research Council Canada.
Ottawa, February 1984.
- [C 6] SEEKAMP, H. BECKER, W. STRUCK, W.:
Brandversuche an Stahlbetonfertigsäulen.
Deutscher Ausschuss für Stahlbeton.
Heft 162, Teil 1. 46 p.
Wilhelm Ernst und Sohn.
Berlin 1964.